

UNIVERSITY OF EAST ANGLIA
FACULTY OF MEDICINE AND HEALTH SCIENCES

Immune System Involvement in Metal Hip Implant Failure

Submitted in accordance with the requirements for the degree of Doctor of
Philosophy by

MUNISE PINAR BLOWERS

May 2015

Acknowledgments

First of all, I would like to express my gratitude to Professor Simon Carding for giving me this opportunity to undertake my PhD study in his lab. I also would like to extend my appreciation to past and present members of his group.

A few names I must mention here in particular; I would like to thank to Dr Louise Wakenshaw for helping me to get up and running in the lab, to Dr Isabelle Hautefort for general scientific advice and discussions over morning coffees we shared together, to Dr Elisabeth Bassity for critical review of some written work and Dr Kamal Ivory for providing me with invaluable scientific advice and in general for being an awesome friend over the years. To the several other students of the lab who came and gone, too many to mention here; thanks for their contributions and their support to the project.

I would like to thank Mrs Anna Mathews for providing me administrative support with great enthusiasm, she was always happy to help, it did not matter what the question might be!

I would like to express my sincere gratefulness to Professor Simon Donell for his advice and support throughout the study. I have massive admiration for his work and it has been great to see his friendly face throughout, especially when things did not go according to the plan. I need to extend my thanks to his staff members especially Ms Tracey Potter for looking after my samples when I was late (only occasionally though!), and Mrs Laura Watson for helping me with ethics applications which I am still trying to learn to do properly...

Mr Darren Ebreo deserves his own paragraph of appreciation for getting up very early to collect clinical samples and also doing his best to explain the study to patients, from which he had a very high consent rate. This study would not be possible without his commitment and hard work.

I would like to acknowledge Dr Stefano Caserta, especially for stimulating discussions and for sharing his passion for immunology with me.

At last but not least I would like to thank my dear husband Lee for standing by me through thick and thin of it. He managed to pretend to understand and even like (it's a strong word, I know) my science over the years for that reason alone he deserves a medal. He survived

through my moans, many late nights and weekend working. His patience and encouragement has been invaluable. I will love him forever.

Statement of Declaration

- This study was funded by DePuy Synthes UK, sponsored by Norfolk Norwich University Hospital (NNUH) and hosted by Institute of Food Research (IFR), Norwich, UK.
- Stipend for PhD maintenance was paid by charity Action Arthritis, Norwich, UK.
- HLA Typing was conducted for a fee-for-service basis by National Health Service Blood and Transplant (NHSBT) Colindale, UK.
- Patient consents and clinical sample collection were conducted by Mr Darren Ebreo.
- Illustrations were created by Paul Pople at Creative Designs, Norwich, UK.
- Statistical advice was provided by Dr Marianne Defernez (Analytical Science Unit, IFR, UK).
- TEM images were acquired by Mrs Kathryn Cross at the Norwich Research Park Bioimaging Centre, UK.
- Laser ablation was processed by Particular GmbH, Germany.

Abstract

Immune system involvement in metal hip implant failure

Osteoarthritis (OA) is the most common debilitating disease, especially in the elderly. Total Hip Replacement (THR) is a last resort treatment for hip OA and Metal-on-Metal (MoM) THR was used commonly for its durability. While this is an effective treatment for many, around 12% of hip implants were revised in 2012. MoM articulations had poor implant survival compared with non-MoM, displaying four times higher failure rate.

Between 1997 and 2004, 652 hip replacement surgeries were undertaken in Norfolk using the Ultima TPS MoM THR system (DePuy) which resulted in a high rate of early implant failure (27.4% at year 7). One of the proposed reasons for MoM THR failure is the adverse reaction to metal wear debris and consequent immune system mediated osteolysis resulting in peri-prosthetic loosening. To understand the immune system involvement in metal hip implant failure, a cohort of OA patients were recruited with and without an Ultima implant.

This study investigated;

- The Human leukocyte antigen (HLA) allelic variation and implant failure association.
- Determined the composition and frequency of immune cells and inflammatory markers in Norfolk cohort.
- And tested the metal particle impact on immune cells.

These experimental approaches were utilised to elucidate whether the metal implant failure is a result of an inflammatory process.

The genetic disposition to metal hip implant failure was tested by conducting HLA typing for 25 different alleles across three MHC class II loci which revealed a protective haplotype against implant failure being DQA1*01:02 - DQB1*06. The analysis of immune parameters showed that all patient groups had normal levels of immune cell composition and cytokine levels apart from the Ultima Asymptomatic group, suggesting a regulatory mechanism in place for metal hip implant survival. Analysis of metal particle effect on immune cells demonstrated that these particles are immune-reactive and results in macrophage-initiated and lymphocyte-mediated failure mechanisms.

Table of Contents

1	CHAPTER 1: Introduction.....	1
1.1	Definition and burden of Osteoarthritis.....	1
1.2	Hip Joint Structure and Pathophysiology.....	2
1.3	OA diagnosis and therapeutic options.....	5
1.4	Metal/Metal-on-Metal hip implant failure.....	8
1.5	Chemistry of Co-Cr-Mo alloys.....	15
1.6	Immunological failure mechanism.....	18
1.6.1	Innate recognition of metals.....	20
1.6.2	Adaptive recognition of metals.....	24
1.7	Hypothesis and Aims.....	30
2	CHAPTER 2: Study Protocol.....	32
2.1	Obtaining ethical approval.....	32
2.2	Patient Recruitment.....	33
2.3	Patient recruitment number and study power.....	34
2.4	Patient demographics.....	35
2.5	Human Tissue Collection.....	37
3	CHAPTER 3: Role of HLA molecules in immune responsiveness to metal hip implants.....	38
3.1	Introduction.....	38
3.1.1	MHC Genetic organisation and structure.....	41
3.1.2	HLA Polymorphisms.....	44
3.1.3	HLA Nomenclature.....	45
3.1.4	HLA expression, antigen processing and presentation.....	47
3.1.5	MHC-Peptide-TCR Interaction.....	48
3.1.6	HLA and Disease.....	50
3.2	Materials and Methods.....	53
3.3	Results.....	57
3.4	Discussion.....	64
3.5	Summary.....	69
4	CHAPTER 4: Investigation of immune parameters in metal hip implant patients.....	70
4.1	Introduction.....	70

4.2	Material and Methods.....	77
4.2.1	Immunophenotyping by Polychromatic Flow Cytometry.....	77
4.2.2	Measurement of serum and SF cytokines	86
4.3	Measurement of serum metal ions.....	88
4.4	Results	89
4.5	Discussion	111
5	CHAPTER 5 – <i>In vitro</i> assessment of metal particle impact on immune cells	116
5.1	Introduction	116
5.2	Materials and Methods	119
5.2.1	<i>In vitro</i> metal nanoparticle generation	119
5.2.2	Characterisation of metal colloid size and particle number.....	121
5.2.3	Characterisation of metal particle shape and cellular uptake.....	123
5.2.4	Measurement of cell proliferation.....	124
5.2.5	Assessment of cytokine production	127
5.2.6	Statistics	127
5.3	Results	128
5.4	Discussion	148
6	CHAPTER 6: General Conclusions.....	154
7	References.....	162
8	Appendices.....	174

List of Figures

Figure 1-1:	Structure of the hip joint	4
Figure 1-2:	Ultima [®] THR TPS.....	11
Figure 1-3:	Photograph of an explanted Ultima [®] stem.....	11
Figure 1-4:	Metal particle associated lymphocytic infiltrate and peri-vascular cuffing	27
Figure 1-5:	Proposed model of immune system contribution to metal implant failure.	28
Figure 3-1:	Structure of MHC class I and MHC class II molecules	43
Figure 3-2:	HLA Nomenclature	46
Figure 3-3:	Odd ratios for MHC class II gene expression	61
Figure 4-1:	T and B cells gating strategy	83
Figure 4-2:	Monocyte gating strategy	84
Figure 4-3:	DC gating strategy.....	85

Figure 4-4: Schematic description of Luminex based assays	87
Figure 4-5: Peripheral blood T and B cell absolute counts with activation markers	93
Figure 4-6: Peripheral blood monocyte counts with activation markers	94
Figure 4-7: Peripheral blood DC counts with activation markers.....	95
Figure 4-8: Standard curves for cytokine measurement	99
Figure 4-9: Serum cytokine levels	100
Figure 4-10: SF cytokine levels	101
Figure 4-11: Comparison of cytokine levels in serum versus synovial fluid.....	103
Figure 4-12: PCA analysis of cytokines in serum.....	104
Figure 4-13: PCA analysis of cytokines in synovial fluid	105
Figure 4-14: Analysis of cytokine correlation coefficients in serum.....	106
Figure 4-15: Analysis of cytokine correlation coefficients in synovial fluid	107
Figure 4-16: Serum cobalt and chromium levels	110
Figure 5-1: Colloid generation by laser ablation.....	120
Figure 5-2: The NanoSight System.....	122
Figure 5-3: Co-Cr-Mo metal alloy particle size and number distribution	128
Figure 5-4: PBMC and metal alloy particle morphology.....	131
Figure 5-5: Time course treatment of PBMCs with metal alloy particles	132
Figure 5-6: Metal particle phagocytosis and its impact on monocytes/macrophages.....	133
Figure 5-7: Cell toxicity, necrosis and apoptosis after metal particle exposure	134
Figure 5-8: PBMC response to metal alloy particles	137
Figure 5-9: Stimulation Index after metal alloy particle induced proliferation	138
Figure 5-10: CFSE Gating Strategy	141
Figure 5-11: PBMC proliferation assessed by CFSE staining.....	142
Figure 5-12: PBMC cytokine secretion after exposure to metal alloy particles	146

List of Tables

Table 1-1: Number of OA patients in the UK by joint site.....	2
Table 1-2: Chemical composition of Ultima alloy.....	15
Table 2-1: Patients Demographics	36
Table 3-1: Number of HLA Alleles	44
Table 3-2: HLA gene frequencies in Cohort 1	58
Table 3-3: HLA gene frequencies in Cohort 2.....	59
Table 4-1: Immunophenotyping of PBMCs in whole blood.....	73
Table 4-2: Soluble immunological mediators affecting bone turnover	75
Table 4-3: Flow Cytometry configuration, filter settings and panel distribution	79
Table 4-4: Peripheral blood immune cell numbers in Norfolk cohort.....	92
Table 4-5: Summated cytokine concentration in patient's serum and SF.....	102
Table 5-1: Live/Dead staining with PI.....	143
Table 5-2: Proliferation Index calculated after CFSE staining	143
Table 5-3: Cytokine production of PBMCs cultured with metal particles	147

List of Equations

Equation 2-1: Formula for sample size calculation for parallel studies.....	34
Equation 3-1: Allelic frequency calculation	54
Equation 4-1: Absolute quantification of the cell events calculation	78
Equation 5-1: Stokes-Einstein formula	121

List of Appendices

Appendix 1: Patient invitation letters and consent forms	174
Appendix 2: Raw data of HLA Typing.....	182
Appendix 3: List of Antibodies.....	183

List of Abbreviations

Ab	Antibody
ADAMTS	A Disintegrin And Metalloproteinase with Thrombospondin Motifs
AF	Allele Frequency
Ag	Antigen
ALVAL	Aseptic lymphocytic vasculitis-associated lesions
ANOVA	Analysis of variance
APC	antigen presenting cells
ARMD	adverse reaction to metal debris
ASTM	American Society for Testing and Materials
Au	Gold
BCR	B cell receptor
Be	beryllium
CD	Cluster of differentiation
CFSE	Carboxyfluorescein succinimidyl ester
CI	confidence intervals
CoC	Ceramic-on-Ceramic
Co-Cr-Mo	Cobalt- Chromium- Molybdenum
CoM	Ceramic-on-Metal
CoP	Ceramic-on-Polyethylene
CTL	Cytotoxic T cells
DC	dendritic cells
DIP	distal interphalangeal
DMSO	Dimethyl sulfoxide
DMT	Divalent metal transporter
DTH	Delayed type hypersensitivity
EDTA	Ethylenediaminetetraacetic acid
ELISA	enzyme-linked immunosorbent assay
ER	Endoplasmic reticulum

ESR	Erythrocyte Sedimentation
FBS	Foetal Bovine Serum
FCS	Flow cytometry standard
FDA	Food and Drug Administration
FMH	Faculty of Medicine and Health Sciences
FSC-A	Forward Scatter-Area
GM-CSF	Granulocyte macrophage colony-stimulating factor
GWAS	Genome-Wide-Association Studies
HBSS	Hank's Balanced Salt Solution
HLA	Human leukocyte antigen
ICP-MS	Inductively coupled plasma mass spectrometry
IFN- γ	Interferon gamma
IFR	Institute of Food Research
IL-10	Interleukin 10
IL-1 β	Interleukin-1 beta
IL-6	Interleukin 6
iNOS	Inducible nitric oxide synthase
IRAS	Integrated Research Application System
LD	linkage disequilibrium
LPB	Lipopolysaccharide Binding Protein
LPS	Lipopolysaccharide
MCP-1	Monocyte chemotactic protein 1
M-CSF	Macrophage colony-stimulating factor
mDC	Myeloid Dendritic cells
MFI	Median Fluorescence Intensity
MHC	Major histocompatibility Complex
MHRA	Medicine and Healthcare products Regulatory Agency
MIC	MHC class I related molecules
MMP	matrix metalloproteinase
MoM	Metal-on-Metal
MoP	Metal-on-Polyethylene
MSD	Meso Scale Discovery
m ϕ	Macrophage
NHSBT	National Health Service Blood and Transplant
Ni	nickel
NICE	National Institute for Health and Care Excellence
NJR	National Joint Registry
NNUH	Norfolk and Norwich University Hospital
NRES	National Research Ethics Service
NSAID	non-steroid anti-inflammatory drugs
OA	Osteoarthritis
OARSI	Osteoarthritis Research Society International
ODEP	Orthopaedic Data Evaluation Panel
OPG	Osteoprotegerin
OR	Odds Ratio
PBMC	Peripheral blood mononuclear cells
PCA	Principal component analysis
PCR-SSOP	Polymerase Chain Reaction- Sequence Specific Oligo Probes

pDC	Plasmacytoid Dendritic cells
PHA	Phytohaemagglutinin
PI	Propidium iodide
PIPES	piperazine-N, N'-bis 2-ethanesulfonic acid
PIS	Patients Information Sheet
PMMA	polymethyl methacrylate
RANKL	Receptor activator of nuclear factor kappa-B ligand
REC	Research Ethics Committee
RH	Rheumatoid Factor
RNS	Reactive nitrogen species
ROS	Reactive oxygen species
SF	Synovial Fluid
SNP	single-nucleotide polymorphism
SOP	Standard Operating Procedures
SSC-A	Side Scatter-Area
TAP	Transporter associated with antigen processing
TCR	T cell Receptor
TEM	Transmission electron microscopy
Th	T helper cells
THR	Total hip replacement
Ti	Titanium
TIMP	Tissue inhibitors of metalloproteinases
TNF- α	Tumor necrosis factor alpha
TPS	Tapered polish stem
WHO	World Health Organization
XAS	X-ray absorption spectroscopy
XTT	2,3-bis-(2-methoxy-4-nitro-5-sulfophenyl)-2H-tetrazolium-5-carboxanilide

1 CHAPTER 1: Introduction

1.1 Definition and burden of Osteoarthritis

Osteoarthritis (OA) is a condition that mainly presents with cartilage damage and pain of joints. Early stage OA starts with mild inflammation of the tissue around joints as a result of cartilage degeneration. OA is typically defined by the presence of osteophytes (bony projections form around joint margins), joint space narrowing, sclerosis, cysts and deformity [1]. Over time, osteophytes may impinge on soft tissues causing pain and stiffness due to increased surface area. The pain and stiffness may limit mobility. Several factors are contributory to the development of OA such as joint injury, obesity, ageing, or secondary to other arthropathies. There are differences between aged cartilage and OA cartilage indicating that OA is not simply wear and tear but involves complex genetic and environmental factors such as excessive load, trauma and injury. OA is now described as a disease of “tear, flare and repair” which encompasses mechanical trauma plus an inflammatory process that results in disease progression [2].

OA is the most common type of arthritis. In the last 7 years, 8.75 million people have been treated for osteoarthritis in the UK. This means 33% of people aged 45 years and over experience arthritic symptoms. Women are more likely than men to seek treatment; it was recorded that 49% of women and 42% of men aged 75 years and over are treated for OA in General Practice [3]. OA can occur in any joint, however, the most commonly affected are the spine, hand, knee and hip. The knee is the most common site for OA followed by the hip with 2.12 million people affected by hip OA (8% of whole population aged 45 and over in the UK) [4]. Table 1-1 shows the estimated number of people with OA by site of body affected in the UK.

Table 1-1: Number of OA patients in the UK by joint site

The estimated number of people in the UK aged 45 or over with OA, adapted from Arthritis Research UK [3]		
Joint	Percentage of population	Estimated number (million)
Knee	18%	4.7
Hip	8%	2.1
Hand and wrist	6%	1.5
Foot and ankle	7%	1.7
Two or more sites	7%	1.7

1.2 Hip Joint Structure and Pathophysiology

The hip joint is a ball and socket joint where the head of the femur (ball shape) articulates with the hip bone at the socket (acetabulum); a cup-like depression on the surface of the ilium (pelvic bone) Fig 1-1. The bony articular surfaces of the hip joint are covered by cartilage and separated from one another by synovial fluid. The hip joint has three components 1) bone tissue 2) cartilage and 3) soft tissue structures around the joint (ligaments, muscles, vessel and nerves).

Progression of hip OA occurs when cartilage loss, disturbance of bone remodelling and intermittent inflammation are present. Histological and cellular changes are seen in the cartilage, subchondral bone, synovium and ligaments. Cartilage consists of around 5% cellular matter (chondrocytes), 65-80% liquid phase (water and ions) and 20-30% solid phase (collagen and proteoglycans) [5]. Cartilage matrix is subjected to a dynamic remodelling process under normal conditions. Degeneration and regeneration occur in

balance such that net matrix volume is conserved in healthy individuals. However in OA, this balance is tipped towards degeneration due to loss of collagen and proteoglycans.

Although OA can be conceptualised as mechanically driven it is modulated by chemical and immunological mediators. Chondrocytes and synoviocytes are the only cells present in healthy cartilage, however inflammatory cell infiltration can be seen in OA. It is hypothesised that first proteolytic breakdown of cartilage matrix occur. This is followed by fibrillation and erosion of cartilage surface. The last stage involves inflammation where synovial cells phagocytose cartilage breakdown products and produce inflammatory cytokines; this process then attracts more inflammatory cells into the site.

Degradation and synthesis of cartilage matrix are driven by mediators that are released from chondrocytes, synoviocytes and immune cells including matrix metalloproteinase (MMPs), cytokines, growth factors and free radicals [6]. Degenerative enzymes such as MMPs and aggrecanases are increased in OA cartilage. Particularly MMP1, MMP3 and MMP13 and a “disintegrin and Metalloproteinase with Thrombospondin Motifs” (ADAMTS) -4&5 have been shown to be involved in cartilage matrix degeneration [7-9]. IL-1 β and TNF- α promote cartilage degeneration by enhancing MMPs synthesis, prostanoic acid synthesis and chondrocyte apoptosis [10]. Several other cytokines including IL-6, IL-15, IL-17, IL-18, IL-21, IL-8 and leukemia inhibitory factor have also been shown to be important in OA [11]. On the other hand the growth factors are found to promote cartilage repair through down-regulating the expression of IL1 β receptor, such as IL-1 β receptor antagonist (IL-1ra), soluble cytokine receptors (TNF receptor I & II) and anti-inflammatory cytokines such as IL-4, IL-10 and IL-13 [12]. Tissue inhibitors of metalloproteinases (TIMP), Type II collagen and proteoglycans that lead to chondrocyte proliferation, can also counteract disease progression [13].

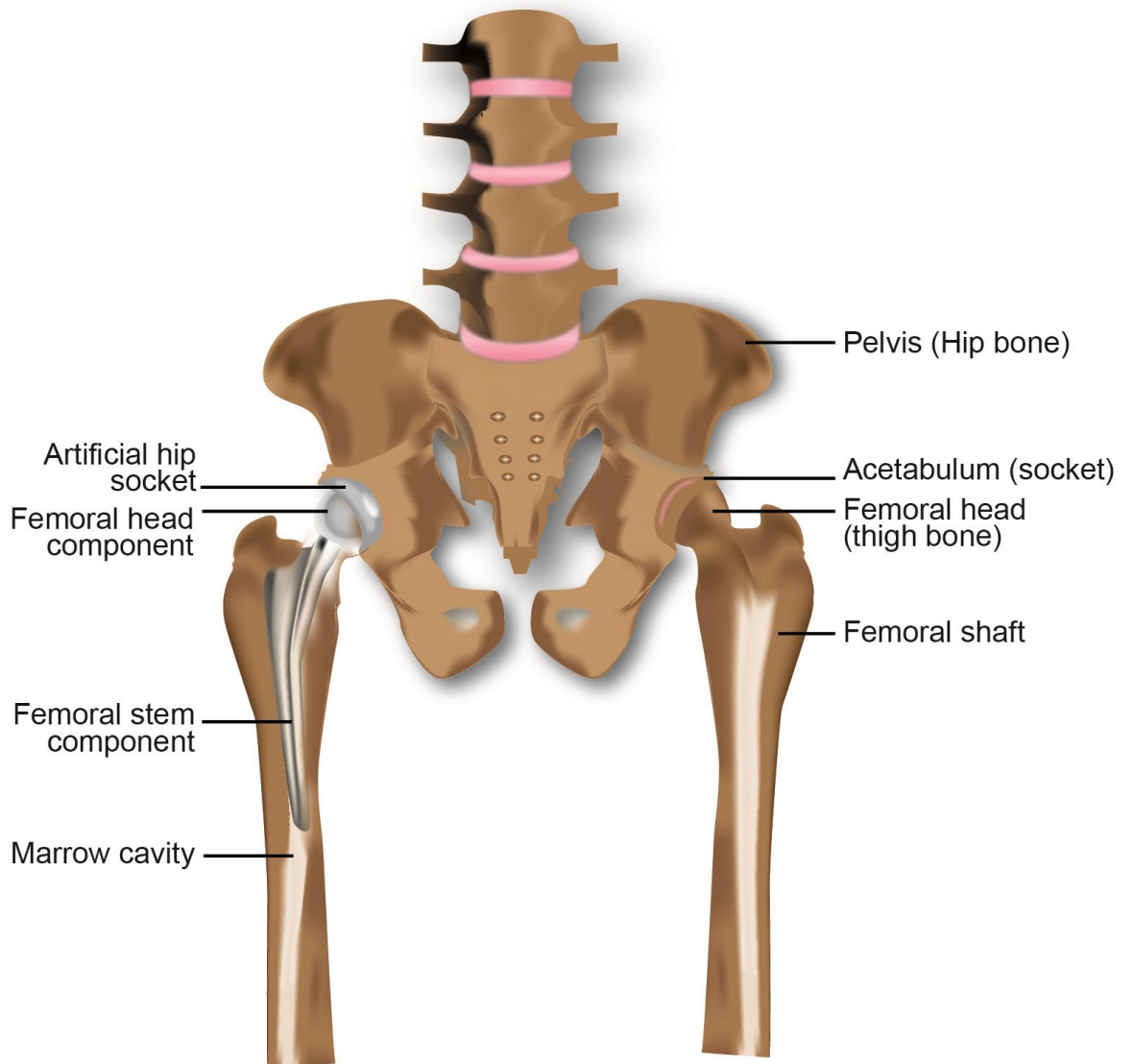


Figure 1-1: Structure of the hip joint

Anterior view showing hip structure and its anatomical components. Right side of the illustration representing natural left hip including pelvis and femur. Left side of the illustration representing right hip with an artificial total hip implant in place (illustrated by Paul Pople at Creative Designs, Norwich, UK).

1.3 OA diagnosis and therapeutic options

OA can be diagnosed pathologically, radiologically, clinically or by a combination of these. The symptoms of OA can vary from patient to patient and the severity of symptoms does not always correlate with the radiological assessment. Because not all people with radiographic OA have clinical symptoms and not all persons who have joint symptoms demonstrate radiographic OA [14]. These differences may indicate varied sub-groups of clinical development.

The American College of Rheumatology established the current classification of hip OA based on clinical and radiographical criteria in 1991 [15]. The diagnostic and therapeutic criteria are designed to separate patients with hip OA from patients with other joint diseases. It also identifies asymptomatic OA from symptomatic OA based on histopathological and radiographical changes. Clinical criteria include the history of the patient, pain score, and physical examination to assess range of motion in the hip. Radiological evaluation consists of findings such as narrowed joint space, sclerosis, formation of osteophytes and cysts. Laboratory tests include the Erythrocyte Sedimentation Rate (ESR) and Rheumatoid Factor (RH). These two parameters are significantly increased in Rheumatoid arthritis but not in Osteoarthritis.

By this classification patients with OA are distinguished from other arthritides and deformities. Furthermore, OA patients are classified into a) Idiopathic OA of the hip b) Idiopathic generalised OA, including hip c) Secondary OA of the hip (caused by another disease or condition).

Similar to other arthritic conditions there is no cure for OA. The therapeutic approach is often based on managing symptoms. Treatment options can be categorised into one or more of the following [16];

- 1) Life style based approaches; losing weight, exercising and physiotherapy.
- 2) Analgesic administration; paracetamol and non-steroid anti-inflammatory drugs (NSAIDs) and disease modifying osteoarthritis drugs (DMOADs), that inhibit matrix-metalloproteinases (MMPs), bisphosphonates, cytokine blockers, calcitonin, inhibitors of inducible nitric oxide synthase (iNOS), doxycycline, glucosamine, and diacerein [17].
- 3) Local administration of corticosteroids and visco-supplementation
- 4) Surgery; usually total joint replacement.

Hip replacement is considered when all alternative therapies have failed. Two different approaches are possible for a hip replacement; resurfacing or Total hip replacement (THR). Resurfacing surgery only replaces acetabular component where the head of the femur is reshaped and resurfaced with an artificial cup. However, total hip replacement involves removing the femoral head and replacing it with an artificial one, then the artificial femoral head is secured by a stem into the marrow cavity (Fig 1-1). Resurfacing is often preferred in younger patients as the larger head size reduces the risk of dislocation. It can also, theoretically, allow the patient to return to a higher level of physical activity. Leaving more bone also may make subsequent revision easier. All resurfacing arthroplasty prosthesis currently on the market are metal-on metal (MoM). However the majority of hip replacement surgery comprise of THR; only around 1% of the hip surgeries were resurfacing in 2012, a decline from 9% in 2005 [18].

Some THRs are fixed with bone cement, polymethylmethacrylate (PMMA) at the bone-implant interface (acetabular or stem compartments or both). A prosthesis where one of its components is fixed with cement and the other is cementless is called a hybrid implant. Different parts of a hip prosthesis are shown in Fig 1-2. Where the head of the hip implant

meets the cup is described as the bearing surface. The bearing surfaces can be made of metal, polyethylene or ceramic. The five main categories of bearing surfaces for THR are;

- 1) Ceramic-on-Ceramic (CoC): both the head and the cup are ceramic
- 2) Ceramic-on-Metal (CoM) : ceramic head with a metal cup
- 3) Ceramic-on-Polyethylene (CoP): ceramic head with a polyethylene cup
- 4) Metal-on-Polyethylene (MoP) : metal head with a polyethylene cup
- 5) Metal-on-Metal (MoM): both the head and the cup are metal

This categorisation describes bearing surfaces only, however, metal alloys are also used in other parts of the implant such as stem and acetabular shell.

Implant selection depends on various factors, such as the patient's age, activity, underlying hip physiology and the surgeon's preferences. For many years the choice of bearing was MoP, however, long term experience from implant registries has shown that frequent failure was seen with these implants in the second decade due to polyethylene wear. This prompted a switch to MoM use for young patients to reduce the risk of wear in the long term. Metal bearings allow use of larger femoral head sizes (36 mm or larger) which more resemble a natural femur head and acetabular socket [19]. Ceramic combinations of bearings are harder than metal, therefore, they display better wear characteristics.

However, these types of bearings experienced fractures and squeaking from the site of the implant. Tribology of manufacturing has been much improved in recent years and historical problems faced with implant design have been reduced currently.

The National Institute for Health and Care Excellence (NICE) technology appraisal guidance, February 2014 [20], recommends that "Prostheses for total hip replacement and resurfacing arthroplasty are recommended as treatment options for people with end-stage arthritis of the hip only if the prostheses have rates (or projected rates) of revision of 5% or

less at 10 years ”. Performances of hip prosthesis are monitored by a panel of experts known as the Orthopaedic Data Evaluation Panel (ODEP). ODEP provides the NHS with an approved list of prosthesis that meet the revision rate standards set out in the NICE guidance.

1.4 Metal/Metal-on-Metal hip implant failure

The majority of hip implants perform well and improve the lives of millions of people every year. In the UK alone around 90,000 hip replacements were conducted in 2012 amounting to around half-a-million procedures since the records started in the UK, according to the 10th annual report published by National Joint Registry (NJR) for England, Wales and Northern Ireland 2013 [18].

One of the earliest hip designs had a MoM bearing (McKee-Farrar THR). Due to poor machining and subsequent wear-related problems this fell out of favour for MoP designs. In the 1990s MoM implants were reintroduced with the aim of increasing longevity by reducing wear. It was thought that better manufacture would overcome the previous problems. However, metal wear debris-associated hypersensitivity was reported [21-24] leading to implant failure from severe tissue reactions. These adverse effects seen in the peri-prosthetic tissue requires a revision surgery where MoM implant replaced with an alternative type of implant. Patients with a failed MoM prosthesis can suffer from groin pain, swelling, squeaking, heat at implant site and the need for an early re-replacement operation due to bone and soft-tissue degradation around the implant. In the UK in 2012, over 10,000 hip revisions were carried out, equating to 12% of all hip operations. The revision burden is now increased compared to previous years and aseptic loosening is

reported as the most common reason (40%) for revision surgery followed by adverse soft tissue reaction (13%) and infection (12%) [18].

The revision rate following primary MoM hip replacement between 2003 and 2010 in the UK was 13.61%. This is around three times higher than non-MoM bearings at 7-year follow-up [19]. The use of MoM articulations has declined dramatically from 10.8% in 2006 to 1.3% in 2012. Currently MoP is the most frequently used articulation type followed by CoC and CoP. The rapid decline of MoM bearings continues in the UK [18]. However, data from the USA indicates that 35% of artificial hips still having a MoM bearing [25].

The 2010 NJR report demonstrated that MoM articulations had an unexpectedly high implant revision rate compared to non-MoM THR [19]. Since then several MoM articulation systems have been recalled by the manufacturers. The UK Medicine and Healthcare products Regulatory Agency (MHRA) issued an alert for all types of MoM hips recommending that patients to be followed up regularly by an orthopaedic surgeon [26]. MHRA advice was updated in 2012 and superseded previous guidelines [27]. The latest recommendation in guidance is that all patients implanted with a MoM articulation must be followed up annually for life by

- a) Measurement of cobalt and chromium ion levels in whole blood
- b) Performing cross sectional imaging including MRI or ultrasound
- c) Monitoring pain, soft tissue reaction, fluid collection or tissue masses

If the imaging is abnormal and metal ion levels are rising, then revision surgery should be considered.

The Norwich metal-on-metal study group first reported issues concerning MoM implants particularly with the Ultima[®] MoM THR TPS, (DePuy Synthes, Leeds UK) in 2006 [28]. Follow up studies of a large cohort of patients, (Donnell *et al* 2010) from the Norfolk and Norwich University Hospital (NNUH) showed that the Ultima[®] system had a high early failure rate (13.8 %)[29]. The latest data (October 2013) on this implant type shows a 27.4% failure rate with a mean time of revision of 6.7 years (Ebreo *et al* 2014, unpublished data).

The Ultima[®] THR is a modular hybrid system, Cobalt- Chromium- Molybdenum (Co-Cr-Mo) alloy with a Tapered polished stem (TPS). A cemented low carbon femoral component with a 28mm Co-Cr-Mo acetabular bearing surface is secured in a titanium (Ti) alloy uncemented shell (Fig 1-2). During the revision operations it was noted that the bearing surfaces were macroscopically undamaged whereas corrosion was seen in the stem where it is in contact with acrylic bone cement (Fig 1-3). An unusual clinical presentation in this cohort was groin pain in the presence of normal radiographs. Collections of fluid around a pseudocapsule of the hip seemed to be causing the pain as it was relieved temporarily after aspiration. Furthermore, soft tissue changes were consistent with a fluid collection. Necrosis of surrounding tissue was found associated with metal released from the stem surface. Histological examination showed diffuse or nodular lymphocytic infiltration with many macrophages present [29].

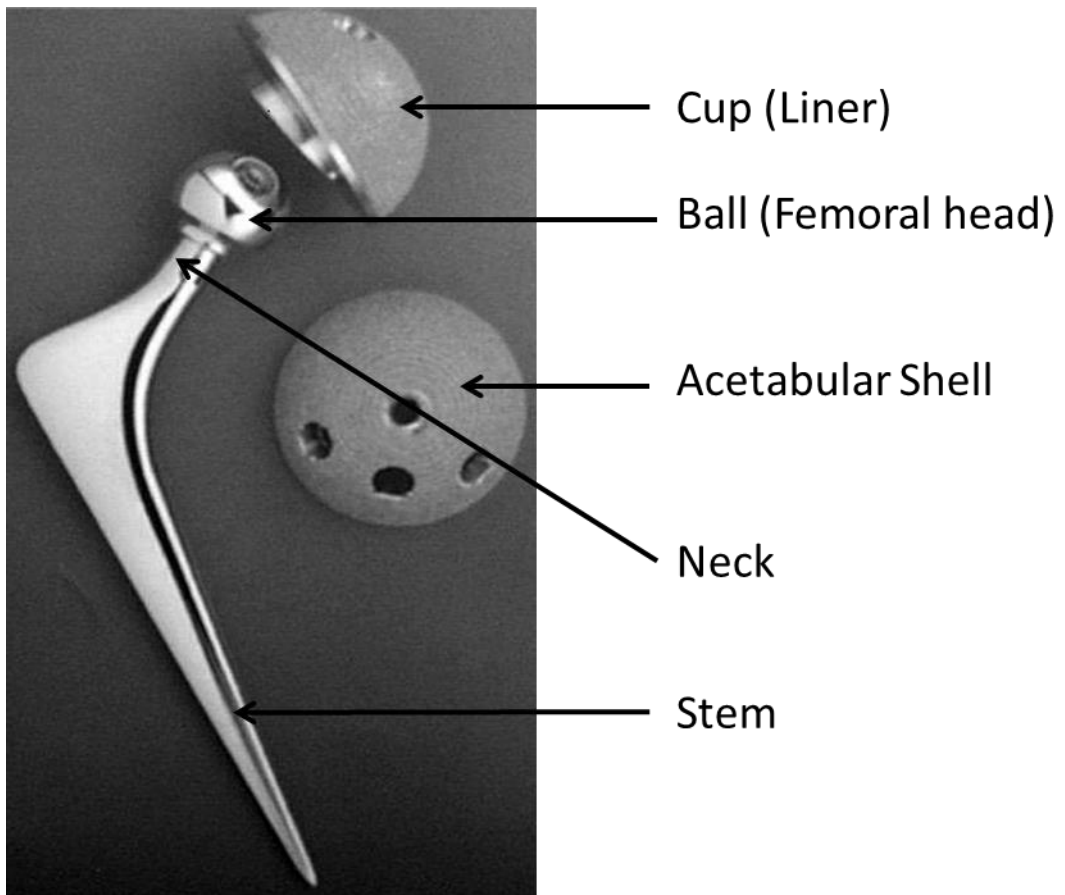


Figure 1-2: Ultima[®] THR TPS

A photograph showing the components of the implant.



Figure 1-3: Photograph of an explanted Ultima[®] stem.

Shows severe corrosion at the interface of the stem and acrylic cement.

Failure of MoM THRs has been attributed to the following reasons;

a) *Implant positioning*

High metal loss due to poor surgical technique resulting in misalignment of components have been reported; an abnormal inclination of the acetabular component can cause impingement on the neck of the femoral implant leading to wear [30]. The friction between the edge of the cup and the head generates metallic debris termed edge-loading. Edge-loading is most pronounced during physical activities, hence it is believed to be more prevalent in younger patients. The association between metal ion levels in blood and cup inclination was reported to be exponential [31].

Malpositioning in large MoM bearings usually involves cup inclinations above 50° and/or anteversion above 15° [32]. However, in the Norfolk cohort the majority of patients had an acetabular inclination within the safe zone. The Ultima® THR TPS system has shown signs of wear mainly on the stem and not on the bearing surfaces, therefore, position related factors are unlikely. This implant was placed by three experienced surgeons with a well-established track record of THR surgery. Only the Ultima® THR TPS had an unprecedented frequency of failure whereas other MoM articulations implanted by these surgeons performed well.

b) *Implant material-related factors*

Tribology is the study of two surfaces in relative motion and their interactions. In the implant field, tribology takes into consideration friction, lubrication and wear of the bearing surfaces. Implant tribocorrosion is a degradation process due to the combined effect of wear and corrosion resulting in the production of bioreactive species. Whilst wear is mechanical, corrosion is a chemical or electrochemical process. Wear may accelerate

corrosion and *vice versa*. Implant wear depends on the structure of the tribological system which means the properties of the material and environmental factors all contribute to wear generation. Considering a commonly cemented THR, there are two dominant types of wear; reciprocating sliding, and fretting. These have been shown to occur at the bearing, head-neck and stem-cement interfaces. Several wear mechanisms are known including abrasion, surface fatigue, adhesion and tribochemical reactions induced by the tribology. These result in changes in surface chemistry and tribofilm formation [33, 34]. Studies have suggested that the mechanism of MoM wear at the bearing interface is governed by predominantly tribochemical reactions and surface fatigue resulting in abrasion of the surfaces [35, 36]. Recent studies have shown that degradation of MoM bearings is a tribocorrosive process; wear is not the full picture. Studies by Hesketh *et al* suggested that wear accounts for 86% of the total material loss, with corrosion accounting for the remaining 14% [37].

Tribocorrosive mechanisms do not only occur on the bearing surfaces but has also been shown to be an important consideration at the stem-cement interface. Bryant *et al* showed that fretting and crevice corrosion at the stem-cement interface were the major reasons for adverse tissue reactions and subsequently large failure rates of the Norwich Ultima TPS MoM patient cohort [38, 39]. The mechanism of crevice corrosion was further demonstrated using an *in vitro* system where Co-Cr-Mo alloy specimens were cemented with PMMA cement for 7 days. Analysis of the metal-cement interface demonstrated a clear distinction between actively corroding areas and the non-corroded sections of the stem and corrosion was accelerated with the use of antibiotics and radio-opaque agents in cements [40]. Under cyclic loading conditions, corrosion was seen to be dominant at this interface with thick layers of blackening (tribological layer) observed, primarily consisting of Cr₂O₃ mixed with organic material, most probably derived from synovial fluid (SF).

Co-Cr-Mo alloys are passive in nature and spontaneously form a protective oxide layer. If the oxide layer is broken down by mechanical wear or corrosion, the base alloy is susceptible to rapid electrochemical oxidation [37]. Under friction the passive film is continuously removed and reformed allowing galvanic coupling between active and passive areas resulting in an increase in corrosion. Electrochemical tests on the Ultima[®] stem demonstrated that 66-80% of all metallic ions released into the bulk environment originated from the stem-cement interface [41]. Galvanic corrosion caused by the combination of a Ti alloy shell and Co-Cr-Mo alloy stem has been reported for other MoM implants where incompatible metals with different electrode potentials come into contact in an electrolyte resulting in one metal corroding another [42].

The literature indicates that total material loss from MoM implants is a combination of mechanical and electrochemical process. Using cement exacerbates this degradation.

c) *Patient related factors*

The Ultima[®] THR TPS population can be divided into two subgroups; successful and unsuccessful. This raises the question of whether patient-related factors are important. Biological disposition can initiate an immune reaction to the metal wear debris in the unsuccessful patients. This thesis examines this third factor by investigating the immunological mechanisms behind the high revision rate that seen in the Ultima[®] THR TPS cohort in Norwich.

1.5 Chemistry of Co-Cr-Mo alloys

The Co-Cr-Mo alloys supplied to the manufacturer for surgical implant production must conform to a certain chemical composition. The American Society for Testing and Materials (ASTM) provides these specifications and sets the standards for medical products. The Ultima[®] THR TPS is an ASTM F799 wrought metal alloy product and chemical composition is shown in the Table 1-2. The main metal elements in the Ultima are chromium (max 30%) and molybdenum (max 7%), nickel (max 1%), iron (max 0.75%) and cobalt. The latter is used to balance up to 100%, approximately 60% of the total composition.

Table 1-2: Chemical composition of Ultima alloy

Chemical composition of Ultima alloy according to ASTM F799 (modified from ASTM original standards document for F799)			
	Min (%)	Max (%)	Permissible variation (%)
Chromium	26.0	30.0	0.30
Molybdenum	5	7	0.15
Nickel	-	1.0	0.05
Iron	-	0.75	0.03
Carbon	-	0.35	0.02
Silicon	-	1.0	0.05
Manganese	-	1.0	0.03
Nitrogen ^{&}	-	0.25	0.02
Cobalt [#]	Balance	N/A	N/A
& If N < 0.10, contents don't have to be reported # Approximately equal to the difference between 100% and the sum percentage of the other specified elements. The percentage of cobalt by difference is not required to be reported.			

Transition metals such as nickel (Ni) are known to be immune sensitisers with a low molecular weight. Ni is the most prevalent contact allergen in the industrialised world. Co, Cr and Mo are also transition metals. Cobalt is a naturally occurring element found in the environment. It is a part of vitamin B12 which is necessary for many biological functions [43, 44]. Chronic exposure to hard metal fumes of cobalt results in “hard metal lung disease” which leads to lung fibrosis [45]. Although the primary sensitising route is the respiratory tract, cobalt poisoning is implicated via skin and gastrointestinal tract [46]. A large cohort study (n = 3042) involving healthy volunteers showed a median Co blood concentration of 0.5µg/L with highest levels not exceeding 1.5 µg/L. Clinical testing of serum Co concentration in MoM patients at an asymptomatic stage and using revision as endpoint revealed levels of 20µg/L associated with metallosis and osteolysis [47].

Chromium is a micronutrient and is essential for biological functions at small doses however, the amount that is needed for optimal health is not well defined. Chromium has been shown to enhance the action of insulin and is involved in carbohydrate, fat and protein metabolism [48]. High doses of Cr are believed to be harmful and chromium toxicity depends on its oxidation state with Cr (VI) being 1000 times more toxic than Cr (III). While Cr (VI) acts as a toxic ion, Cr (III) has been shown to be antigenic causing inflammatory and allergic reactions [49]. Cr (VI) is unstable in the body and reduces to Cr (V)→Cr (IV)→Cr (III) in cells [50, 51] releasing free radicals. The toxicity of Cr may result from damage to cellular components during this process. In the blood the majority of Cr (III) is bound to proteins such as transferrin, whereas a small proportion is associated with low molecular weight proteins. Cr (III) is poorly absorbed and is mainly taken up by cells when organically coupled to serum proteins. Peri-prosthetic tissue analysis of failed ASTM F75 alloy (as in the Ultima[®]) showed that the majority of wear debris contained Cr³⁺ with trace amounts of oxidised cobalt [52]. Also, a further study reported that

Chromium (III)-phosphate was the predominant metallic species in the tissues surrounding MoM hip replacements, which could have arisen from corrosion, wear or a combination of both [53].

Molybdenum is found naturally in soil and it is a trace element which is essential for human metabolism. The daily recommended intake of Mo is 0.1-0.3 mg for adults [54]. Apart from medical implants Mo is also used in the production of tungsten and pigments. Mo is an essential constituent of enzymes that catalyse redox reactions in animals and plants. It is a component of coenzymes necessary for the activity of xanthine oxidase, sulfite oxidase, and aldehyde oxidase. Mo also form complexes with carbohydrates, amino acids, flavins, porphyrins [55]. Excessive dietary intake of molybdenum induces secondary copper deficiency that leads to osteoporosis often manifesting in by bone fracture. Molybdenum competes with phosphorus utilisation, resulting in reduced mineralisation of bone in animals [56].

Although Co, Cr, Mo are needed for biological functions and materials used in orthopaedics hip implants are chosen for their inertness, the dose and valency of these elements appear to be decisive factors in whether they are bio-active or not.

1.6 Immunological failure mechanism

Histological examination of peri-prosthetic tissue in failed implant patients has been shown to display aseptic lymphocytic vasculitis-associated lesions (ALVAL) characterised by tissue necrosis and a dense perivascular lymphocytic infiltrate, also known as lymphocytic cuffs, characterised by the absence of infection. After hip implant surgery a neocapsule forms around the implant consisting of fibrous tissue, fat, muscle and bone. It is important that post-surgical empty spaces are filled by regenerated bone rather than fibrous tissue to ensure implant stability. The neocapsule is contained at the inner surface with the pseudosynovial membrane. Studies on surgical tissue from revised MoM patients reveal that high lymphocytic infiltration in perivascular tissue is present at the implant-neocapsule interface. Surface ulceration of the neocapsule in MoM was reported to be extensive compared to well-fixed MoP implants (Fig 1-4) [57-59]. This phenomenon raises the question of whether the immune system is involved in MoM implant failure. The most predominant cause of implant failure is aseptic loosening which happens when the bone tissue around the implant starts to degrade and loses its mass with histological evidence of hypersensitivity. Inflammation and oedema are seen in many patients and are believed to be the cause of joint pain. Pseudotumours have been found in 60% of patients both failed and well-functioning MoM implants [60] [61]. The pathological spectrum consisting of all symptoms and histological findings is collectively described as Adverse Tissue Reaction to Metal Debris (ARMD).

The main concept in the peri-prosthetic osteolysis is that osteo-resorption dominates over osteogenesis therefore high rate of bone loss results in aseptic loosening of implants. The effects of metal particles on osteogenesis might be direct via disruption of osteoclast

functions or indirect orchestrated by other cells in the area such as fibroblasts, osteoblasts and immune cells (Figure 1-5).

There is some debate about whether the nature of the immune response to particulate debris is driven by innate and/or adaptive immune cells [62]. The prevailing view is that prolonged exposure to metal debris results in a non-specific and continuous immune reaction initially involving innate cells such as monocytes and granulocytes, which may self-resolve. However, if such response is persistence, it can result in a more specific T cell-mediated response, reported in a subset of patients experiencing implant failure. It has been suggested that this might be similar to metal contact sensitivity [63] as seen in delayed type IV hypersensitivity [64].

Metal debris that break away from implants could be in several different forms including, particles, colloidal organometallic complexes, inorganic metal salts/oxides and metallic ions [65]. The fate of these particles depends on the cell-type they encounter. Clearance of metal particles is attempted by phagocytes, mainly neutrophils, macrophages and dendritic cells. Histopathology data from failed implant patients suggests that macrophages and lymphocytes are the main immune cells that infiltrate the peri-prosthetic tissue. Neutrophil infiltration is not often reported in peri-prosthetic tissue, presumably because it might be long passed by the time of sample collection.

This is also seen in other chronic conditions such as asthma and tuberculosis. Wear debris exposure also results in resident cell damage to generate danger signals (DAMPs: damage associated molecular pattern molecules) that are recognised by immune cells in the absence of any pathogen. This is termed sterile inflammation because large quantity of immune cells migrate from blood circulation and infiltrate the inflamed site even in the absence of infecting pathogens. This however results in local inflammation and may perturb

osteoclastogenesis and/or any regulatory mechanism away from check-points for bone homeostasis. Although there is almost no literature on altered regulatory mechanisms in osteolysis and subsequent implant failure, in the absence of the negative feedback loop from regulatory cells, a pro-inflammatory local response may persist for longer and favour osteolysis.

The chemical elements that cause hypersensitivity in humans often fall into the transition metals group of the periodic table, such as titanium (Ti), chromium (Cr), cobalt (Co), nickel (Ni), molybdenum (Mo) and palladium (Pd). These elements are characterized by their valence electrons that are present in more than one atom shell resulting in several oxidation states. Metal elements which cause hypersensitivity appear to share common properties; for example, the presence of two electrons in the outer atomic shell which allows creating coordination sites with organic molecules. How these metal elements are recognised by immune cells and how they activate neighbouring resident bone cells are theorised by various mechanisms.

In the following paragraphs current understanding of immune system activation by metals is discussed;

1.6.1 Innate recognition of metals

Macrophages are believed to be the main cell-type involved in response to chronic metal exposure, this is because:

- a) As highly phagocytic cells, macrophages promote the clearance of metal debris by phagocytosis
- b) Macrophages have been reported to localise in high numbers at inflamed sites in peri-prosthetic tissue.

- c) Mechanistic studies had shown that these cells respond to both metal particles and metal ions

The proposed mechanisms of macrophage activation by metal wear debris include; (i) direct ligation of cell surface receptors such as Toll-like receptors (TLRs) and/or internalization of metal particles and subsequent intra-cellular processing (Fig 1-5 ii, ii, iv).

Direct TLR engagement and subsequent macrophage activation was shown with several *in vitro* models. In a mouse model of C57BL/6J, it has been demonstrated that bone marrow macrophages incubated with Ti activate and produce of TNF- α , IL-1 β and IL-6 [66].

Ligation of TLRs was also reported with Co and Pd in monocyte derived dendritic cells (MoDC) through TLR4 ligation shown in TLR4/MD2 transfectant cell lines [66]. Other groups also showed TLR4 activation by Co, similar to endotoxin triggered response [67].

Using mutant receptor proteins revealed that His 456 and His 458 of TLR4 (non-conserved) are required for activation by Ni⁺² [68]. Polyethylene wear particles are also shown to upregulate TLR2 in mice models recently [69]. This is an indication of direct activation by metal ions without any further ligation requirements. Other TLRs such as TLR2, may be involved in particle recognition even though so far only polyethylene particles were shown to activate TLRs.

It should be noted that the readouts measured in the above studies are generally late events, downstream of TLR receptor signalling including the induction of cytokine expression such as IL-1 β , IL-6, TNF- α and IL-8. Hence it is yet unclear whether metal ions effect directly the conformational changes of TLR and/or its signalling.

Metal particles effects on macrophages viability also have been documented. It has been shown that Co⁺² and Cr⁺³ induce macrophage mortality in a concentration dependent

manner *in vitro* [70]. Short-term exposure (24 hours) of metal ions results in macrophage apoptosis at low concentrations ($\text{Co}^{+2} < 6$ ppm, $\text{Cr}^{+2} < 250$ ppm). However increased metal ion concentrations ($\text{Co}^{+2} = 6-10$ ppm, $\text{Cr}^{+3} = 250-500$ ppm) with longer exposure (48 hours) results in macrophage necrosis [71]. This highlights the fact that necrosis is likely to be the main mechanism of macrophage death after chronic exposure to high concentrations of metal ions. While apoptosis is an active form of cell death and part of the body homeostasis, necrosis results in an inflammatory response facilitated by the release of proteolytic enzymes, DAMPs and cytokines (Fig 1-5).

Toxic metal particles/ions enter the cells via several different pathways. Three main transport mechanisms are proposed in the literature;

- 1) Through non-specific ion transporters followed by metal ion oxidation in the cytosol (Fig 1-5 ii).
- 2) Phagocytosis followed by a series of oxidative processes in the phagosome leading to generation of metal ions and free radicals (Fig 1-5 iii).
- 3) Binding to metal-binding proteins such as transferrin and ferritin via the divalent metal transporter 1 (DMT1) (Fig 1-5 iv). In the cytosol, metal ions are reduced and eventually reduced/oxidised [64].

Metal ion oxidation/reduction generates free radicals such as reactive oxygen species (ROS) and reactive nitrogen species (RNS) which are detrimental to cellular function. Metal wear debris released from a MoM implant cannot be eliminated by metabolic degradation and has to be excreted via the renal or gastrointestinal route. Indeed animal studies suggest that Co/Cr ions accumulate in the liver and kidney [72]. Accumulated particles can be phagocytised by macrophages [73, 74], leading to cellular toxicity. It is thought that macrophages eventually lyse, thus resulting in local inflammation. This

recruits more phagocytes and other antigen presenting cells (APC) to the site of metal ion accumulation [58, 59], potentially followed by a specific adaptive immune response. After the innate recognition of metals, internalised metal ions are thought to be presented by macrophages to T cells which results in T cell activation (Fig 1-5 v, vi). Activated T cells proliferate and undergo expansion and differentiation into cytokine producing effectors, leading to production of RANK-L, M-CSF [75] [76] which mediates transformation from pre-osteoclast into osteoclast (Fig 1-5 vii) and this promotes bone destruction. Other T cells differentiate into IFN- γ , IL-6 and IL-10 producing effectors which block osteoblast and fibroblast functions (Fig 1-5 viii). Thus, these two T cell mediated mechanisms synergistically promote bone damage.

Fibroblasts recovered from peri-prosthetic tissue in the presence of metal particles have shown to affect the differentiation and the bone reposition capacity of osteoclasts [77, 78]. Phagocytosis of metal ions by fibroblasts results in RANKL, and TNF- α productions two cytokine known to be osteoclastogenic, plus differentiation from pre-osteoclasts to osteoclast requires cell to cell contact between osteoclast precursors and fibroblasts (Fig 1-5 x).

It has been reported that osteoblast are also respond to metal particles. Ti induced IL-8 and MCP-1 production from these cells [79]. This activation was time and concentration dependent. Mechanistic study showed that the chemokine expression was via NF-KB-mediated transcriptional activation and controlled by the MAPK signal transduction pathway. IL-8 and MCP-1 are both chemoattractant for macrophages, particle induced expression of these chemokine would results in macrophage infiltration from periphery (Fig 1-5 xi).

1.6.2 Adaptive recognition of metals

T cell activation in presence of metals involves four components: TCR, MHC, antigen and metal ions. TCRs recognise their cognate antigens through complementary determining regions (CDR) on them. The germ line-encoded residues in CDR loops of the TCR are evolutionary conserved for interaction with matched MHC. Therefore metal induced T cell activation may be due to an aberration of either the conformational interactions of these molecules or the recognition of antigens presented by these molecules in the presence of metal ions.

In general, metal ions lead to the generation of neo-antigens by one of the proposed mechanisms. Four different models explain possible T cell recognition of metal ions (Fig 1.5. v and vi):

v. a) Metal ion binds at TCR recognition site of MHC molecule involving both peptide and MHC polypeptide: The most common hypothesis for non-peptide moieties recognition by T cells that they act hapten-like. Haptens are molecules with low molecular weight which have the potential to covalently modify proteins therefore they are strong inducer of immune system. It is postulated that metal ions are associated with or covalently bound to the surface of an MHC-self peptide complex, near to Ag binding groove. This interaction creates a new site for TCR interaction which results in T cell activation. The exact structure of the “MHC-peptide-metal ion” complex is not known, however Yin *et al* showed that Ni^{+2} becomes part of such ligand [80]. By generating *in vitro* mimotope libraries, as a surrogate for Ni^{+2} -reactive T cell epitopes, the authors demonstrated that, even in the absence of Ni^{+2} , reactive ANi2.3 T cell clone can be activated. Depending on a DR52c molecule consisting lysine at p7 position. They have shown that this positively charged lysine occupies the same position in the mimotopes as

the Ni^{+2} does in the natural complex. In summary, metal ion occupies a space at MHC coordination site which results in altered steric conformation leading to neo-antigen formation.

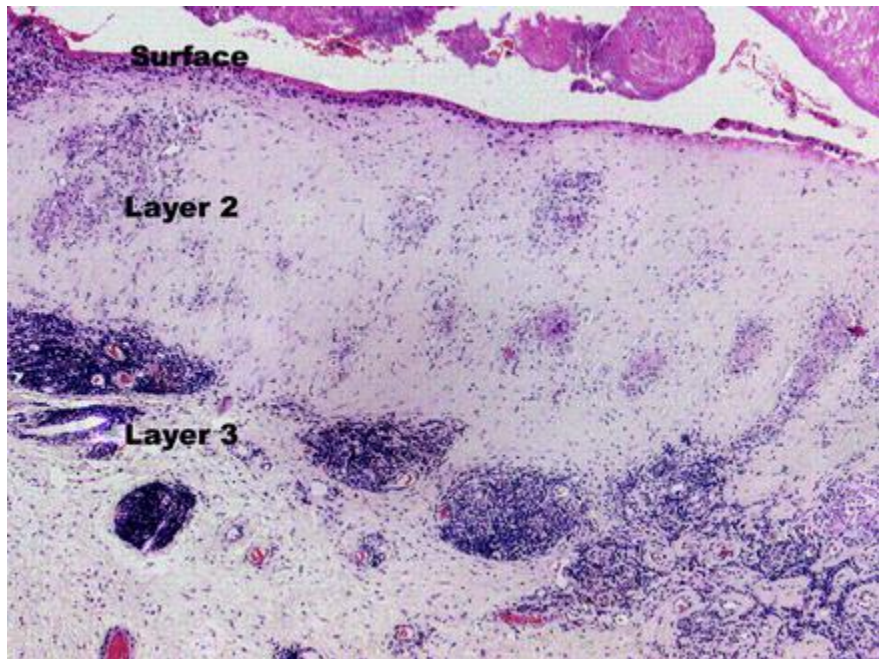
v. b) Modified self-peptide binding to specific MHC molecules: Metal ions bind inside of the MHC-peptide binding groove to drastically change the repertoire of self-peptides normally bound to MHCs. The continuous presence of metal ions perturbs the loading and the stability of self-peptides during endosomal loading skewing the peptide repertoire presented by MHC molecule away from cognate self-peptide and providing a site for new antigen in the periphery. It has been shown that there is a change in the endogenous self-peptides bound to MHC II when Be^{+2} complex recognised by HLA-DP2 restricted CD4+ T cells in Chronic Beryllium disease (CBD). These peptides possess residues of aspartic acid at p4 and glutamic acid residues at p7 which represents Be^{+2} coordination sites [81]. Metal ion capture in this way can result in conversion of a self-peptide into a neo-antigen. Creation of neo-antigens in peripheral organs, after thymic selection, can lead to non-self recognition and T cell-mediated response. In summary, MHC peptide loading is altered which results in aberrant antigen presentation.

v. c) Transition metal ion interference at inside of the MHC polypeptide: Chelating of metal ions alters the structure of MHC molecules α/β chains. TCR recognise metal-modified amino acid residues of the MHC molecule itself or metal provokes conformational changes potentially in the MHC molecule, effectively providing a new structure for different TCRs to bind. It has been shown in the CBD that the TCR does not interact directly with the Be^{+2} ion but instead recognizes changes in the surface of HLA-DP2/peptide complex. This induced by the internally bound Be^{+2} which by changing the MHC polypeptide loops favours the formation of a new TCR ligand coordinated by both

MHC and peptide amino acids [82]. In summary, MHC structure is modified which results in autoimmune reaction to self MHC molecules.

vi) Antigen independent mechanism: Metal ions are sufficient to form a coordination complex between the TCR and MHC molecules in a peptide independent manner [83]. This model proposes a mechanism independent of requirement for antigen and antigen processing. It has been demonstrated that fixed APCs resulted in activation of Ni-reactive T cell clones. This scenario is similar to T cell activation by superantigens which bridge TCR with MHC molecule independent of the peptide or TCR specificity. However the difference from superantigen activation is that metal ion recognition requires a more specific contact within the TCR α - significantly enhances the specificity of this interaction. However the interaction of metal ions between TCR and MHC requires a much more specific sequence recognition in the TCR chain than what seen with superantigens, which in contrast can activate many TCR clonotypes. For instance Ni⁺² hypersensitivity involves with the SE9 T cell clone activation by Ni crucially depends on Tyr29 in CDR1 α , Tyr94 in CDR3 α , and a conserved His81 in the HLA-DR β -chain [84]. Thus also the MHC sequence is specifically affecting such TCR: MHC bridging coordination products mediated by metal ions. Due to positive selection in thymus all peripheral cells possess the ability of a short and instable MHC interaction. In the presence of metal ions, self-peptide/MHC molecules may stabilise interactions with TCR, resulting in T cell activation.

A



B

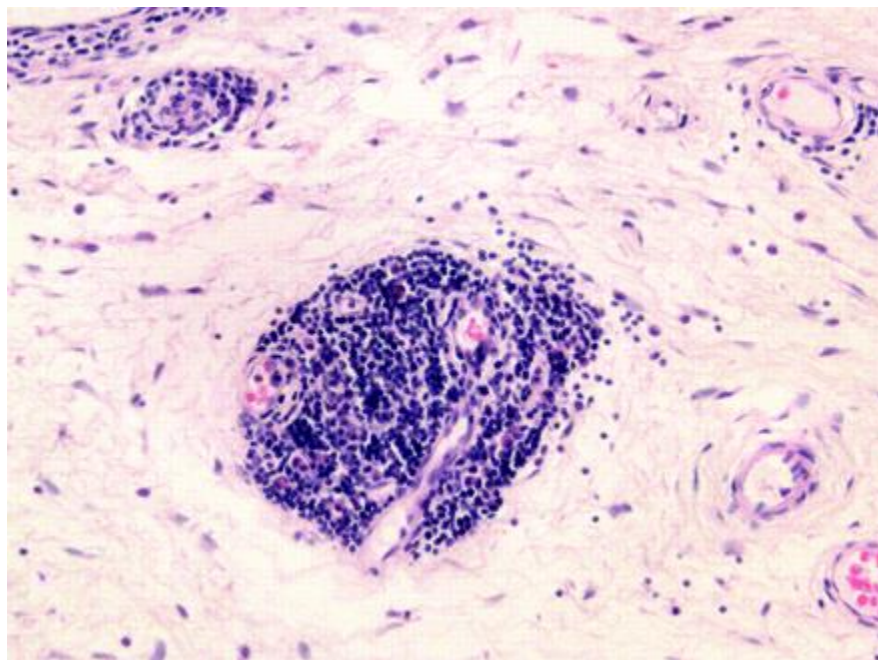


Figure 1-4: Metal particle associated lymphocytic infiltrate and peri-vascular cuffing

A representative micrograph of tissue section stained with Hematoxylin and eosin from a failed MoM hip implant replacement. **A:** Displaying demarcated tissue layers of neocapsule Surface layer (Layer 1) shows sign of ulceration with loss of the pseudosynovial lining. Subsurface layer (Layer 2), between the tissue surface and the vascular layer, contains limited cellular infiltration. Layer 3 displaying vasculated tissue with cuff of lymphocytes are present predominantly. (x40 magnification). **B:** Lymphocytic cuffs with higher magnification (x100). Adapted from Davies *et al* 2005 [56].

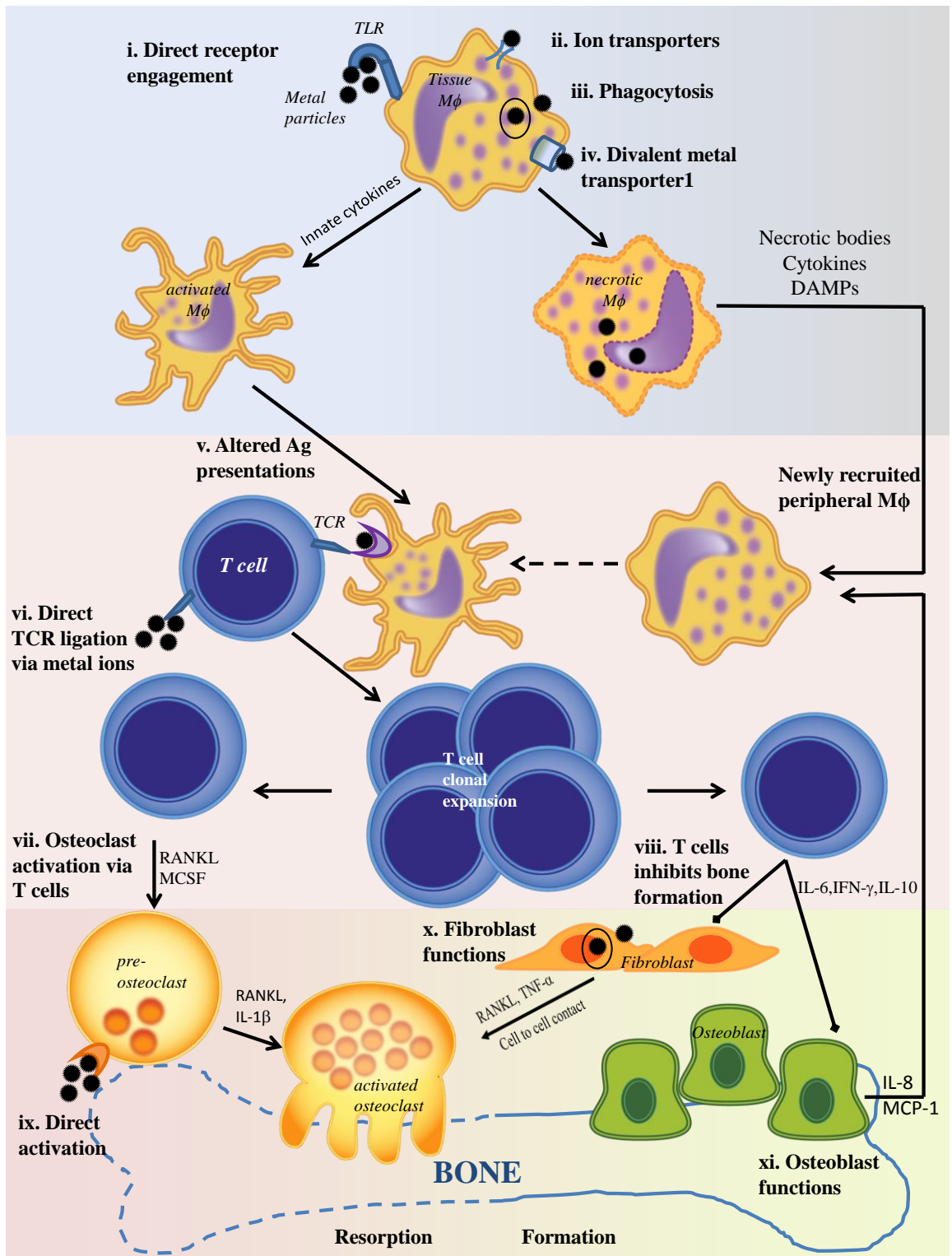


Figure 1-5: Proposed model of immune system contribution to metal implant failure.

Legend for Figure 1-5: Macrophages can be activated directly by metal particles via TLR receptors on them (i) or internalisation of these particles are mediated by various mechanism such as through ion transporters (ii), through phagocytosis (ii) or through DMT1 (iv) which all can lead to macrophage activation. On the other hand metal particles can also be toxic to macrophages, resulting in necrosis of these cells. Necrosis will lead to production of pro-inflammatory mediators and subsequently, infiltration of newly recruited peripheral macrophages. Macrophages and other APCs are involved in altered antigen presentation to T cells in the presence of metal ions (v). T cells also can be directly activated via metal particles (vi). Activated T cells produce cytokines such as RANKL and MCSF facilitate osteoclast formation (vii). Subset of T cells thought to have inhibitory effects on tissue resident cells such as Fibroblast and Osteoblast (viii), which slow down tissue formation. Direct particle exposure to osteoclasts results in differentiation of pre-osteoclast to activated osteoclast (ix). Fibroblasts can activate osteoclasts either by cytokine mediated manner or cell to cell contact (x). The other tissue resident cells such as osteoblast also are involved in osteoclast activation and further recruitment of macrophages through cytokine and chemokines (xi), which result in bone resorption. This cascade of pathways, perhaps all not mutually exclusive result in perturb bone homeostatis therefore osteolysis that seen in metal hip implant failure.

1.7 Hypothesis and Aims

This thesis set out to test the following hypothesis;

Metal implant wear debris modifies the function of antigen presenting cells (APCs) leading to the activation of T cells that results in inflammation and destruction of bone tissue causing implant failure.

The hypothesis has been tested by addressing the following aims.

1. *To define the HLA allele types in Ultima patients;*

Do the patients with failed metal implants have different HLA genotype, predisposing to metal hip implant failure? HLA genotyping was aimed at identifying whether there is allelic variation between failed versus well-functioning hip implants. Identifying the distribution of MHC alleles would be the first step towards understanding adaptive immune response in metal hip implant failure (Chapter 3), as most likely adaptive responses could be MHC-restricted.

2. *To determine If Adverse Reactions to Metal Debris (ARMD) an inflammatory process;*

What is the evidence of immune system dysregulation in the Norfolk cohort? Immune cells composition and activation status were investigated in the Norfolk cohort of Metal-on-Metal (MoM) patients. Cytokine and growth factors were analysed in serum and synovial fluid of these patients (Chapter 4). Any difference in cytokine levels or activation status of the cells may suggest an inflammatory ongoing *in vivo* response to metal hip implants.

3. *To investigate if immune cells mount a response to implant wear debris?*

The impact of the Ultima wear-particles on peripheral blood mononuclear cells (PBMCs) was determined by investigating phagocytosis, proliferation and cytokine production profile upon exposure to Ultima particles *in vitro* (Chapter 5).

2 CHAPTER 2: Study Protocol

2.1 Obtaining ethical approval

The National Research Ethics Service (NRES) facilitates ethical review through its Regional Ethics Committees (REC) based across England. The application for research ethics approval was made via the Integrated Research Application System (IRAS), which is an online file management system for completion of all required documentation. After registration and completion of the IRAS forms, the application was accompanied by the research protocol and supporting documents including but not limited to Patient Information Sheets (PIS), Consent Forms, Invitation Letter, GP Information Letter, Contracts with the sponsor and the funder, Investigator's CVs and Standard Operating Procedures (SOPs) where relevant (Appendix 1). A "favourable opinion" for the study was gained in February 2012 by Cambridge East REC, reference number 11/EE/0488.

It was also necessary to obtain ethical approval for procuring blood samples from healthy volunteers for assay development and *in vitro* assessment. This required approval from the local UEA Faculty of Medicine and Health Sciences (FMH) Research Ethics Committee, which was approved in January 2012, reference number 2011/2012-13.

This study was registered in the clinical trials website as per the funder's (DeyPuy Synthes, UK) terms and conditions, reference number NCT01517737. Details can be found at <http://clinicaltrials.gov/ct2/show/NCT01517737?term=2011+Orth+04S+%2868-06-11%29&rank=1>

This prospective cohort study was also approved by the Research Governance Committee of the Norfolk & Norwich University Hospital and conducted in accordance with the Declaration of Helsinki.

Laboratory experiments were conducted in Institute of Food Research (IFR), Norwich UK. The study was approved by IFR Research Governance Committee (March 2012).

2.2 Patient Recruitment

This study was designed to investigate the immune system involvement in MoM Ultima[®] THR TPS implant failure. The other type of metal implants were also studied as control including the MoP and MoC since NJR data suggest that MoM implants are three times more likely to fail compared to other types [19]. Patients undergoing primary or revision total hip replacement were recruited at the NNUH Orthopaedics Department during their routine visit to hospital. Whole blood, serum and synovial fluid were collected from these patients. Non-operative patients were recruited in the Outpatient Clinic during routine follow-up and asked to donate blood samples only.

Patient Inclusion Criteria:

- Undergone an Ultima[®] TPS THR in Norwich
- Ultima[®] TPS THRs undergoing revision
- Undergoing primary hip replacement with osteoarthritis
- Other metal THRs undergoing revision

Patient Exclusion Criteria:

- Undergoing primary THR with rheumatoid arthritis
- Other inflammatory arthritides
- Secondary infection
- Taking immunosuppressant medication
- Unable to provide informed consent

2.3 Patient recruitment number and study power

It is not well established as to which immunological parameter is the most relevant biomarker in diagnosis of metal implant failure. So far blood ion levels are the best wet-biomarker available for clinicians. For this reason serum metal ion levels were used to calculate the sample size for this study; considering the view that elevated serum ion levels are an indication of metallosis leading the implant failure.

Null hypothesis: Metal ions released from failed MoM implants are NOT different than non-MoM implants.

A power test was performed to ensure that the study was adequately planned and the appropriate number of patients was recruited. Statistical considerations for a parallel testing were utilised using the online tool at

http://hedwig.mgh.harvard.edu/sample_size/js/js_parallel_quant.html

For this calculation the following factors were considered.

α : Probability of type I error (false positive) = $p < 0.05$

β : power — the probability of avoiding Type II error (false negative) = 80%

Δ : the effect size that study should be able to detect; difference between control and tested patients

σ : Standard deviation in the population (between subjects) =1

Z_α : Z is a constant (set by convention according to the accepted α error =1.96 (2-sided, 5%))

Equation 2-1: Formula for sample size calculation for parallel studies

$$n = 2 (Z_\alpha + Z_{1-\beta})^2 \sigma^2 / \Delta^2$$

Metal ion concentrations in the blood were used to establish study effect size. Maroni *et al* compared MoM with normal controls and found the effect size to be 1.7 for chromium [85]. Pretest power analysis, performed by using one standard deviation of the control subjects, indicated a sample size of 14 had an 80% power to detect a difference between groups and sample size of 18 gave 90% power. As for the quantification of soluble biomarkers in serum and synovial fluid, Osteoarthritis Research Society International (OARSI) & Food and Drug Administration (FDA) guidelines were followed [86]. Based on 2-sample t-test (2-sided $\alpha = 0.05$) effect size: 1.23 with 2 SD. The number needed was 15 per group provided 90% of study power whereas 12 patients per group provided 80% study power. Therefore it was aimed to recruit between 12-18 patients/per clinical group.

2.4 Patient demographics

A total of 56 patients were recruited for this study. The patient's demographics are depicted in Table 2-1. The study cohort was stratified into four groups according to the radiological screening and clinical status as follows;

1. Pre-Implant group: OA patients that have no metal implant and undergoing primary hip replacement (n = 15)
2. Ultima Asymptomatic group: OA patients that have an Ultima implant and tolerating well (n = 17)
3. Ultima Symptomatic group: OA patients that have a failed Ultima implant and awaiting a revision operation (n = 12)
4. Other Symptomatic group: OA patients that have another type of failed metal implant and awaiting a revision operation (n = 12)

Table 2-1: Patients Demographics

	Pre-Implant	Ultima Asymptomatic	Ultima Symptomatic	Other Symptomatic
Clinical Status	No implant present	Implant present, not failed	Implant present, failed and revised	Implant present, failed and revised
Number Recruited	15	17	12	12
Mean age (in years with range)	70 (41-83)	68 (55-84)	64 (45-80)	70 (54-86)
M/F ratio	2/13	10/7	8/4	5/7
<i>In situ</i> implant time (months \pm SD)	N/A	130 \pm 26	139 \pm 23	123 \pm 54

2.5 Human Tissue Collection

Operative patients were identified from the NNUH institutional database (Bluespier Int, Worcs, UK) by a member of the clinical team. Outpatient patients were recruited during their hospital visit to routine MoM clinics run by consultant orthopaedic surgeons at the NNUH. Patients were approached to provide informed consent for collection and analysis of blood and synovial fluid at the time of providing consent for their surgical procedure by a member of the clinical team. For the outpatients group, 50 mls of blood was collected. For the operative groups, 50mls of blood was obtained from each patient in the anaesthetic room. Blood sampling was performed using standard venepuncture techniques with a Vacutainer system (Becton-Dickinson). Samples were aspirated into glass silicone tubes for serum assay, Na-Heparin tubes for PBMC analysis, K₂EDTA for immunophenotyping, HLA typing, and trace element analysis. Intra-operatively once the capsule of the hip joint had been identified, synovial fluid was aspirated via a 21G stainless steel needle through the capsule so as to prevent contamination with blood from the general circulation. Synovial fluid was transferred aseptically to a Na-Heparin tube for further analysis.

Down-stream processing of samples and details of data analysis are described in the relevant chapters.

3 CHAPTER 3: Role of HLA molecules in immune responsiveness to metal hip implants

3.1 Introduction

MHC molecules in humans are named Human Leukocytes Antigens (HLA). Following on from earlier mouse work involving recognition of the differential antigens responsible for tumour rejection led to the discovery of the first human HLA antigen [87]. In 1958 three separate groups published [88] [89] [90] their findings studying sera from multiple blood transfused donors showing the antisera detecting alloantigens on human leucocytes. The discovery of HLA molecules is attributed to Dausett and his associates who received the Nobel Prize in 1980 sharing with it Snell and Benacerraf. This led to our understanding that human leukocytes possess mismatched determinants (antigens) that mount an immune response.

HLA tissue mis-matching was initially noted in organ transplantation where allogenic MHC molecules of a donor were recognised by the recipient's immune system leading to graft-versus-host disease and therefore resulting in transplant failure [91]. Vredevoe *et al* first showed the positive correlation between HLA matching and kidney allograft survival in 1965 [92]. Even though earlier work by many groups had shown that HLA molecules possess strong histocompatibility antigens [87], the immunobiological functions of MHC molecules were demonstrated using mouse models. Mozes and McDevitt *et al* used a mouse model which had eight different HLA serotypes of different genetic backgrounds [93]. On injection of synthetic antigens only certain MHC serotypes of mice responded strongly to the antigen whilst other mice did not; even though each sero-group of mice had different genetic backgrounds. From control experiments, including using those different antigens, serotypes and different strains of mice, it was concluded that genes linked to the HLA-complex control the immune response. It was also postulated that,

either there are multiple HLA gene loci, or a single gene locus expresses many alleles.

Using modern investigation tools, we now know that both assumptions were true.

The actual function of HLA molecules was not elucidated until the 1970s. It was first shown that T cells and B cells were involved in MHC compatibility [94]. Then the same was true for macrophage MHC antigens [95] highlighting the requirement for histocompatible macrophages and lymphocytes. T cell recognition of an antigen directly involves the MHC-complex termed MHC restriction which was first demonstrated by Doherty and Zinkernagel [96, 97].

Even though traditionally the role of MHC molecules is associated with adaptive immunity, our current understanding of MHC molecule's role in innate immunity is also expanding. The evidence suggests that MHC class II molecules synergize with TLR-2 and TLR4 in inducing an innate immune response where MHC-II knock-out mice shows reduced responsiveness to ligation of these receptors [98]. The mechanism of MHC involvement in innate immune response was elucidated where MHC class II deficiency resulted in attenuated development of endotoxic shock. Intracellular MHC class II molecules interact with the Btk (tyrosine kinase) via the costimulatory molecule CD40 and maintains Btk activation. The Btk interacts with adaptor molecules MyD88 and TRIF. The absence of this interactions results in defective TLR signalling [99]. Therefore, intracellular MHC class II molecules can act as adaptors, promoting full activation of TLR-triggered innate immune responses. These findings highlight the fact that apart from central role in adaptive immunity MHC molecules are also important in innate inflammatory response.

The genes encoding the HLA molecules are mostly located on the short arm of chromosome 6. HLA molecules are key immune determinants and an individual possesses a particular HLA type. HLA type and its disease association have been well described for some time now. This has led to an understanding that a wide range of autoimmune and malignant diseases occur more frequently in individuals with a certain HLA haplotype. The HLA molecules can mediate disease-promoting effects by presentation of modified disease-triggering peptides. On the other hand, HLA molecules can also be protective by promoting regulatory cells thus resulting in homeostasis. HLA association has been shown to have diagnostic value in clinics where the relative risk value (disease frequency among individuals carrying associated MHC antigens) is well established in several conditions (e.g. HLA-B27 and ankylosing spondylitis).

3.1.1 MHC Genetic organisation and structure

The MHC can be divided into three genetic loci;

- a) Class I containing HLA-A, B, C loci
- b) Class II containing HL-DR, DQ, DP loci
- c) Class III containing non-classical HLA genes of immune function such as TNF, complement factors, and heat shock proteins.

By the early 1980s, it was generally understood that there were at least six different series of determinants (loci) causing variation in HLA types. Molecules A, B and C are present on most nucleated cells and are named Class I, whereas DR, DP and DQ are mainly present on antigen presenting cells and named Class II. These six main loci are now called classical HLA antigens. Since then other antigens have been discovered with more limited tissue distribution. These newer HLA molecules are not routinely involved in antigen presentation and are named non-classical HLA (class III) molecules.

The MHC class I molecule is a heterodimer consisting of two polypeptide chains; an α and a β_2 -microglobulin chain. The α chain contains 3 domains, α_1 , α_2 and α_3 ; the α_3 domain spans through the cell membrane and is non-covalently bound to β_2 -microglobulin. The α_3 domain and β_2 -microglobulin show similarities to immunoglobulin C domain and have similarly folded structures. However the α_1 and α_2 domains fold together into a single structure (Fig 3-1 A). The folding of α_1 and α_2 creates the peptide binding groove for MHC class I molecules (red in Fig 3-1 A).

MHC class II molecule is also a heterodimer consisting of 2 α and 2 β domains. However, the MHC class II molecule has two trans-membrane glycoprotein chains (Fig 3-1 B). Each

chain has two domains and two chains which together form the four domain MHC class II structure. Again $\alpha 2$ and $\beta 2$ domains are similar to the immunoglobulin C domain where these two span through the cell membrane. The MHC class II molecule peptide binding groove is comprised of $\alpha 1$ and $\beta 1$ chains (Fig 3-1) are formed by different chains and therefore not covalently bonded. The peptide binding groove sits on $\alpha 1$ and $\beta 1$ chains (red in Fig 3-1 B).

Genes encoding the α chains of MHC class I molecules and the α and β chains of MHC class II molecules are linked within the complex on the short arm of chromosome 6 whereas the genes for $\beta 2$ -microglobulin of MHC class I complex are on chromosome 15 with the invariant chain of the MHC class II complex located on chromosome 5.

Different alleles of MHC class molecule have specificity to bind different peptides.

Allelic variation occurs only at specialised sites within the MHC molecules. In the MHC class I molecule, both $\alpha 1$ and $\alpha 2$ chains display polymorphism. However within the MHC class II DR molecule only the $\beta 1$ chain is significantly polymorphic; the DR $\alpha 1$ chain virtually invariant. As for the DQ and DP molecules, both $\alpha 1$ and $\beta 1$ chains displays variation at the peptide binding groove [100, 101].

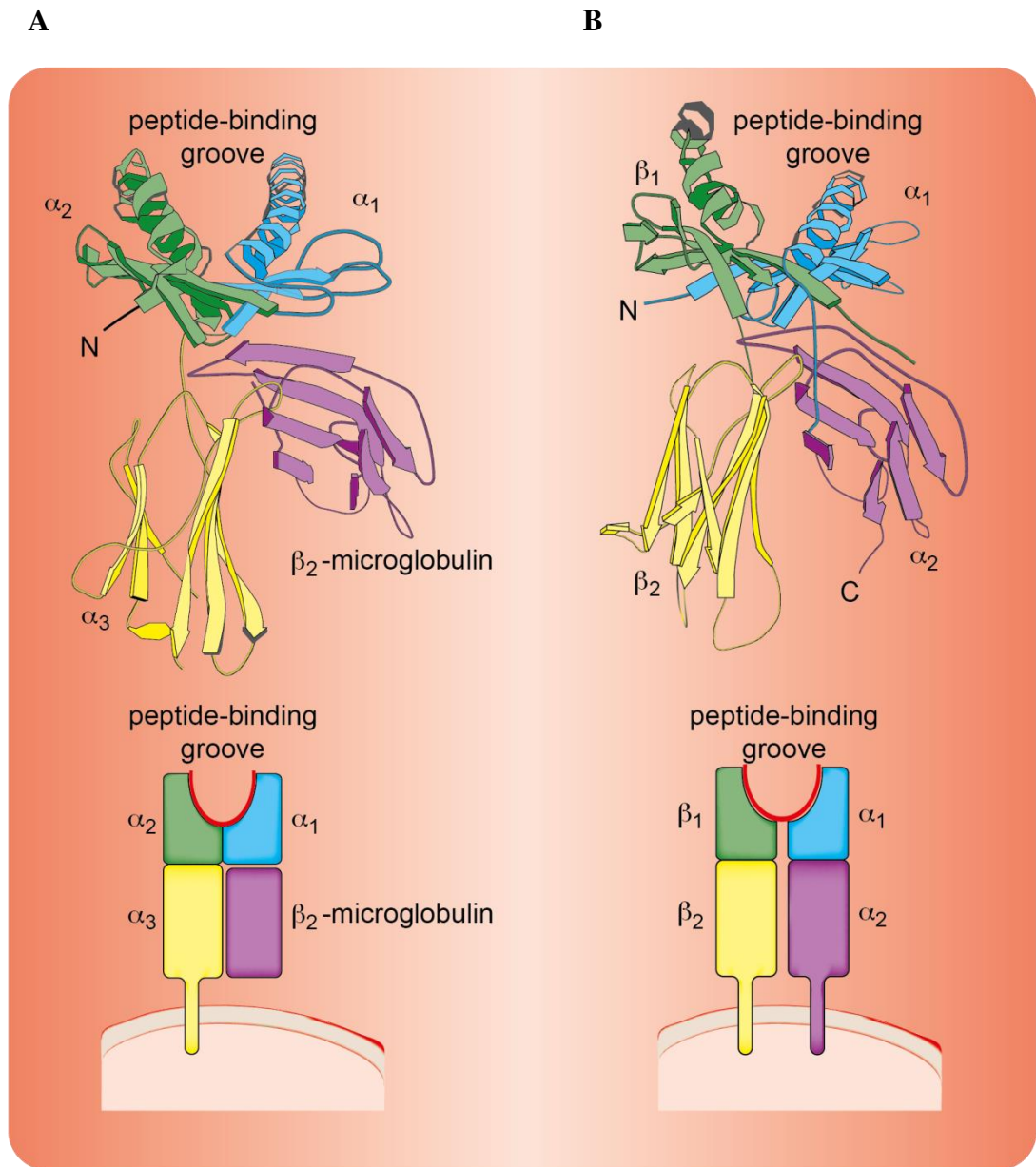


Figure 3-1: Structure of MHC class I and MHC class II molecules

A) Schematic depiction of MHC class I molecule. Top panel showing a ribbon diagram of subunits for MHC class I molecule. It is composed of two polypeptide chains, a long α chain and a short β chain (β_2 -microglobulin). Peptide binding groove consist of two α helices forming a wall on each side and eight β -pleated sheets forming a floor. Bottom panel is showing MHC I molecule interaction with cell. Transmembrane α_3 domain of the molecule anchors to cell. Peptide binding region shown in red where most of the allelic variation occur **B)** MHC class II molecule is composed of two polypeptide chains. Top panel showing a ribbon diagram depicting protein structure of subunits. α_1 and β_1 domains consisting of peptide binding groove. Bottom panel displaying transmembrane region (β_2 and α_2 domains). Peptide binding regions marked in red (Illustrated by Paul Pople at Creative Designs, Norwich, UK).

3.1.2 HLA Polymorphisms

MHC genes are highly polygenic and polymorphic giving immune cells an advantage in recognising many different antigens and differentiating self from non-self. MHC genes are the most polymorphic genes in humans indicative of their rapid and constant evolution. Much of the allelic variation is limited to the peptide binding groove. The number of alleles assigned to different HLA molecules is ever expanding. The number of alleles that have been assigned by World Health organisation (WHO) as of July 2014 are shown in Table 3-1.

Table 3-1: Number of HLA Alleles

HLA Alleles assigned by WHO as of July 2014 [102]	
HLA Class I Alleles	8,976
HLA Class II Alleles	2,870
Other non-HLA Alleles (MICA, MICB, TAP1, TAP2)	164
Number of confidential Alleles (waiting to be published)	4

3.1.3 HLA Nomenclature

The WHO oversees the coordination of the nomenclature for HLA typing. An example is as shown in Fig 3-2 [103] which was used for genotyping in this study. Each allele has a unique number corresponding to a specific allele with up to four sets of digits separated by colons. Each section separated by a colon is called a “field”. The length of the allele designation depends on the sequence of the allele and its nearest relative. Most of the alleles are named up to field 1 and field 2. Longer names are used if necessary to separate it from close relatives. The first field describes the allelic group, the second and so on describe the specific allele. These numbers are assigned for a specific DNA sequence to determine allelic classification. If it differs in amino acid sequence of the encoded protein, another number is then assigned. The third field shows alleles that differ for synonymous nucleotide sequences within the coding region whereas field 4 indicates the differences in the untranslated region. A number in field 4 may have a suffix attached to it such as N for Null or S for secreted.

The HLA nomenclature was updated in 2010. The WHO Nomenclature Committee for Factors of the HLA System, determines assigned allele types and is also responsible for maintaining the HLA nomenclature. Details can be found at <http://hla.alleles.org/nomenclature/index.html>. Additionally, laboratories input their finding into this database called “The expert assigned types” which represents more cells and therefore more alleles.

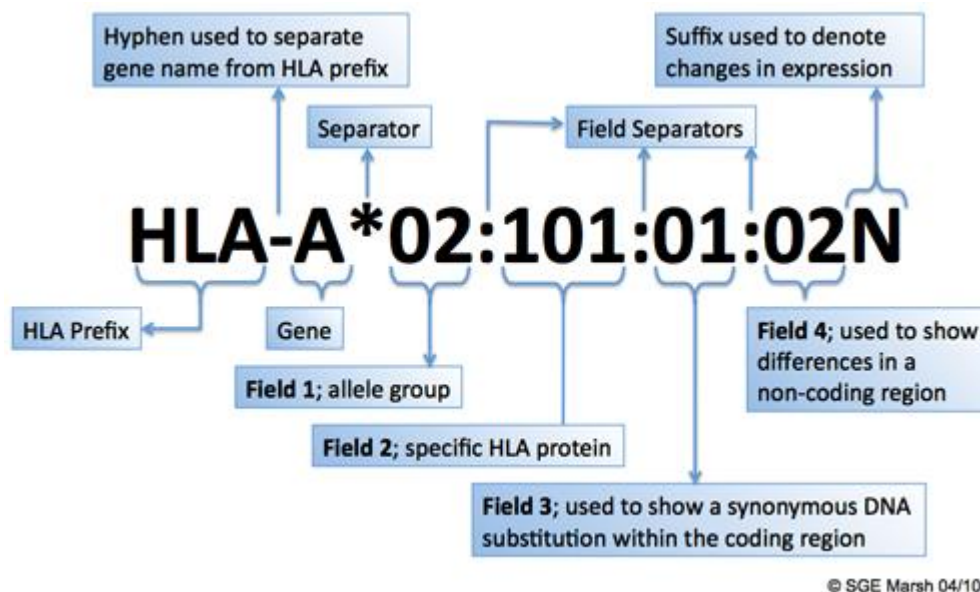


Figure 3-2: HLA Nomenclature

Schematic illustration of HLA tissue typing results. Numbers, letters and symbols are explained for interpretation. <http://hla.alleles.org/nomenclature/naming.html>

Common notations are;

HLA → the HLA region and prefix for an HLA gene

HLA-DRB1 → a particular HLA locus i.e. DRB1 *HLA-DRB1*13* a group of alleles which encode the DR13 antigen or sequence homology to other DRB1*13 alleles

*HLA-DRB1*13:01* → a specific HLA allele

*HLA-DRB1*13:01:02* → an allele that differs by a synonymous mutation from *DRB1*13:01:01*

*HLA-DRB1*13:01:01:02* → an allele which contains a mutation outside the coding region from *DRB1*13:01:01:01*

*HLA-A*24:09N* → a 'Null' allele, an allele which is not expressed

*HLA-A*30:14L* → an allele encoding a protein with significantly reduced or 'Low' cell surface expression

*HLA-A*24:02:01:02L* → an allele encoding a protein with significantly reduced or 'Low' cell surface expression, where the mutation is found outside the coding region

*HLA-B*44:02:01:02S* → an allele encoding a protein which is expressed as a 'Secreted' molecule only

*HLA-A*32:11Q* → an allele which has a mutation that has previously been shown to have a significant effect on cell surface expression, but where this has not been confirmed and its expression remains 'Questionable'

3.1.4 HLA expression, antigen processing and presentation

T cells only recognise antigens presented by antigen presenting cells through the MHC. There are two different classes of MHC molecules, MHC class I and MHC class II, involved in antigen presentation. All nucleated cells express MHC class I molecules as many as 100,000 (apart from erythrocytes and sperm cells). MHC class II molecules are conditionally expressed (around 30,000) by professional antigen presenting cells such as B cells, macrophages and dendritic cells, as well as by thymic epithelial cells.

Antigens might be derived from an intracellular or extracellular source; MHC class I molecules process antigens derived from cytosol and deliver them to the cell surface where they are recognised by CD8⁺ T cells. However, MHC class II molecules process antigens that originate from extracellular sources. These antigens are internalised by a vesicular system where the MHC II molecule gets loaded and is then delivered to the cell surface. The MHC class II-peptide complex is recognised by CD4⁺ T cells.

Therefore, the HLA class I pathway deals with endogenous pathogens and immunogens such as viruses, intracellular bacteria and products of proteasome degradation (nonapeptides). Peptides that bind to MHC class I are actively transported from the cytosol to the endoplasmic reticulum (ER) by transporters associated with antigen processing (TAP) proteins where they are processed. Cytosolic proteins are degraded by a multicatalytic protease complex called a proteasome. The proteasome chops up peptide ligands for the MHC class I molecule. Antigens are then transported from the cytosol to the ER by TAP1 and TAP 2 proteins. These two TAP proteins form a heterodimer and load peptides to the MHC class I molecule in the ER. A fully-loaded MHC class I molecule with peptide then leaves the ER and is transported to the cell surface within the Golgi apparatus where it is recognised by CD8⁺ T cells. CD8⁺ T cells are specialised to kill any

cells that present with foreign peptides. This process is crucial for homeostasis hence almost every cell in the body serves the class I pathway. Proteasome also can degrade proteins in the cytosol that originate from the vesicular system. This process is called retrograde transportation and allows APCs to release peptide into the cytosol and then be presented by the class I pathway, termed cross-presentation [100, 101].

On the other hand the HLA class II pathway deals with intra-vesicular peptides that are generated by receptor mediated endocytosis, phagocytosis and pinocytosis. These peptides originate from exogenous pathogens and immunogens and only APCs can present such antigens. MHC class II molecules are also located in the ER however they cannot bind to their antigens readily due to an accompanying invariant chain which binds to and blocks their peptide-binding groove. The MHC II molecule binds to its peptides in the endosome where active proteases catalyse invariant chain release. Once dislodged from the invariant chain, peptides are loaded onto class II molecules. MHC class II molecules can also capture molecules within the endosome that are derived from metabolic degradation where cytosolic proteins move into the vesicular system through the process of autophagy. Loaded MHC class II molecules within Golgi apparatus then move to the cell surface where they can be recognised by CD4+ T cells. CD4+ T cells are specialised in activating macrophages, helping B cells to produce antibodies, and regulate immune responses [101] [100].

3.1.5 MHC-Peptide-TCR Interaction

In the adaptive immune system, B cell receptor (BCR) recognises antigens directly, whereas T cell receptor (TCR) will only recognises antigens in the context of an MHC molecule. MHC molecules, when loaded with antigen, form a ligand, then a TCR

recognises the matched MHC molecule-antigen complex. Antigen, MHC molecule and TCR altogether form an immunological synapse. This formation only occurs where foreign/self-antigens are presented by matched MHC molecules to their cognitive T cells; this mechanism is called MHC restriction. MHC restriction dictates that the epitope seen by a given TCR is a combination of a cognitive peptide with a matched MHC molecule. This means that the TCR must recognise both antigen and MHC molecule type concomitantly.

Two main factors are involved in the immune responsiveness against a given antigen that are not necessarily mutually exclusive; determinant selection and T cell repertoire. Different alleles of MHC molecules in an individual select a given determinant with varying affinity with the higher the strength of the binding resulting in a greater likelihood of a potent response. The discrimination of a non-self/immunogen from a self/non-immunogen is determined by the T cell repertoire. T cell clones capable of recognising self-antigens are deleted in the thymus during T cell development and the establishment of central tolerance. This is the result of positive and negative selection events in the thymus which are determined by MHC-self protein TCR interactions. The interaction between a selected T cell clone and its cognate antigen could be weak or strong and thus determines the extent of the response. It is also important to consider that the reaction to non-self-antigens might be due to a breakdown in central and/or peripheral tolerance where self-reactive T cell clones escape thymic deletion and enter into the periphery. It is likely that a combination of these two mechanisms result in an autoreaction. Hence an individual's MHC genotype controls the ability of the immune system to detect or respond to a specific immunogen. Therefore a particular HLA allele with a certain haplotype may predispose or protect an individual to a specific disease.

3.1.6 HLA and Disease

Many studies have demonstrated that expression of MHC molecules are closely associated with auto-immune diseases. Amiel *et al* reported in 1967 that patients with Hodgkin's disease displayed a higher frequency of HLA-B5 antigens (51%) compared to healthy individuals [104]. The HLA-DQ2 and HLA-DQ8 alleles are strongly predispose to type 1 diabetes [105]. Ninety per cent of Caucasian ankylosing spondylitis patients carry HLA-B27 allele whereas only 9% of healthy population do [106]. Rheumatoid arthritis, narcolepsy, coeliac disease, and multiple sclerosis, have all been shown to have an association with HLA alleles [107] [108]. Many chronic inflammatory diseases are associated with MHC class II genes, due to their central role in presenting immunogens to T cells. It has been shown in rheumatoid arthritis that some of the autoantigens responsible for this condition are derived from type II collagen, which has a single immunodominant T cell epitope that is bound by both HLA-DQ1 and HLA-DQ4.1 molecules [109] [110] [111].

Regarding OA, the literature is limited and conflicting. It is not known if any autoantigens are primarily involved. There are a few previous reports of HLA association with OA using different typing techniques, classification systems and varying ethnic background, making it difficult to compare studies or demonstrate any association.

Riyazi *et al* studied OA of the distal interphalangeal (DIP) joint's association with HLA-DR alleles. They have found no association of DIP compared to healthy population. However comparison between OA patients revealed that HLA-DR2 (DRB1*15/16) was more common in DIP + OA patients compared to DIP- OA patients (OR = 2.4 ;95% CI = 1.1-5.0) whereas HLA-DR4 (DRB1*04) showed decreased frequency (OR = 0.3; 95% CI = 0.1-0.7) in their comparison [112]. Suggesting DR2 might be a risk factor to develop

DIP in OA patients. DR4 involvement has not been reported before; this allele may need further scrutiny.

Merlotti *et al*, showed over representation of HLA-B35, B40, DQ1 and CW4 (*B15 and *B35, *B40, DQB1*05 and DQB1*06, *C04) alleles in primary OA of the hand.

Haplotype analysis showed an association of B35-DQ1, B40-DQ1 and DR2-DQ1 with increased OA risk [113]. Rovetta *et al* indicated that haplotype DRB1:07*e *04 is more frequent in OA compared to healthy controls, HLADR*13 was most prevalent in patients with OA of the hand [114]. Moos *et al* analysed HLA-DRB1 loci in primary OA patients [115] and showed increased DR2 (*15/*16) , frequency of this allele was 26.5% compared with only 17% in the control (OR = 1.58). On the other hand, decreased DR5 (*11, *12, *13) frequency was observed in patients compared to controls indicating a negative association (OR = 0.542). These results are varied largely and inconsistent and the only common finding of these studies is allele DR2 (*15/*16)'s association with OA.

Metal sensitivity to Ni and beryllium (Be) through T cell involvement is well documented with both being associated with particular MHC class II alleles (HLA-DR52c and HLA-DP2) [116]. There are almost no reports on Co-Cr-Mo sensitivity and MHC association.

Fisher *et al* studied labourers working in hard metal manufacturing and reported no deviation in HLA phenotype in cobalt-sensitive individuals [117] . No MHC allele or isotype association have been reported regarding sensitivity to metal alloy debris generated by hip prostheses. It has been shown in Ni allergy that metal-specific T cell clones require autologous APC for response to metal ions, indicating a role of specific peptide and/or specific MHC variants in metal binding and therefore interactions with the TCR [83]. How metal ions influence MHC + peptide complex recognition by TCR is not fully understood. It has been proposed however that metal ions may bind to MHC molecules and this interaction induces changes in MHC+ peptide complexes leading to alteration in ligand and

presentation as neo-antigens. This altered ligand is recognised by T cells and causes hypersensitivity. This may be a mechanism for the immune response to metallosis seen in hip implant failure.

Traditionally, HLA tissue typing used to be conducted by serology using reactive antibodies for MHC molecules. Serotyping yields low resolution results by today's standards since the exact amino-acid sequence or nucleotide sequence cannot be determined. As the technology has advanced, molecular typing tools have become the choice for tissue typing where higher resolution results can be achieved. The Polymerase Chain Reaction- Sequence Specific Oligo Probes (PCR-SSOP) method is the most commonly used technique today to type HLA molecules and gives intermediate resolution. Sequencing can be further conducted on the samples in case higher typing resolution is required. This would determine the exact sequence of the HLA gene and resolves most of the degeneracy seen in the results. Disease association studies only look at the general allelic group, therefore intermediate resolution is often sufficient.

Since literature is very limited on OA and metal implant failure in terms of HLA association the current study was undertaken to determine whether there is an association between HLA class II gene frequencies and metal hip implant failure by investigating, first, the whole cohort for their allelic frequencies (OA patients), then looking at the failed hip implant group. HLA-DR and -DQ frequencies are often altered in auto-immune diseases, arthropathies and recognition of transition metals hence these two alleles were investigated in the current study.

3.2 Materials and Methods

Patients

A total of 56 consecutive patients were recruited for this analysis consisting of Cohort 1 of OA patients considered for hip arthroplasty, Cohort 2 of 24 OA patients (sub group of Cohort 1) that had a failed metal hip implant requiring revision. The control group was matched with patient groups for ethnic background and geographic location. The 537 control subjects were all Caucasians from Norfolk, England [118].

Sample processing

PBMCs were isolated from EDTA-blood using Ficoll Hypaque density gradient separation. 6 mls of anti-coagulated blood was layered onto Histopaque-1077 (Sigma, Cat No: 10771) in Accuspin tubes (Sigma, Cat No: A2055-10EEA) and centrifuged at 800 g for 15 minutes. Opaque interface containing mononuclear cells were aspirated with a 3 ml Pastette. Cells were washed and transferred into cryovials containing freezing media consist of 90% Foetal Bovine Serum (FBS) + 10% Dimethyl sulfoxide (DMSO) and stored at -80⁰C for further use in tissue typing.

HLA Typing

This was undertaken by the National Health Service Blood and Transplant (NHSBT) Colindale Laboratory, on a fee-for-service basis. HLA Class II typing was carried out for HLA-DRB1, -DQA1, -DQB1 using commercial PCR-SSOP kits (LABType®, One Lambda). In this method DNA is amplified with PCR with locus-specific biotin-labelled primers. The products were interrogated with oligonucleotide probes attached to beads which were analysed on a Luminex™ platform. HLA types were obtained at intermediate resolution which resolves major allele groups to a minimum of two digits (within the first

field). Analysis of HLA-DRB1, -DQA1, -DQB1 types were performed at the two digit level except for HLA-DQA1*01 (4 digit).

This level of resolution can produce a certain degree of degeneracy between related alleles however it identifies main allelic groups.

The allele frequency (AF) is described as the frequency of possessing a particular copy of an HLA allele amongst all alleles being considered at a genetic locus. HLA genes are expressed as co-dominant meaning both parental and maternal phenotypes are present in off-spring. AF is calculated as in equation 3-1.

Equation 3-1: Allelic frequency calculation

$$AF = \frac{(\text{number of alleles positive of MHC variant}) \times 100}{\text{total number of chromosomes } (2n)}$$

Statistical analysis

Allelic frequencies of investigated genes were compared between patients and controls using the Fisher Exact test and associations were expressed as Odds Ratios (ORs) with 95% confidence intervals (CIs). $P < 0.05$ value was considered significant.

OR is a measure of association between an exposure and an outcome. The OR represents the odds that an outcome will occur given a particular exposure, compared to the odds of the outcome occurring in the absence of that exposure [119].

In the current study it was tested whether possessing certain allele increase the risk of developing implant failure. Statically significant differences then were interpreted as

- OR=1 Exposure does not affect odds of outcome (no association)
- OR>1 Exposure associated with higher odds of outcome (Predisposing)
- OR<1 Exposure associated with lower odds of outcome (Protective)

High polymorphism is seen at HLA loci (20 or more alleles per locus), in addition to extensive linkage disequilibrium (LD) between immunogenetic loci is present which requires correction of analysis. Multiple testing correction was done using a technique developed by Benjamini and Hochberg called the “false discovery rate ” [120], based on the number of tests and the original p-values using R software. p_c represents corrected P values.

Study Power Calculation

Retropective assessment of the study power was calculated for failed implant group.

Effect size (OR) calculation was conducted using Stata software (Texas, USA).

The calculation was based on recruitment number for case (2n = 48) and control (2n = 1074) groups, $\alpha = 5\%$ was considered statically significant and 80% study power deemed to be desirable.

The difference in allele frequencies between case and control was assessed by conducting a simulation test to determine required OR value to achieve a study power ≥ 0.8 . Following Stata script was utilised.

Stata commands used:

```
cci 1 47 11 1063 / cci 8 40 11 1063
```

```
cci 25 23 365 709 / cci 43 5 365 709
```

```
sampsi 0.02 0.01, alpha(0.05) n1(48) n2(1074)
```

```
sampsi 0.17 0.01, alpha(0.05) n1(48) n2(1074)
```

```
sampsi 0.52 0.34, alpha(0.05) n1(48) n2(1074)
```

```
sampsi 0.90 0.34, alpha(0.05) n1(48) n2(1074)
```

The worst case scenario (lowest allele frequency) and best case scenario (highest allele frequency) in controls were calculated and compared with patient's allele frequencies for given loci.

3.3 Results

Molecular typing was conducted for a total of 25 different alleles across three MHC class II gene loci, DRB1, DQA1 and DQB1 (for complete raw data See Appendix 2). 13 HLA-DRB1, 7 HLA-DQA1 and 5 HLA-DQB1 alleles were interrogated. “A” represent α chain of the respective molecule whereas “B” represent β chain. HLA-DR α chain does not have any variation hence only B chain was investigated, on the other hand at the DQ loci both α and β chains display allelic variation.

Table 3-2 shows the comparison of HLA-DRB1, -DQA1, -DQB1 gene frequencies in Cohort 1 OA patients, and normal controls. HLA-DRB1*01 ($p = 0.0405$) showed increased frequency in OA patients compared with controls. HLA-DQA1*01:02 ($p = 0.0089$) and DQB1*06 ($p = 0.0342$) showed decreased frequency in OA patients compared to controls. After correcting for multiple comparisons significance was lost for the differences in frequency of HLA-DRB1*01 ($p_c = 0.3375$), -DQA1*01:02 ($p_c = 0.2225$) and -DQB1*06 ($p_c = 0.3375$) alleles (Table 3-2).

Analysis of Cohort 2, the failed implant group, was also conducted against the control population (Table 3-3). There was an increased frequency of DQA1*05 ($p = 0.0303$) whereas DQA1*01:02 ($p = 0.0003$) and DQB1*06 ($p = 0.0026$) showed decreased frequencies in patients compared to controls. The difference in frequency of DQA1*05 did not withstand multiple testing correction ($p_c = 0.1889$) although both DQA1*01:02 ($p_c = 0.0075$) and DQB1*06 ($p_c = 0.0325$) were still significant after correction.

Table 3-2: HLA gene frequencies in Cohort 1

HLA-DR and HLA-DQ gene frequencies in Cohort 1, OA patients (2n=112) compared with controls (2n=1074) [118]					
HLA type	Patients	Control	Odds Ratio with "Confidence Interval "	p	p _c
	% (n)	% (n)			
DRB1*01	19.6 (22)	12.5 (135)	1.700 "1.031 to 2.803"	0.0405	0.3375
DRB1*03	17.0 (19)	15.3 (165)	1.126 "0.6687 to 1.894"	0.6805	0.8953
DRB1*04	15.2 (17)	20.1 (217)	0.7067 "0.4129 to 1.210"	0.2607	0.5013
DRB1*07	17.0 (19)	12.8 (138)	1.386 "0.8198 to 2.342"	0.2401	0.5002
DRB1*08	3.6 (4)	3.5 (38)	1.010 "0.3536 to 2.884"	1.0000	1.0000
DRB1*09	0 (0)	1.1 (12)	0.3778 "0.02220 to 6.428"	0.6177	0.8680
DRB1*10	0 (0)	0 (1)	3.184 "0.1288 to 78.68"	1.0000	1.0000
DRB1*11	9.8 (11)	5.8 (63)	1.748 "0.8921 to 3.424"	0.1020	0.3642
DRB1*12	1.8 (2)	1.0 (11)	1.757 "0.3844 to 8.031"	0.3515	0.5543
DRB1*13	4.5 (5)	9.3 (101)	0.4502 "0.1794 to 1.130"	0.0835	0.3642
DRB1*14	0.9 (1)	2.8 (31)	0.3031 "0.04096 to 2.243"	0.3548	0.5543
DRB1*15	10.7 (12)	11.0 (119)	0.9630 "0.5137 to 1.806"	1.0000	1.000
DRB1*16	0 (0)	1.2 (13)	0.3495 "0.02062 to 5.922"	0.6250	0.8680
DQA1*01:01	20.5 (23)	14.1 (152)	1.568 "0.9607 to 2.558"	0.0914	0.3642
DQA1*01:02	10.7 (12)	20.7 (223)	0.4579 "0.2471 to 0.8486"	0.0089	0.2225
DQA1*01:03	4.5 (5)	2.2 (24)	2.044 "0.7642 to 5.469"	0.1849	0.4622
DQA1*02	17.0 (19)	12.8 (138)	1.386 "0.8198 to 2.342"	0.2401	0.5002
DQA1*03	15.2 (17)	20.7 (223)	0.6829 "0.3992 to 1.168"	0.1755	0.4622
DQA1*04	2.7 (3)	2.2 (24)	1.204 "0.3567 to 4.065"	0.7358	0.9158
DQA1*05	29.5 (33)	21.2 (228)	1.550 "1.006 to 2.387"	0.0546	0.3412
DQB1*02	26.8 (30)	22.5 (242)	1.258 "0.8083 to 1.957"	0.3443	0.5543
DQB1*03	33.9 (38)	34.2 (368)	0.9852 "0.6531 to 1.486"	1.0000	1.000
DQB1*04	3.6 (4)	2.9 (32)	1.206 "0.4185 to 3.475"	0.7693	0.9158
DQB1*05	20.5 (23)	14.9 (161)	1.465 "0.8994 to 2.388"	0.1313	0.4103
DQB1*06	15.2 (17)	24.2 (260)	0.5602 "0.3282 to 0.9564"	0.0342	0.3375

Table 3-3: HLA gene frequencies in Cohort 2

HLA-DR and HLA-DQ gene frequencies in Cohort 2, OA patients (2n = 48) compared with controls (2n=1074) [118]					
HLA type	Patients	Control	Odds Ratio with "Confidence Interval "	p	p _c
	% (n)	% (n)			
DRB1*01	14.6 (7)	12.5 (135)	1.188 "0.5221 to 2.701"	0.6572	0.9894
DRB1*03	20.8 (10)	15.3 (165)	1.450 "0.7083 to 2.967"	0.3093	0.7732
DRB1*04	16.7 (8)	20.1 (217)	0.7899 "0.3643 to 1.712"	0.7124	0.9894
DRB1*07	22.9 (11)	12.8 (138)	2.016 "1.005 to 4.047"	0.0513	0.1889
DRB1*08	4.2 (2)	3.5 (38)	1.185 "0.2773 to 5.067"	0.6874	0.9894
DRB1*09	0 (0)	1.1 (12)	0.8763 "0.05109 to 15.03"	1.0000	1.000
DRB1*10	0 (0)	0 (1)	7.385 "0.2967 to 183.8"	1.0000	1.000
DRB1*11	10.4 (5)	5.8 (63)	1.866 "0.7140 to 4.877"	0.2064	0.645
DRB1*12	0 (0)	1.0 (11)	0.9534 "0.05533 to 16.43"	1.0000	1.000
DRB1*13	6.3 (3)	9.3 (101)	0.6422 "0.1960 to 2.104"	0.6146	0.9894
DRB1*14	2.1 (1)	2.8 (31)	0.7159 "0.09561 to 5.360"	1.0000	1.000
DRB1*15	2.1 (1)	11.0 (119)	0.1707 "0.02333 to 1.250"	0.0529	0.1889
DRB1*16	0 (0)	1.2 (13)	0.8106 "0.04746 to 13.85"	1.0000	1.0000
DQA1*01:01	16.7 (8)	14.1 (152)	1.213 "0.5570 to 2.642"	0.6716	0.9894
DQA1*01:02	2.1 (1)	20.7 (223)	0.0811 "0.0111 to 0.5920"	0.0003	0.0075
DQA1*01:03	4.2 (2)	2.2 (24)	1.902 "0.4362 to 8.296"	0.3066	0.7732
DQA1*02	22.9 (11)	12.8 (138)	2.016 "1.005 to 4.047"	0.0513	0.1889
DQA1*03	16.7 (8)	20.7 (223)	0.7632 "0.3522 to 1.654"	0.5867	0.9894
DQA1*04	2.1 (1)	2.2 (24)	0.9309 "0.1232 to 7.032"	1.0000	1.0000
DQA1*05	35.4 (17)	21.2 (228)	2.035 "1.106 to 3.743"	0.0303	0.1889
DQB1*02	35.4 (17)	22.5 (242)	1.885 "1.026 to 3.466"	0.0523	0.1889
DQB1*03	39.6 (19)	34.2 (368)	1.257 "0.6952 to 2.272"	0.4421	0.9894
DQB1*04	2.1 (1)	2.9 (32)	0.6928 "0.09263 to 5.182"	1.0000	1.0000
DQB1*05	16.7 (8)	14.9 (161)	1.134 "0.5212 to 2.468"	0.6833	0.9894
DQB1*06	6.3 (3)	24.2 (260)	0.2087 "0.0643 to 0.6774"	0.0026	0.0325

Statistically significant increased frequencies are indication of disease susceptibility whereas decreased frequencies are interpreted as disease protection. Both the OA and failed implant group had protective alleles in common (DQA1*01:02 and DQB1*06), whereas DRB1*01 was specific to OA predisposition and DQA1*05 was specific for the metal hip implant failure in this cohort of patients. The summary of these findings depicted in Fig 3-3. Genetic association in multi-factorial diseases such as OA often produce small OR values (1.2 to 2.0), because of large number of alleles involved conferring small risk that combined with environmental factors confers a greater range of susceptibility. Taking this into consideration predisposing alleles showed considerably large OR values; DQB1*01 = 1.7 and DQA1* 05 = 2.035 (Table 3-2 and 3-3).

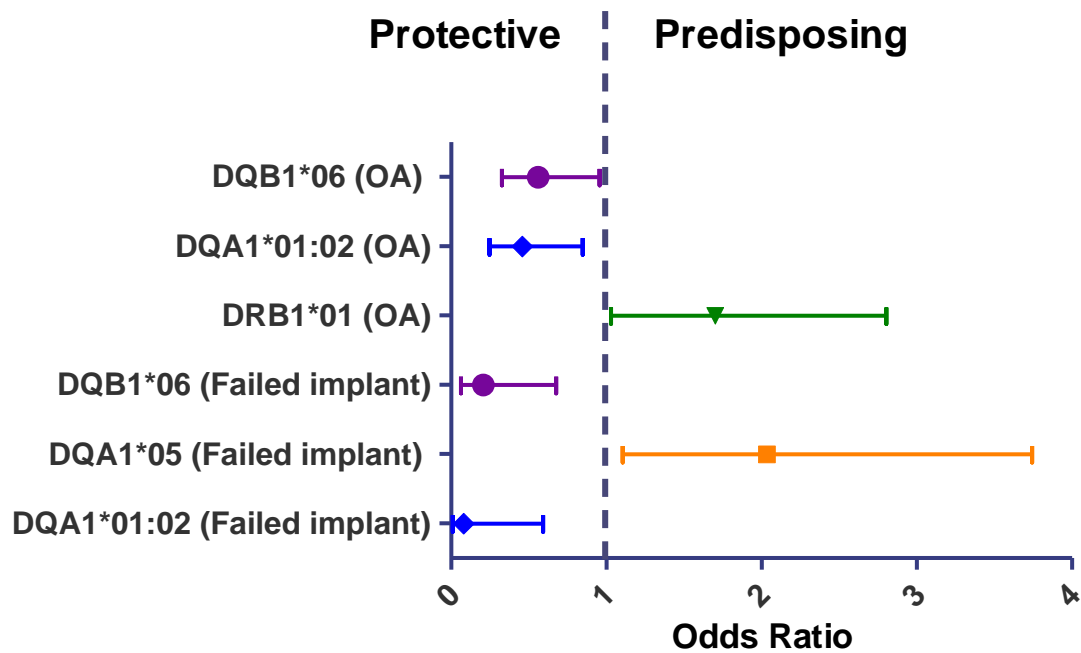


Figure 3-3: Odd ratios for MHC class II gene expression

A forest plot depicting Odd Ratios calculated for patient's MHC class II allelic variation versus control population. "OA" denotes total study population (Cohort 1) of Osteoarthritis patients. "Failed implant" denotes (Cohort 2) patients with failed metal implant undergoing revision operation. Statically significant differences plotted with 95% CI. OR < 1 indicating protective effect, OR > 1 indicating Predisposing effect.

Retrospective assessment of statistical power in the study of HLA association with implant failure was conducted for “worst case scenario” and “best case scenario” to assess effect size in this population.

Worst case scenario: The HLA allele with lowest frequency in controls was DRB1*12, allele frequency with 1.0 %. The statistical power for a range of odds ratios given that this sample size of controls was $2n = 1074$ and sample size of cases was $2n = 48$ (odds ratio considered as the effect size in a case-control study).

Table 3-4: Effect size calculation for worst case scenario

Allele frequency in controls (% , [n])	Allele frequency in patients (% , [n])	Odds ratio	Statistical power
0.01 [11]	0.02 [1]	2.1	0.0816
0.01 [11]	0.04 [2]	4.2	0.3440
0.01 [11]	0.08 [4]	8.8	0.7490
0.01 [11]	0.10 [5]	11.2	0.8518
0.01 [11]	0.17 [8]	19.3	0.9803

Best case scenario: The HLA allele with highest frequency in controls was DQB1*03 allele frequency with 34.2%.

Table 3-5: Effect size calculation for best case scenario

Allele frequency in controls (% , [n])	Allele frequency in patients (% , [n])	Odds ratio	Statistical power
0.34 [365]	0.52 [25]	2.1	0.6654
0.34 [365]	0.56 [27]	2.5	0.8352
0.34 [365]	0.69 [33]	4.3	0.9984
0.34 [365]	0.83 [40]	9.1	1.000

Statistical power increases with increasing sample size, increasing allele frequency and increasing effect size (odds ratio). The sample size was fixed and the tables (Table 3-4 & Table 3-5) above shows statistical power for two extreme allele frequencies for a range of odds ratios. It is clear that for the worst case scenario where the allele frequency is very low, only associations with unrealistic odds ratios (11.2) could reach statistical significance with 85% study power (Table 3-4).

In the best case scenario for the HLA allele with the highest frequency in controls, an association with an odds ratio of 2.5 or higher would reach statistical significance. Thus, for the range of allele frequencies, the minimum odds ratio would have to be 2.5 for an association to reach statistical significance. For any allele other than the one with the highest frequency, it has to be greater than 2.5. This equates to number of alleles in patients that are required, $n = 27$ with 83 % study power (Table 3-5).

3.4 Discussion

Only a small proportion of hip prostheses progress to implant failure. In the Norfolk cohort the same type of implant was used for arthroplasty by the same set of surgeons of which the majority were successful. The failure rate for most MoM implants is approximately 9.5% at 6 years follow-up but was 24.6% for the Ultima[®] THR TPS. However the Ultima performed well in other clinical centres (Richard Farrar, personal communication). This implies that host-related determinants may cause an aberrant immune response in Norfolk cohort.

No clear HLA association with OA has been documented previously apart from -DR2 (*15/*16). In this study an increased frequency of HLA-DRB1*01 was observed in OA group. This might be attributed to the presence of other arthropathies. HLA-DRB1*01 have been reported to increase in RA. And DRB1 is known to be the principal locus contributing to RA development. Although RA patients were excluded from recruitment procedure, subclinical RA might be present in some patients. RA presents itself as a co-morbidity in some of the OA patients , but there was no observed increase in the frequency of HLA-DRB1*04, which is the HLA type primarily associated with RA [121].

The comparison of HLA type frequencies between Cohort 2 Patients (failed implants) and controls revealed several significant differences. HLA-DQA1*05 is present at increased frequency in failed patients. HLA-DQA1*05 includes both HLA-DQA1*05:01, associated with HLA-DRB1*03, and HLA-DQA1*05:05 associated with HLA-DRB1*11 [122]. Both HLA-DRB1*03 and HLA-DRB1*11 were present at higher frequencies in Cohort 2 Patients than in controls but the differences were not significant. The frequencies of HLA-DRB1*07, -DQA1*02 and -DQB1*02 were present at increased

frequency in Cohort 2 patients than in controls; these HLA types occur in strong association with each other (HLA-DQB1*02 are also associated with HLA-DRB1*03). This represents an increase in the presence of this haplotype which is an indication of biological link in failed cohort.

The frequency of differences identified was not significant following correction of p values for the number of comparisons. However, the most striking differences in HLA frequencies between Cohort 2 Patients (failed implants) and controls are those of HLA-DQA1*01:02 and HLA-DQB1*06, the decreased frequencies of which remain significant following correction. HLA-DRB1*15 e DQA1*01:02 e DQB1*06 occur together as a haplotype in the UK and other populations [123]. There was only one instance of HLA-DRB1*15 in Patient Cohort 2 (2.1%) whereas the frequency in controls is 11.0%, which suggests that this HLA type or haplotype might be protective against implant failure. HLA-DQB1*06 is also associated with HLA-DRB1*13 in the UK and is also present in patient Cohort 2 at a reduced frequency compared with controls. But whilst HLA-DRB1*15 is strongly associated with HLA-DQA1*01:02 e DQB1*06:02 in the UK, HLA-DRB1*13 it is generally found associated with HLA-DQA1*01:02 and found with a variety of different HLA-DQB1*06 alleles e.g. HLA-DQB1*06:03 and -DQB1*06:09. The results showed that DQA1*01:02 and DQB1*06 were decreased in frequency in the OA cohort suggesting a protective effect of these alleles. This may be a unique finding in OA, as it has not been previously reported.

The general UK distribution of allele DQA1* 01:02 is 18.11% (n =1245, Dr Colin Brown, personal communication) whereas it was 2.1 % in our failed cohort. This data is agreeable with current analysis where there is a significant reduction of this allele in failed cohort compared to controls of Norfolk. There is no data available for this allele in other geographical regions of the UK. It would be a great interest to compare DQA1*01:02

frequency and correlation to both failed and survived implants in other parts of the UK. Regional comparisons could help to establish if high rate of failure is due to regional bias in Norfolk population where this allele is expressed in significantly low frequency in failed groups.

On the other hand, UK distribution of allele DQB1*06 is 1.21% (n = 132119, Dr Colin Brown, personal communication) whereas it was 6.3% in failed cohort which suggesting an increase in frequency of this allele in failed group. This contradicts the current analysis where decreased allele frequency was observed in failed groups compared with control group of healthy Norfolk population. This highlights the fact that Norfolk group in general shows very high frequency of DQB1*06 allele compared to UK population. This allele may not be related to the hip implant survival hence both survived and failed groups show high frequency in our study compared to rest of the UK.

HLA-DQA1*05 showed a higher prevalence in the failed implant group. This allele has also been recently reported as predictive of non-responsiveness to anti-TNF- α treatment in RA patients, suggesting anti-TNF α therapy is unable to control inflammation within this group of patients [124]. A similar situation may exist in inflammation caused by metal wear debris. By comparison, frequencies of HLA-DRB1*15, -DQA1*01:02 and -DQB1*06 are decreased in the failed implant group suggesting a “protective” effect.

These phenotypes were also protective in Cohort 1, implying that it might have an overall protective effect in inflammation. In the failed implant group this phenotype stood up to multiple testing correction, which is stronger evidence for a “protective” association. The HLA-DRB1*15, -DQA1*01:02 and -DQB1*06 haplotype has been shown to be “protective” against type 1 diabetes [125], whilst it is a susceptibility factor for multiple

sclerosis [126]. DRB*15 allele is also shown to be a susceptibility factor for OA [112] [115] however frequency of associated DQ alleles have not been reported before.

Genome-Wide-Association Studies (GWAS) are utilised to investigate disease association with HLA genes and non-HLA genes. Nakajima *et al* reported two single-nucleotide polymorphism (SNPs) that are associated with knee OA [127]. These variants are in the region containing HLA class II/III genes, namely rs7775228 and rs10947262 in Japanese subjects (n~4800). These two SNPs sequences are located between the upstream region of HLA-DQA2 and HLA-DQB1 suggesting OA is an immunological disorder. However, Shi *et al* studied Han Chinese and Australian populations in knee OA for the same SNP association demonstrating that there was no disease association between the two SNPs and knee OA in either population [128]. Another large scale replication study was unable to show any association of these two SNP regions in European Caucasian OA populations [129].

The discrepancy seen in different reports might be due to large Linkage Disequilibrium in different populations of these genes. Analysis of the Japanese data by Valdes *et al* showed that Japanese populations have a high frequency of protective haplotype (DRB1*15:02 e DQA1*01:03 e DQB1*06:01) compared to European populations [129]. This might explain failed repeat experiments in different populations. Even though GWAS is an accurate method for gene association studies of genetic contribution to disease susceptibility it is limited to looking at a few SNPs at a time. HLA typing produces more comprehensive outcomes generally.

The results reported here indicate that there are differences in HLA class II frequencies in the Norfolk Ultima cohort compared to controls especially in “protective” alleles of the failed implant group. However analysis of greater patient numbers and different

populations to compare these results might help to achieve conclusive answers. The findings of this study need to be confirmed in another MoM cohort. Achieving a larger cohort size was not possible with Ultima hence this prosthesis was discontinued in 2005 and many patients have already been revised since. The number of patients who still have an Ultima *in situ* is very limited.

HLA-DQA1*01:02 e DQB1*06:02 haplotype showed strong under-representation in the current study. Further studies can focus on functional roles of these alleles in metal hip implant failure. These variants might be involved in regulatory functions and in the absence of given alleles, immune response might be overwhelmed with metal ions and resulting in aberrant immune reaction. A follow up study could be conducted by recruiting patients with and without given haplotype and metal processing functions of immune cells can be assessed via delayed type hypersensitivity for antigen specific regulation, such as demonstrated in lung transplantation patients [130, 131].

Each MHC allele has a distinct peptide binding motif which favours certain amino acids at particular regions in their sequence (anchor residues). MHC binding motifs for metal-protein complexes can be identified for under or over represented variants by nucleotide sequencing of MHC molecules. Matching amino acid sequences can then be determined by MHC-II binding predictions. MHC binding assays shown to identify potential immunogenic motifs [132, 133] therefore metal haptens for these motifs could be investigated additionally. Peptide bound HLA molecules can be identified by biochemical analysis by elution of MHC+protein complexes. Antigen loading and presentation can be shown functionally to see if these specific MHC molecules have a role in T cell expansion and antigen specific clone generation for epitope specificity. Phenotype of the functional cell types involved and immunogenic epitopes could be determined using combination of these approaches in future studies.

HLA type and disease association have been long reported however there are no reports of HLA type of patients with failed MoM implants. Metal ions are small molecules and may be acting in a similar fashion to other small molecules such as drugs. Small molecule interactions with MHC class I alleles are demonstrated in various drug treatments; HLA-B* 57:01 for abacavir [134], HLA-B*15:02 e –A*31:02 for carbamazepine [135] and HLA-B*58:01 for allopurinol hypersensitivity [136], all of which are MHC class I alleles. More studies are needed to identify HLA type and molecular interactions with metals in failed MoM cohorts. It should perhaps include class I alleles too. This can be used as a screening process before deciding on choice of implant type.

3.5 Summary

This study investigated the association of metal implant failure and polymorphism of MHC class II molecules. The analysis of data identified under represented alleles in patients with failed MoM implants namely HLA-DQA1*01:02 and HLA-DQB1*06. Not having these alleles in the germline might be a confounding factor in metal hip implant failure. These molecules might be involved in regulatory mechanisms of immune cells such as regulatory T cell education. There is no HLA data available at present for other centres where Ultima implants were used. Comparing HLA frequency with implant survival rate across different part of the country would help to understand if the Ultima failure was HLA associated or other confounding factors involved, perhaps not all biological. Larger and further studies are required to determine frequencies in failed implant patients and to elucidate functional role of these alleles.

4 CHAPTER 4: Investigation of immune parameters in metal hip implant patients

4.1 Introduction

The metal sensitivity seen in MoM THR patients is thought to be caused by reactivity of immune cells to metal particles/ions. Many different cell types are involved in the immune reaction process as detailed in Chapter 1. In the reaction to metal implant wear debris, high levels of monocytic and lymphocytic infiltration have been observed histologically in the peri-prosthetic tissue, resulting in ALVAL [56, 58, 137]. It is postulated that metal particles elicit phagocyte responses of monocytes and dendritic cells initially which then these cells involved in recruitment of adaptive immune cells (T or B lymphocytes) into site of corrosion.

Aberrant cell counts are observed in several conditions such as autoimmune diseases, viral infections and malignancies. A comprehensive immunophenotyping permits to find out if there is also any alteration of these immune cell's composition in metal implant failure. To investigate phagocytes and lymphocytes, peripheral whole blood was assayed using a 18 parameter flow cytometry for each patient (Table 4-1) consisting of three panels (Table 4-3). The first panel identifies B cells (CD19+HLADR+) and T cells (CD3, CD4, CD8) plus their activation status (HLADR) and commitment to secondary lymph organ homing (CD62L) (Fig 4-1). Cell surface CD62L expression by T cells was analysed as this protein facilitates recirculation between blood and lymph nodes, which is important in immune surveillance and therefore timely responses to challenge. Naïve and memory T cells are CD62L+ whereas effector cells are CD62L- [138]. Immune activation correlates with an increase in HLADR expression by memory T cells, while naïve T cells express HLADR only following antigenic stimulation.

The second panel defines monocytes in detail with their involvement in metal implant failure well documented [139-141]. They readily uptake metal wear debris as demonstrated in Chapter 5 and by others [71, 142]. Macrophages are also involved in the activation of lymphocytes through antigen presentation and release of inflammatory cytokines that mediate osteoclast differentiation and maturation. Increased osteoclastogenesis results in implant loosening which is the lead cause of implant failure. Investigation of monocyte subsets was conducted according to the nomenclature established by Zeigler-Heitbrock *et al* [143-145]. Peripheral monocytes are divided into three groups (Fig 4-2);

- 1) CD14+CD16- classical (inflammatory) monocytes
- 2) CD14-CD16+ non-classical (resident) monocytes
- 3) CD14+CD16+ intermediate (transitional) monocytes

The expression of HLADR was also utilised for monocyte identification as they all express high levels of HLADR. Additionally, expression of migration (CX3CR1), activation (CD86) and maturation (CD83) markers in these myeloid lineage cells were studied (Table 4-1). CD86 and HLADR expression are upregulated upon Co/Cr metal exposure *in vitro* [146]. CD86 is a co-stimulatory molecule expressed by APCs that works in tandem with CD80 to activate T cells. Upregulation of these molecules is indicative of APC activation. After activation, the myeloid cells mature to become effector cells; CD83 is a marker for maturation and involved in cell-to-cell interaction during antigen presentation. Interferon- α mediated antigen presentation, T cell proliferation and phagocytosis were demonstrated by CD14+CD83+ cells and these cells were able to stimulate memory responses [147].

De novo activation of lymphocytes requires DCs. Even though these cells are rare in blood and tissues, they are very potent APCs. DCs are often overlooked in metal implant failure

with very few reports showing DC presence in periprosthetic tissue [148]. This might be due to their scarcity plus difficulty of determining specific markers for these cells. DC response to polyethylene wear particles has shown that these particles cause increased MHC II expression and IL-12 production, which are hallmarks of DC activation [149]. In blood, DC are divided into two main groups, myeloid DC (mDC) and plasmacytoid DC (pDC). They both represent heterogeneous group of cells leading to further subdivisions. mDCs are mainly involved in T cell activation, produce large amounts of IL-12, drive Th1 differentiation and CTL responses. On the other hand pDCs seem to be involved mainly in viral infections and produce type-I interferons. Four different subtypes of DCs were investigated in the current study (Fig 4-3).

- 1) Myeloid CD11c+
- 2) Myeloid CD1c+
- 3) Plasmacytoid CD123+
- 4) Plasmacytoid CD303+

The role of DCs and other APCs in metal implant failure is unknown. Therefore antigen presenting cells along with B and T cells were phenotyped in failed implant patients and compared to patients with well-functioning *in situ* implant.

Table 4-1: Immunophenotyping of PBMCs in whole blood

	Target antigen	Cellular expression in peripheral blood	Function
1	CD3	T cells	Associates with TCR and involved in signal transduction
2	CD4	T subset, monocytes	MHC class II co-receptor, T cell differentiation/activation
3	CD45	Haematopoietic cells apart from platelets and erythrocytes	Enhanced TCR and BCR signalling
4	HLA-DR	APC, Tact	Presentation of peptides to CD4+ T lymphocytes
5	CD303	pDC	Type II C-type lectin. Endocytic receptor; mediating antigen uptake and presentation. Inhibit IFN- α production.
6	CD11b	Myeloid cells, NK	Binds CD54, fibrinogen and iC3b
7	CD62L	B, naïve and memory T, monocytes, granulocytes, NK	CD34, GlyCAM and MAdCAM-1 receptor Leukocyte homing, tethering and rolling
8	CD19	Immature B cells	Complex with CD21 and CD81, BCR co-receptor. B cell activation/differentiation.
9	CD14	Monocytes and granulocytes (low)	Receptor for LPS/LBP
10	CX3CR1	NK cells, CD8 cells, DC, monocytes	Receptor for Fractalkine on endothelial cells. Leukocyte migration and adhesion.
11	CD86	Monocytes, DC, Bact Tact cells	Binds to CD28, CD152, T cell costimulation
12	CD83	Bact, Tact, DC	Marker for DC maturation, may play a role in cell-cell interaction during antigen presentation
13	CD16 α	Neutrophils, monocytes, NK	Component of low affinity Fc γ III receptor, phagocytosis and ADCC
14	Lin	CD3, CD14, CD16, CD19, CD20 & CD56	Peripheral blood DCs and basophils can be distinguished from other leukocytes by their lack of Lin antigen expressions
15	CD1c	mDC, B subsets	MHC Class I-like molecule, associated with β -microglobulin. Has specialised role in presentation of non-protein antigens
16	CD11c	DC, myeloid cells, NK, B, T subsets	Binds CD54, fibrinogen and iC3b
17	CD123	Lymphocyte subsets, basophils, m ϕ . DC	IL-3 receptor α -chain
18	CD8	Cytotoxic T cells, NK, DC subset	Co-receptor for MHC Class I. T cell differentiation and activation

Bone metabolism is a dynamic process and bone cells rely on complex signalling pathways involving cytokines, hormones and growth factors to maintain healthy bone structure. Any disruption of bone metabolism may result in conditions such as periprosthetic loosening leading to implant failure. Investigation of bone-related soluble biomarkers in our cohort of patients may aid to understand this complex condition. Cellular composition and cytokine profile have been shown in revised hip implant tissue with *in situ* hybridisation, demonstrating high T lymphocyte and macrophage infiltrates expressing IL-6, IL-1 and TNF- α mRNA [150]. However, various other cytokines have not been studied in metal implant failure.

The effects of cytokine signalling work in two different manners;

1) Pleiotropic: where each cytokine acts on multiple targets

2) Redundant: where several cytokines respectively elicit similar cellular response.

Therefore, investigating multiple cytokines collectively may be more informative than individually in immune dysregulation. Table 4-2. details important cytokines and their biological function in bone metabolism. These cytokines were identified as significant soluble mediators which may potentially affect bone turnover in metal implant patients.

Table 4-2: Soluble immunological mediators affecting bone turnover

Analyte	Producer cells	Actions	Role in bone metabolism
GM-CSF	mφ, T cells, mast cells, NK cells, endothelial cells and fibroblasts	Stimulates stem cells to produce monocytes and granulocytes especially neutrophils.	Found high levels in arthritic joints. Regulates mononuclear osteoclast fusion and activation [151].
IFN-γ	T cells, NK and NKT cells	Activates mφ and inhibit viral replication directly, promotes Th1 cell differentiation, suppress Th2, Ig class switching.	Inhibits RANKL-induced osteoclastogenesis, Suppresses osteoclast formation by degrading RANK adaptor protein TRAF6 [152].
IL-10	Monocytes and CD4+ T cells, T regs, activated T cells and B cells	Down regulates mφ activity and activates B cells and antibody production. Dampens NK cell action.	Anti-inflammatory cytokine. Most haematopoietic cells express IL-10R. Immunoregulatory, blocks NF-κB activity.
IL-1β	mφ, epithelial cells	T cell and mφ activation, induce fever.	Proinflammatory cytokine associated with cartilage degeneration [153]. IL-1 receptor antagonists treatment slows down bone erosion [154].
IL-6	T cells, mφ and endothelial cells, osteoblasts, stromal cells	T and B cell growth, induction of fever, stimulates acute phase protein production. Effects are interrelated with IL-1, THF and PTH.	Enhances bone resorption by increasing the pool of osteoclastic progenitors and their differentiation into mature osteoclasts [155]
Leptin	Adipose tissue secreted cytokine (adipokine)	Stromal cell, osteoblasts.	Mediator of metabolic homeostasis and joint remodelling. Stimulate osteoblast activity and proliferation [156, 157] and inhibits osteoclastogenesis.
RANKL	Osteoclasts, osteoblasts, activated T cells, DC, stromal and epithelial cells	Ligand for RANK which is mainly expressed on cells of myeloid lineage such as DC, pre-osteoclasts and osteoclasts.	Lymphocyte development and osteoclast differentiation/activation. Inhibition of osteoclast apoptosis. RANKL knock-out mice show severe osteopetrosis and loss of osteoclasts [75].
OPG	Osteoblasts and stromal cells	Decoy receptor for RANKL. Inhibits osteoclastogenesis by preventing RANK-RANKL interactions.	Blocks osteoclasts differentiation from precursor cells, prevents bone loss [158].
M-CSF	T cells, bone marrow stromal cells, osteoblasts, fibroblasts.	Stimulates growth of monocytic lineage cells.	M-CSF is necessary along with RANKL for the complete differentiation of osteoclastic precursors into mature osteoclasts [76].
TNF-α	Activated mφ, NK cells, T cells also non-haematopoietic cells.	Activation of many cells, cytotoxic, antiviral, pro-coagulatory and growth stimulatory effect. Potent bone-resorbing factor.	Osteoclast stimulating molecule, promotes RANKL production by stromal cells hence induce osteoclast formation indirectly [159].

MoM implants are made of around 60% Co, 30% Cr and 7% Mo. Even though these elements are required for biological functions, they are toxic at high concentration in biological systems [160, 161]. MoM THR patients are advised to have their Co-Cr levels checked periodically as increased ion levels could be a surrogate measure of *in vivo* device wear. MHRA issued an alert in June 2010 and updated this alert in June 2012 stating, “soft tissue reaction may be caused by metal wear debris”. MHRA highlighted the high failure rate with MoM THR and resurfacing and recommended annual monitoring of the hip using imaging and measurement of metal ion levels in the blood to determine whether a revision is needed in people with MoM hip replacement prostheses who have symptoms. The diagnostic positive cut off level for both Co and Cr is 7µg/l. Hart *et al* found this cut-off level to be useful in distinguishing failed versus well-functioning implants. They also reported that lowering cut of levels to 4.97 µg/l showed increased sensitivity but reduced specificity for identifying failed implants [162]. It is not certain if raised serum levels of metal ions are indicative of metallosis in the peri-prosthetic tissue. However De Smet *et al* found that serum Co and Cr levels in patients with metallosis were approximately ten times higher compared to patients without metallosis [163]. They also studied metal ion levels in joint fluid of revision patients. There was a good correlation between serum and joint fluid metal concentrations and implant failure. For practical reasons it is not always possible to assess metal ion levels of joint fluid, therefore monitoring serum levels serves as a pragmatic option for the clinical management of these patients.

This work aimed to investigate the immune status in the Norfolk cohort with a detailed characterisation of antigen presenting cells (monocytes, dendritic cells and B cells) plus T cells. Levels of soluble biomarkers such as cytokines and growth factors were tested. Correlation of these immune parameters with metal ions levels was examined.

4.2 Material and Methods

4.2.1 Immunophenotyping by Polychromatic Flow Cytometry

The frequency and composition of human leukocytes in the body can be used as an indicator of health or disease. These cells are monitored in patients by identifying their surface markers by immunophenotyping using flow cytometry. To investigate blood leukocytes in metal implant patients, three polychromatic flow cytometry panels were designed. Target molecules included subset-defining lineage-specific markers, co-stimulatory molecules, activation-associated markers, cytokine and chemokine receptors. These panels were specifically designed for the project and were adapted from a published protocol [164], which required extensive refinement, optimisation and validation. The immunophenotyping panels consist of three panels of 9 Abs each, i.e. 18 different parameters in total (Table 4-3). An absolute quantification protocol was also standardised for whole blood samples using the “Lyse-no-wash” method [165] which provides the exact cell number of interest in the sample by normalising cell readings to known amounts of bead count (equation 4-1). The flow cytometry panels that were developed for this study used minimally manipulated *ex-vivo* blood samples plus absolute counting beads, which is the gold standard in immunophenotyping.

Compensation is an integral part of multi-colour flow cytometry. It became apparent that compensation beads are more suitable than single colour cell controls due to the low level expression of some antigens in these panels. The OneComp beads were used for this purpose (eBioscience, Cat No: 01-1111-42).

Since multiple antibodies (Ab) in a single tube were used, an appropriate concentration of each Ab was determined by titration preliminary experiments to avoid non-specific binding. The second step was to test isotype-matched control Abs utilising the same

fluorochrome as the test antibody to assess background signals. Isotype control Abs were used at the same concentrations as the test Abs. Low background levels were confirmed before proceeding to staining study samples.

The functions of the markers investigated are detailed in Table 4-1. Details of the lasers, filters, and the long pass dichroic mirrors are shown in Table 4-3. Appendix 4-1. shows details of Abs used, suppliers and catalogue numbers plus isotype controls for these Abs.

Flow cytometry staining was carried out by adding appropriate amount of Ab to TruCOUNT™ tubes (BD, Cat No: 340334) followed by 100 µl of fresh EDTA-blood.

Tubes were centrifuged for 30 seconds, vortexed gently and left to incubate for 30 mins in the dark at 21°C for staining. Following Ab staining, erythrocytes were lysed by adding 0.5 ml of RBC Lysing Buffer (BioLegend, Cat No: 420301) and incubated 10 mins at 21°C.

Samples were acquired using BD FACS ARIA II. Events were threshold at 1,000 fluorescence units in CD45: PerCP-Cy5.5 channel to eliminate majority of debris. A minimum of 50,000 events were acquired in the monocytic/lymphocytic gate.

Equation 4-1: Absolute quantification of the cell events calculation

$$\frac{\text{number of events in cell gate}}{\text{number of events in beads gate}} \times \frac{\text{number of beads per pellet}^*}{\text{sample volume (ul)}} = \text{absolute count} \left(\frac{\text{cells}}{\text{ul}} \right)$$

*This value is found on the TruCOUNT Absolute Count Tube foil pouch label and might vary from lot to lot.

Table 4-3: Flow Cytometry configuration, filter settings and panel distribution

Instrument configuration, filter settings and panel distribution				
	Laser/Filter/ LP mirror	Panel 1	Panel 2	Panel 3
FL1	B 530/30 520LP	CD3:FITC	CX3CR1:FITC	Lin:FITC
FL2	B 585/42 556 LP	CD4:PE	CD86:PE	CD1c:PE
FL3	B 695/40 655 LP	CD45:PerCP- Cy5.5	CD45:PerCP- Cy5.5	CD45:PerCP- Cy5.5
FL4	B 780/60 735 LP	HLADR:PE-Cy7	HLADR:PE-Cy7	HLADR:PE-Cy7
FL5	R 660/20 N/A	CD303:APC	CD83:APC	CD11c:APC
FL6	R 730/45 710 LP	CD11b:AF700	CD16:AF700	CD11b:AF700
FL7	R 780/60 750 LP	CD62L:APC-Cy7	CD62L:APC-Cy7	CD62L:APC-Cy7
FL8	V 450/40 N/A	CD19: PacBlue	CD19: PacBlue	CD123:EF450
FL9	V 530/30 520 LP	CD8:PacOrg	CD14:V500	CD14:V500

Gating Strategy and Data Analysis

Flow cytometry standard (FCS) data files were manually curated and analysed according to the panel design and protocol (Table 4-3) using Kaluza[®] Flow Analysis Software, (Beckman Coulter, Inc). Representative gating strategies are shown in Figs 4-1 to 4-3. Events are displayed as “dot plot counter with density” for clarity to distinguish populations. Absolute cell numbers / μ l were calculated using equation 4-1 and results between clinical groups were compared using one way ANOVA (mean \pm SD) with Tukey post-hoc correction in GraphPad Prism5. Statistical significance was denoted to the symbols below throughout the document.

<u>Symbol</u>	<u>Value</u>	<u>Interpretation</u>
ns	$p \geq 0.05$	Not significant
*	$p \leq 0.05$	Significant
**	$p \leq 0.01$	Very significant
***	$p \leq 0.001$	Highly significant
****	$p \leq 0.0001$	Extremely significant

Identification of T and B cell subsets

At first PBMCs were identified according to their characteristically low side scatter profile and high CD45 expression with a polygonal gate constructed around the relevant populations (Fig 4-1 A). In this way, granulocytes with a high side scatter and low CD45 expression were excluded from further analysis. Beads were identified in the same cytograph through their inherent far red fluorescence intensity that falls in the PerCP-Cy5.5 channel and by their high side scatter; two characteristics that set them apart from either granulocytes or PBMCs. All subsequent subset identification was effected within

the PBMC gate. B cells were identified and gated by their CD19+HLADR+ surface expression and their numbers per μ l blood were evaluated within this gate (Fig 4-1 B). It was necessary to include CD3 as a T cell lineage-specific marker in the panel as CD4 and CD8 molecules are also expressed by non-T cells within the PBMC gate; T cells were identified as either CD3+CD4+ T helper cells (Th) or CD3+CD8+ cytotoxic T lymphocytes (CTL) and, relevant gates were constructed (Fig 4-1 C and D). CD3+CD62L+ and CD3+CD62L- T cells were gated for absolute cell counting (Fig 4-1 F). At the same time the activation status of CD3+ T cells present within peripheral blood was determined through their enhanced HLADR expression. CD3+HLADR+ T cells were selected (Fig 4-1 E) as an indicator of T cell stimulation. `

Identification of monocytes

HLADR molecules are highly expressed on monocytes hence they are the most abundant APCs. PBMC gating was followed by gating HLADR +ve events to identify monocytes (Fig 4-1 D). In peripheral blood, the low affinity Fc receptor, CD16, is found on natural killer cells, neutrophils and monocytes [166] . Neutrophils were excluded from analyses by gating on PBMC prior to defining membrane expression of surface antigens (Fig 4-2 A). CD14 is a receptor for LPS/LPB and the main lineage marker for monocytes. It is weakly expressed by granulocytes. Again the PBMC gate was used to first identify both CD14+HLADR+ monocytes. Also this gating strategy allowed the identification of transient monocytes CD14+CD16+HLADR+ (Fig 4-4 E). CD86 is involved in antigen presentation and T cell activation. CD86 expression of monocyte subsets were determined using dot plots CD16 vs CD86, (Fig 4-2 B) and CD14 vs CD86 (Fig 4-2 C).

DCs identification

DCs are rare cells in peripheral blood consisting of less than 1% of PBMCs. One of the current conventions of identifying these cells is to use a lineage marker (lin) to exclude other major cell populations (T/B/NK cells and monocytes) from analysis. Hence some DC markers are also expressed on non-DC populations. Therefore, this strategy identifies DCs as Lin-HLADR⁺ phenotype in blood (Fig 4-3 B). This strategy was utilised to assess total numbers of DCs with DC subsets identified as CD11c⁺ mDCs and CD123⁺ pDCs (Fig 4-3 D). CD1c is a MHC I class like molecule and highly expressed by mDCs. CD1c⁺ mDCs were also identified with this strategy. It was observed that all CD1c⁺ cells also express CD62L hence this double expression was utilised to identify this subset of DCs (Fig 4-3 E). Specific expression of CD303 identifies a subset of pDCs using this marker only. pDCs also express high levels of HLADR molecule. This double positive expression was utilised to identify this subset of DCs (Fig 4-3 C).

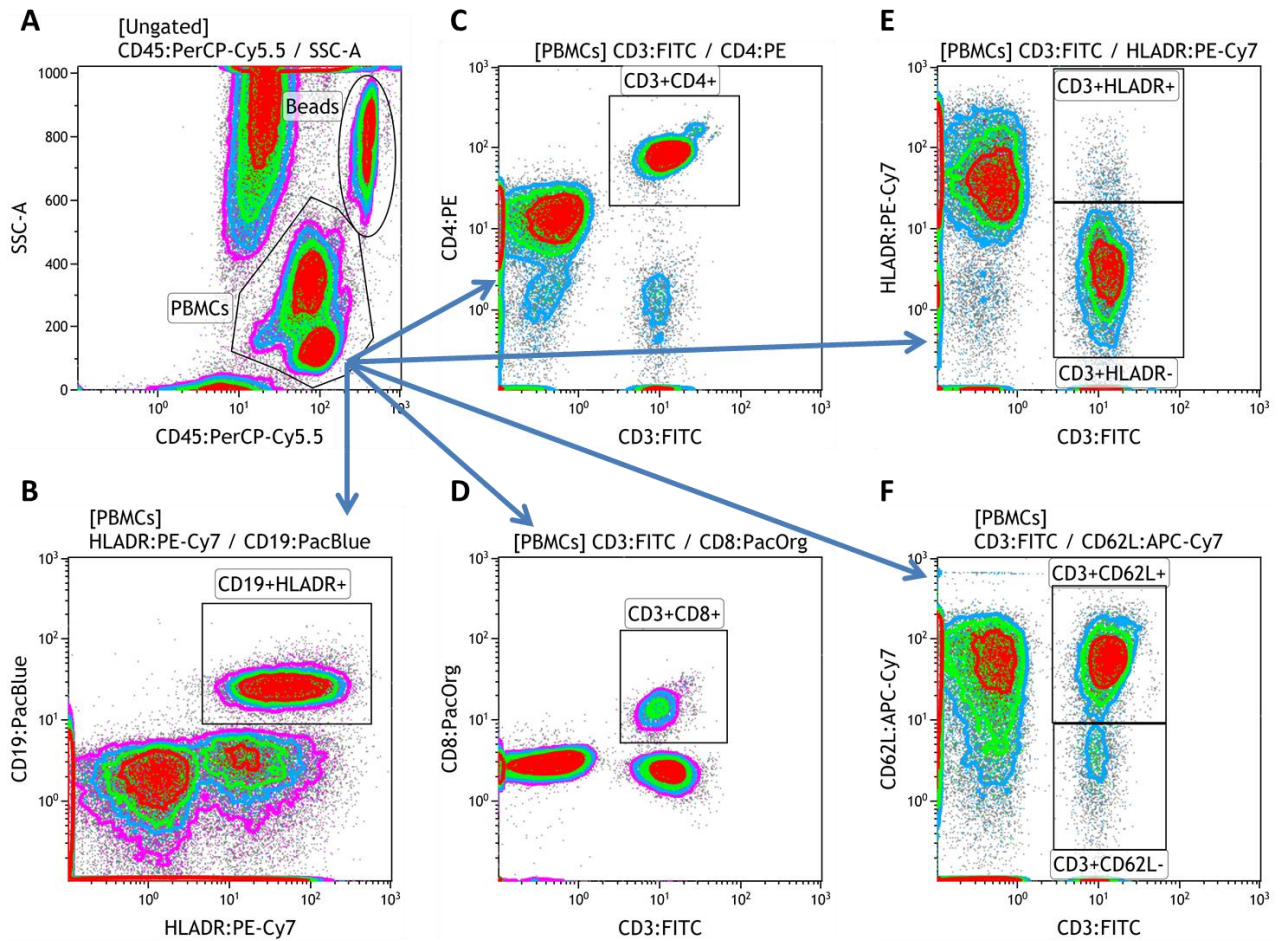


Figure 4-1: T and B cells gating strategy

Representative data of peripheral whole blood obtained from patients with/without metal hip implants. Blood was stained within an hour of phlebotomy and acquired subsequently. PBMC fraction was analysed using gating strategy below. Representative sample shown using pseudocolor bivariate dot plots. **A:** Ungated total events: cell events for CD45 (pan leukocyte lineage marker) vs SSC (indicative of granularity). This plot type permits distinguishing PBMCs from granulocytes, debris and counting beads (labelled as “Beads”). Subsequent cytographs are displayed within PBMCs gate. **B:** Identification of B cells are conducted by plotting events for CD19 (B cell-specific marker) expression versus HLADR positivity (highly expressed on APCs). **C:** CD4+ T cells identified by CD3 positivity (T cell-specific marker) and CD4 expression. **D:** CD8+ cells identified by CD3 vs CD8 positivity. **E:** Activated T cells are shown by CD3 vs HLADR expression (CD3+HLADR+). Non-activated T cell numbers are shown in the gate of CD3+HLADR-. **F:** CD62L positivity (L-selectin, lymph node homing marker for lymphocytes) used to distinguish naive (CD3+CD62L+) vs effector (CD3+CD62L-) T cells.

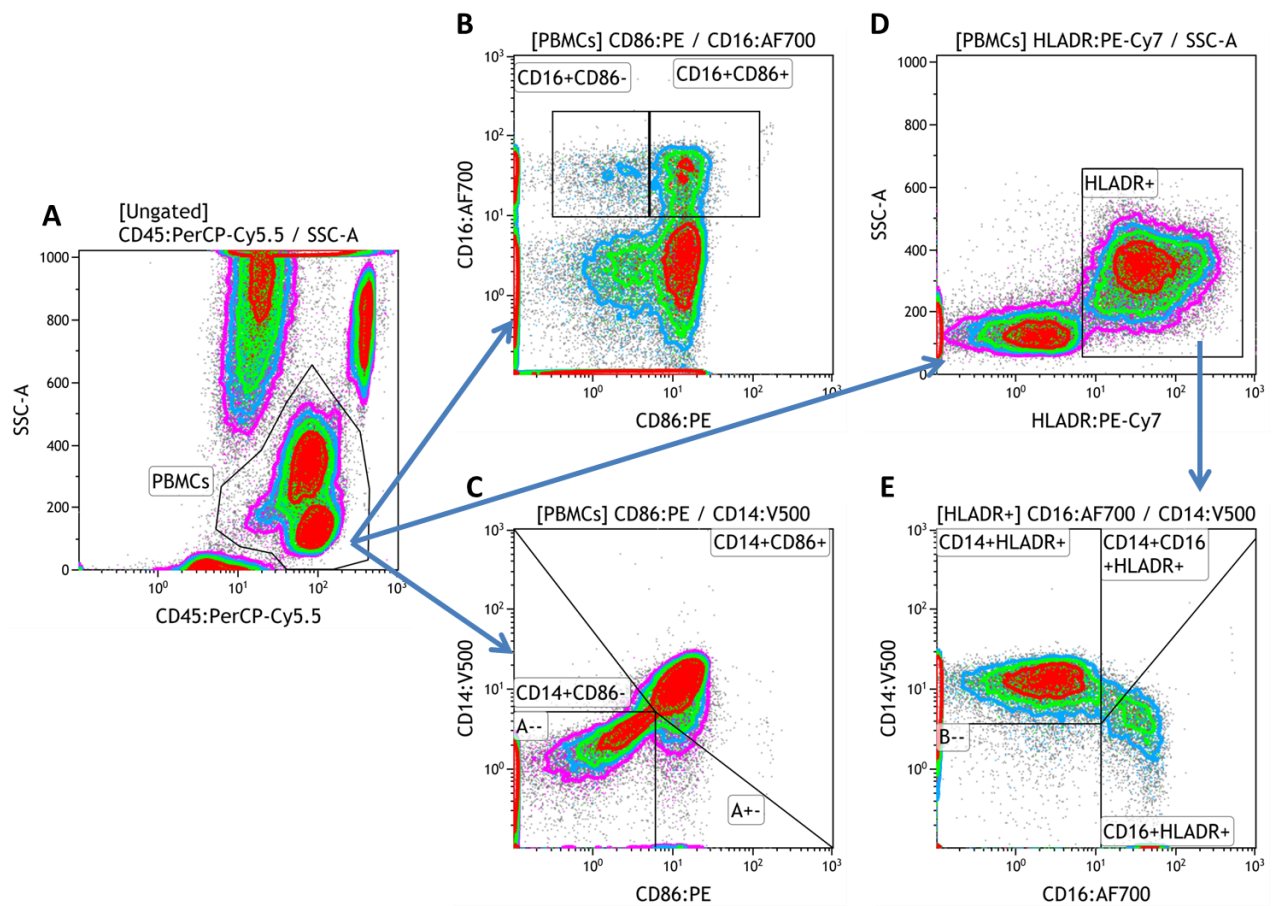


Figure 4-2: Monocyte gating strategy

Representative data of peripheral whole blood obtained from patients with/without metal hip implants. Blood was stained within an hour of phlebotomy and acquired subsequently. PBMC fraction was analysed using gating strategy below. Representative sample shown using pseudocolor contour bivariate dot plots.

A: CD45 (pan leukocyte lineage marker) vs SSC distinguishes PBMC population from other cell types and debris. Further plots are derived from the PBMC gate. **B:** CD86 expression on the CD16+ monocytes, CD86+ve and -ve events gated accordingly. **C:** CD86 expression on the CD14+ monocytes, CD86+ve and -ve events gated accordingly. **D:** pre-gating for high HLADR expression before sub-classification of monocyte subsets. **E:** monocytes segregated according to CD14 vs CD16 expression into either CD14+CD16- (classical monocytes), CD14-CD16+ (non-classical monocytes) or CD14+CD16+ (intermediate monocytes) gates.

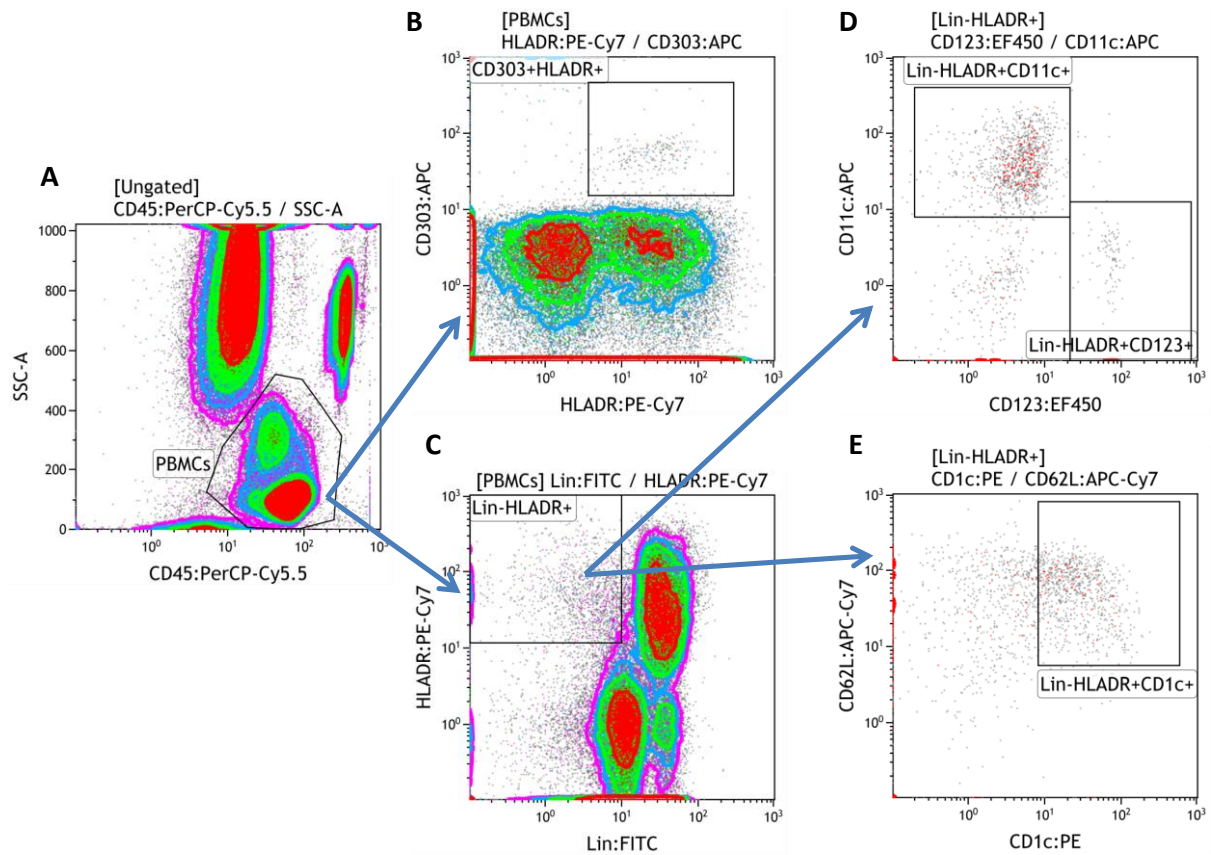


Figure 4-3: DC gating strategy

Representative data of peripheral whole blood obtained from patients with/without metal hip implants. Blood was stained within an hour of phlebotomy and acquired subsequently. PBMC fraction was analysed using gating strategy below. Representative sample shown using pseudocolor contour bivariate dot plots.

A: PBMCs identified utilising $CD45^{high}$ vs SSC^{low} characteristics. **B:** $CD303+$ alone identifies another subset of pDCs, directly derived from from PBMC gate **C:** $Lin-HLADR+$ gate donates all DCs. Lineage antibody is a combination of $CD3$, $CD14$, $CD19$, $CD20$ and $CD56$ markers and absence of this staining provides specificity of DC identification. **D:** $CD11c+$ mDCs and $CD123+$ pDCs determined within $Lin-HLADR+$ gate. **E:** $CD1c+$ DCs all displaying high levels of $CD62L$ in peripheral blood (Pre-gated in $Lin-HLADR+$).

4.2.2 Measurement of serum and SF cytokines

Soluble analytes were measured in serum and synovial fluid (SF) using a commercial kit in 10-plex format (Procarta Immunoassay kit, Affymetrix), according to the manufacturer's instructions. SF samples were centrifuged at 10,000 x g for 10 mins and the supernatants collected for assay. The kit utilises xMAP beads and Luminex technology. Briefly, xMAP (magnetic microspheres) which are internally labelled with red and infrared fluorophores with different intensity. Red laser excites both of these dyes which produce spectral signatures to locate the bead for a given analyte. Proteins of interest in test sample are captured by antibody coated beads followed by biotinylated detection of Ab. The sample is then incubated with a Streptavidin-PE conjugate, which is the reporter dye, and excited by the green laser. The digital signal generated from both red and green laser excitations are collected through photomultiplier tubes in Luminex200 instrument. Fig 4-4. demonstrates the details of experimental work flow. Luminex assays have a greater dynamic range of ~1-10,000 pg/ml than alternatives i.e. ELISA, MSD. Hence it was chosen as method of choice.

Serum and SF levels of GM-CSF, IFN- γ , IL-1 β , IL-6, IL-10, Leptin, M-CSF, TNF- α , OPG, RANKL were determined. All samples were assayed in duplicate. Data was generated using StarStation 3.0 software, (Applied Cytometry Systems). Median Fluorescence intensity (MFI) was determined for each analyte with concentration calculated using 5PI algorithm for the best curve fit, displayed as pg/ml. Serum versus SF read outs were compared with two-tailed student t-test using GraphPad Prism 5.0. Multivariate analysis was conducted in MATLAB, MATWorks, inc. The Matlab commands script was written by Dr Marianne Defernez, (Analytical Science Unit, IFR).

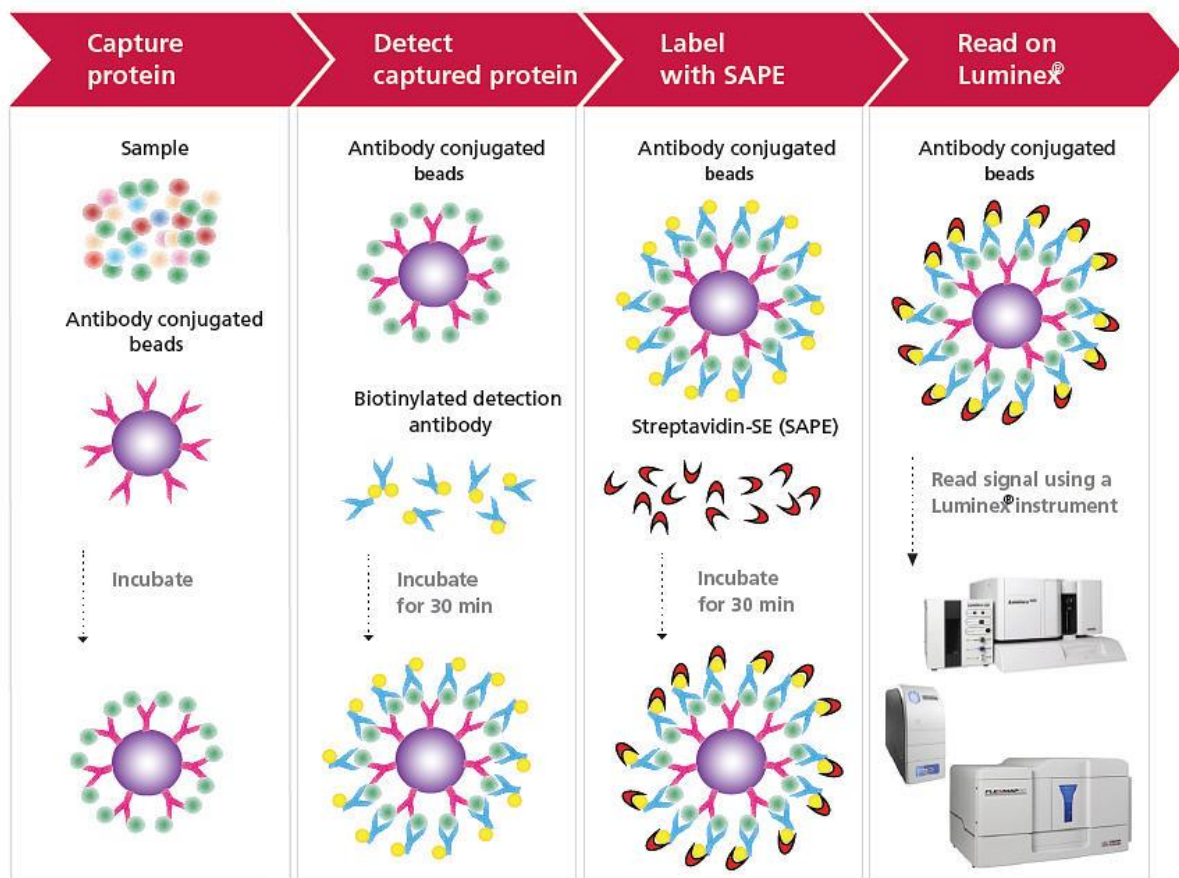


Figure 4-4: Schematic description of Luminex based assays

How Luminex based assays work. **Capture protein:** samples are incubated with magnetic beads overnight on a rocker. **Detect capture protein:** after a wash, biotinylated detection Ab is added and incubated for 30 mins. **Label with SAPE:** after a wash, reporter dye added to sample and incubated for 30 mins. **Read on Luminex:** after the final wash, beads are resuspended in read buffer and run at Luminex 200 instrument. Further details can be found at

(<https://www.panomics.com/products/multiplex-immunoassays/procarta-immunoassays/overview>)

Copyrights permission for the schema was granted from Procarta, Affymetrix , March 2014.

4.3 Measurement of serum metal ions

Serum samples were collected in Vacutainer Trace Element tubes (BD, 368380) and analysed by University Hospital of Wales, Cardiff. Serum levels of chromium and cobalt were analyzed using an Agilent 7700x Inductively Coupled Plasma Mass Spectrometer (ICP-MS), (Agilent Technologies UK LTD, Berkshire, UK). Samples, standards and quality control material were diluted 1 in 15 with diluent (0.1% EDTA, 0.01% Triton x100, 0.2% ammonia and 20ppb of germanium) as an internal standard. Aqueous standards were used for calibration. Cr was analyzed at mass 52 and Co at mass 59 with helium as a correction gas.

4.4 Results

The aim was to develop a rapid and sensitive assay which could be used during routine blood work to establish immune status of arthroplasty patients. Therefore a high content-high dimension, 18 parameter flow cytometry assay was developed and this assay was used to detect immune cell numbers and composition in these patients. Absolute cell numbers were calculated along with expression of activation and adhesion molecules using *ex-vivo* whole blood samples. Cytographs were manually curated. Immune cells first were subdivided into T cells, B cells, monocytes and DCs based on specific lineage markers thereafter expression of activation and adhesion molecules were investigated. Patients comprising the four study groups were stratified according to their clinical status detailed in Chapter 2. G1: Pre-implant, G2: Ultima Asymptomatic, G3: Ultima Symptomatic and G4: Other Symptomatic.

Immune cells composition

All four patient groups displayed normal absolute levels of CD3+CD4+ T cells, CD3+CD8+ T cells and CD19+HLADR+ B cells (Table 4-4) compared with standard blood counts of healthy individuals. There were no significant alterations between clinical groups when group means were compared (Fig 4-5 A, B and C) however a few individuals showed increased number of CD8+ T cells (Fig 4-5 B) in the Ultima Asymptomatic group. Further, T cell analysis revealed that HLADR expression by CD3+ cells was also increased in Ultima Asymptomatic groups. HLADR expression by T cell is an indication of their activation. Analysis of CD62L expression demonstrated that CD62L+ T cells were increased in Ultima Asymptomatic group compared with Ultima Symptomatic group. This shows expansion of a less polarised T cell, consisting of naïve and central memory T cell population in this group (Fig 4-5 E). On the other hand there were no significant

differences between clinical groups in effector T cell populations, CD3+CD62L- (Fig 4-5 F). No alterations of CD11b expression was observed between either cell type or clinical groups hence this parameter was excluded from further analysis.

Monocyte subsets were categorised into three groups; investigation of first category classical monocytes, CD14+HLADR+ (Fig 4-6 A) showed elevated numbers of these cells in the Ultima Asymptomatic group. Further the myeloid cell activation marker CD86 was utilised to investigate activation status of these cells. Although the Ultima Asymptomatic group had a slightly increased mean signal for this group, the result was not statistically significant compared with other groups (Fig 4-6 B). Analysis of the second monocytes subsets, non-classical monocytes, CD16+HLADR+ did not reveal any differences between clinical groups (Fig 4-6 C). There were also no alterations in CD86+ expression (Fig 4-6 D). A very similar picture was also present for the third monocyte subsets, intermediate, CD14+CD16+HLADR+. Cell numbers and activation status were comparable between the four clinical groups (Fig 4-6 E & F).

Reference values for classical monocytes are well established and in this study classical monocytes were within the normal range for all groups (Table 4-4) with the only exception being the Ultima Asymptomatic group. This group of patients had an elevated monocyte count above reference values which was statically significant compared to Ultima Symptomatic group ($p = 0.0170$). Non-classical and intermediate monocytes are emerging subsets therefore their reference values are not established. However, on average it is estimated that classical monocytes counts for around 90%, non-classical monocytes for 10% and intermediate monocytes consist of very small and variable percentage of total monocytes. The results of this study also reflect this proportional distribution above Fig (4-6 A, C & E).

There was very low or no detectable expression of CX3CR1 and CD83 by monocytes using *ex-vivo* samples in this study. Analysis of these markers was not possible on fresh non-manipulated blood.

Total dendritic cell population plus four different subsets were investigated. The mean total blood DC number was 29.6 ± 17.2 $\mu\text{l}/\text{cells}$ for all study groups. Table 4-4 details the average numbers for the individual groups. The results show that the total DC number was increased in the Ultima Asymptomatic group compared with the Symptomatic patients ($p = 0.0018$) (Fig 4-7 A). Detailed analysis of DC subsets revealed that this increase was due to CD1c+ DCs (Fig 4-7 B) whereas all other DC subsets displayed numbers within the normal range (Fig 7-4 C, D, E & F).

Overall immunophenotyping of this cohort of patients elucidated that immune cells investigated were within the normal range for all groups apart from Ultima Asymptomatic group. Specifically these alterations were confined to naïve/central memory T cells, classical monocytes and CD1c+ mDCs.

Table 4-4: Peripheral blood immune cell numbers in Norfolk cohort

Normal range of immune cell numbers compared with patient's results (mean \pm SD) stratified into clinical subgroups					
	Reference values (cells/ μ l) [100, 101]	Pre-implant (n = 15)	Ultima Asymptomatic (n = 17)	Ultima Symptomatic (n = 12)	Other Symptomatic (n = 12)
Th cells CD3+CD4+	500-1600	1014 \pm 372.3	951.6 \pm 425.8	639.0 \pm 188.9	772.3 \pm 392.5
CTL CD3+CD8+	300-900	360.5 \pm 189.6	535.8 \pm 456.2	255.2 \pm 180.7	256.1 \pm 106.4
B cells CD19+HLADR+	72-460	194.0 \pm 89.75	159.9 \pm 92.48	118.6 \pm 90.42	172.9 \pm 104.0
Monocytes CD14+HLADR+	150-600	417.9 \pm 133.3	631.6 \pm 348.6	394.8 \pm 203.2	346.7 \pm 176.7
Dendritic cells Lin-HLADR+	13-37 [167]	28.22 \pm 16.82	41.61 \pm 18.73	22.22 \pm 7.979	21.99 \pm 14.44

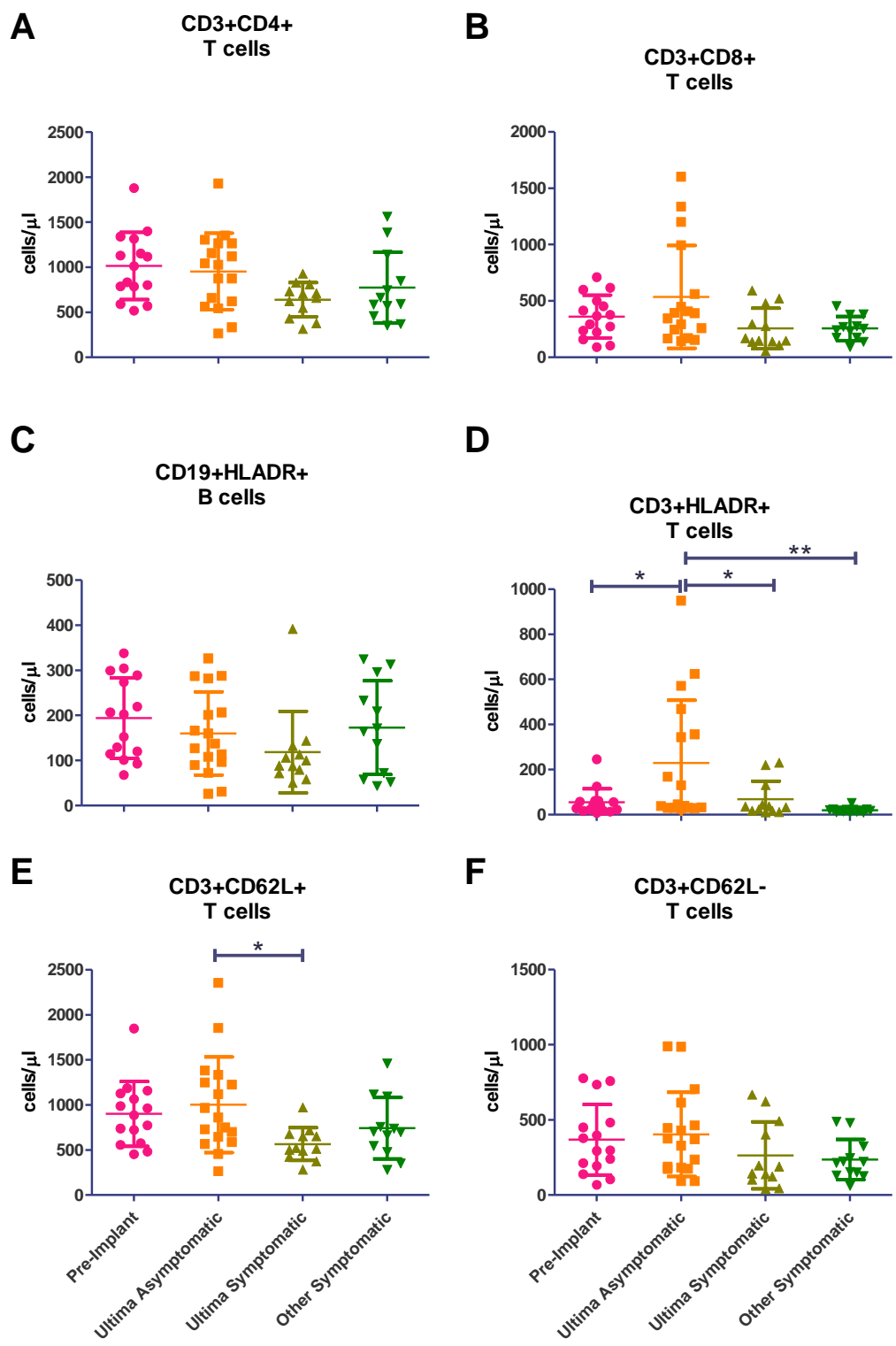


Figure 4-5: Peripheral blood T and B cell absolute counts with activation markers

Peripheral blood was analysed *ex vivo*. Patients were stratified into 4 groups according to clinical presentation. A: CD4+ T cell numbers. B: CD8+ T cell numbers C: B cell numbers D: Activated T cell numbers. E: Naïve and central memory T cell numbers F: Effector T cell numbers

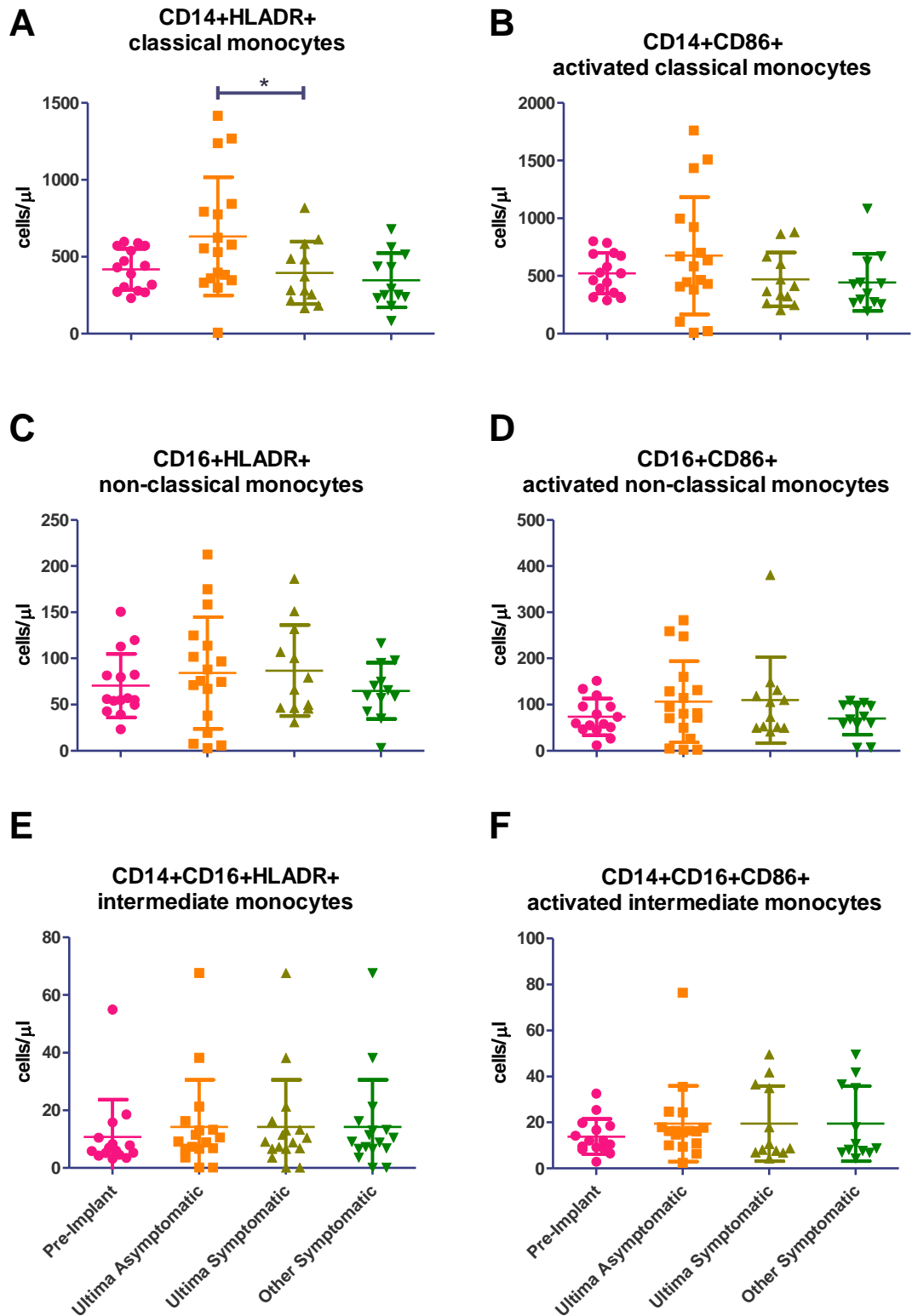


Figure 4-6: Peripheral blood monocyte counts with activation markers

Peripheral blood was analysed *ex vivo*. Patients were stratified into 4 clinical groups. **A:** Presents classical monocytes. **B:** CD86 expression on monocytes is indicative of activation. **C:** Presents non-classical monocytes. **D:** activated non-classical monocytes. **E:** Transitional monocytes express both CD14 and CD16 markers named as intermediate monocytes **F:** activated intermediate monocytes, CD14+CD16+CD86+ .

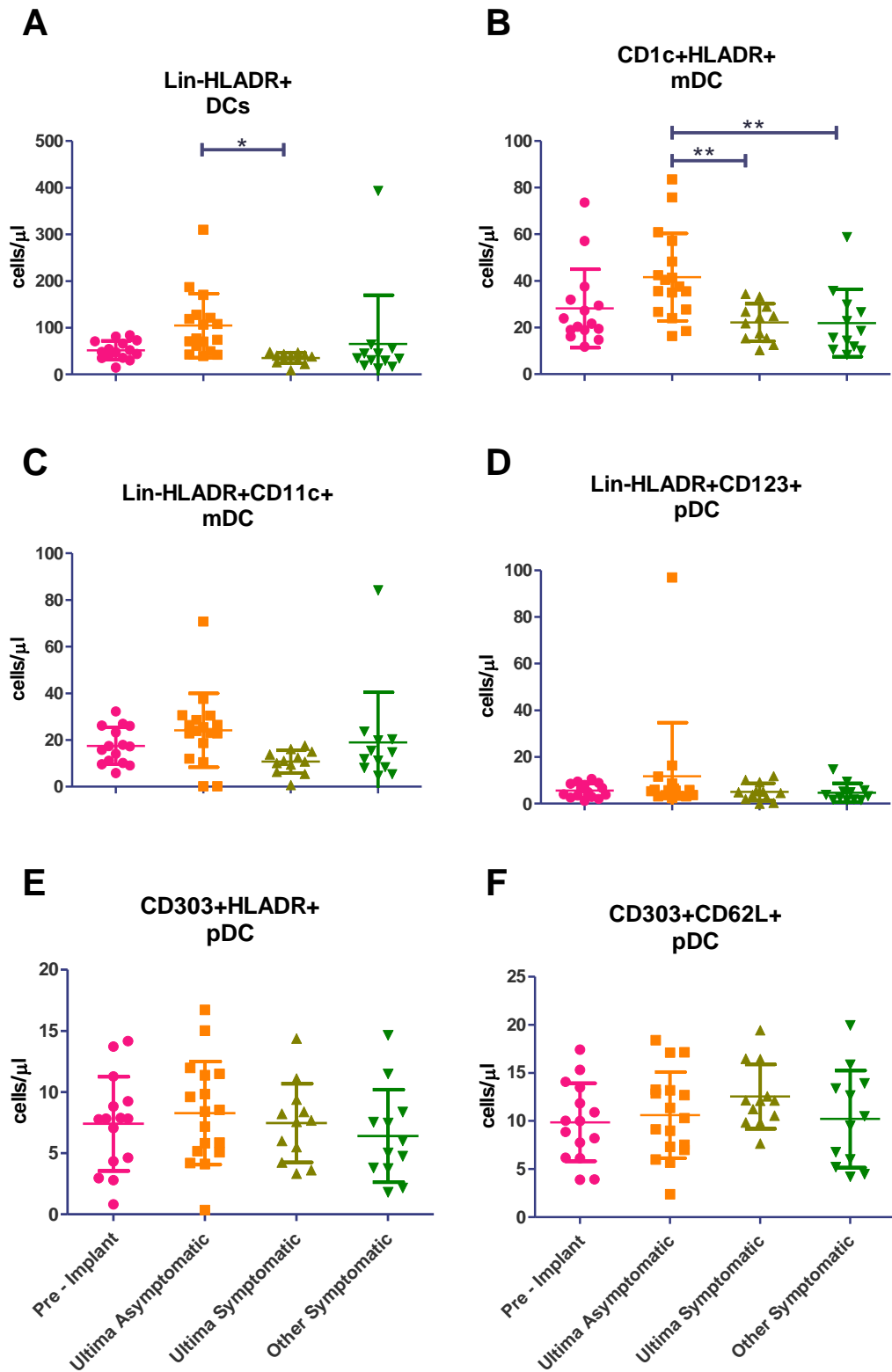


Figure 4-7: Peripheral blood DC counts with activation markers

Whole blood was analysed for dendritic cell constitution. All DCs express high levels of HLADR molecule hence used for identification. **A:** total number of dendritic cells shown across different clinical groups. **B:** Representing CD1c+ myeloid DCs. **C:** Representing CD11c+ mDCs. **D:** Representing CD123+ plasmacytoid DCs **E:** Representing CD303+ plasmacytoid DCs. **F:** Dendritic cells almost always positive for CD62L.

Ex vivo cytokine measurement

The Luminex assay displayed high sensitivity and robust experimental outcome technically as shown by the standard curves generated (Fig 4-8). The patient's serum contained very low or undetectable levels of IFN- γ , IL-10, IL-6, IL-1 β , M-CSF, TNF- α and RANKL (Fig 4-9 & Table 4-5) whereas GM-CSF, Leptin and OPG were detectable. SF levels of IFN- γ , IL-10 and TNF- α were also low however GM-CSF, IL-1 β , IL-6, Leptin, M-CSF, OPG and RANKL were readily detectable in this sample type (Fig 4-10 & Table 4-5). There were no significant differences in the levels of cytokines between the clinical groups analysed either in serum (Fig 4-9) or SF (Fig 4-10). However when the data was paired for the individual's serum versus SF readings, there were significant differences in summated cytokine levels favouring SF samples. Seven out of 10 analytes investigated showed higher concentrations in SF compared to blood (Fig 4-11). The respective p values are displayed in the graphs.

The data was further scrutinised with multivariate analysis using an unsupervised data-reduction method; Principal Component Analysis (PCA). PCA considers all measurements at once and expresses the data in a simplified manner. PCA has the potential for more vigorous assessment of the immune status in accordance with the multifunctional nature of cytokines. This method was applied to both serum and SF data with and without scaling. Data scaling did not influence the outcome therefore results was presented without scaling. Patient 35 was excluded from analysis of PCA in serum, hence identified as an outlier skewing analysis.

First the loading characteristics of each measurement were tested in serum and SF (Fig 4-12 A & Fig 4-13 A). Loading indicates the weight of each measurement in the combination of analytes measured. Leptin (PC1) and OPG (PC2) were the main principal components

in serum. Leptin was also the main variable in SF (PC1) however PC2 was IL-6 in this sample type.

PC1 versus PC2 was plotted to see if there was any clustering effect firstly for individual patients (Fig 4-12 B & Fig 4-13 B), secondly for clinical groups (Fig 4-12 C & Fig 4-13 C) and thirdly for gender (Fig 4-12 D & Fig 4-13 D).

Having compared all the analytes together, there was no clustering effect between any of the individuals either in serum or in SF samples. Analysis of clinical groups also did not reveal any confounding differences between groups. Stratifying patients into male and female also did not correspond to any gender-related effect in this cohort. Apart from analysis of Leptin showed that this cytokine is at higher concentrations in females compared to males (Fig 4-12 D and Fig 4-13 D). Leptin is produced by adipose tissue and females tend to have higher percentage of body fat compared to males, therefore this result was expected.

Correlation between every single analytes against each other was investigated using Pearson correlation test for both serum and SF readings. In order to deal with multiple testing error, a simulation test was carried out. Statically significant ($p < 0.05$) threshold value was calculated for R values by carrying out simulation test. Simulation was applied 10,000 repeats of normal distributed random numbers using the same sample size as study, (10 columns x $n = 55$) for serum and (10 columns x $n = 24$) for SF. Correlation matrix then interrogated for R values. The results revealed that $r = 0.42$ was statically significant for serum and $r = 0.62$ for synovial fluid.

A large number of analytes were correlated in the serum, respective correlation coefficient are displayed in the Fig 4-14. This is expected since all of these patients are representing

osteoarthritis and co-morbidities are common in this age group. However there were no differences in cytokine levels between the groups as shown in Fig 4-9.

There were not any considerable correlations in synovial fluid (Fig 4-15).

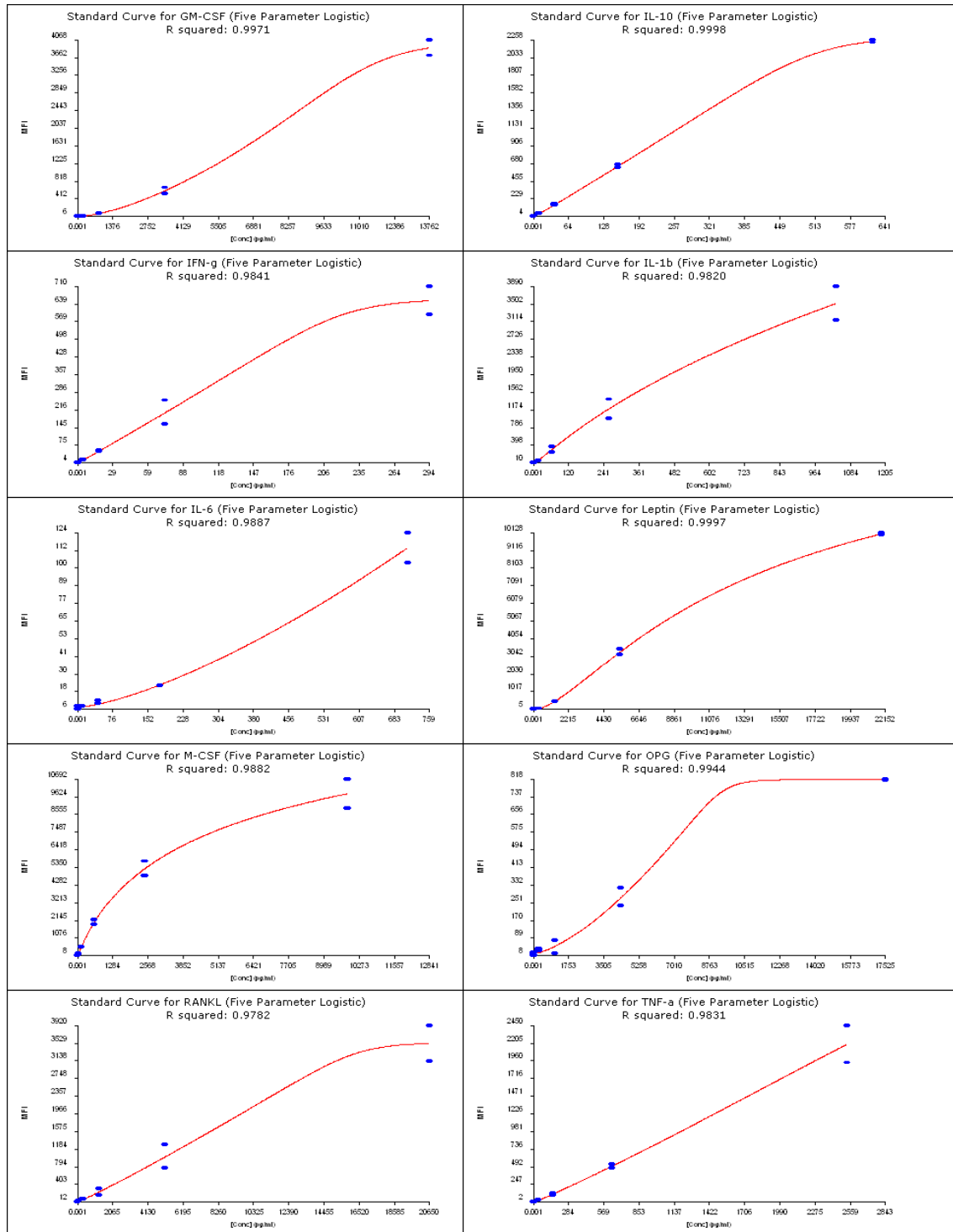


Figure 4-8: Standard curves for cytokine measurement

Standard curves generated for Luminex assay using 5 Parameter logistic curve fit and sample concentration was calculated by extrapolating mean fluorescence intensity from these plots. Correlation Coefficient value (R^2) is presented on relevant graphs.

Serum

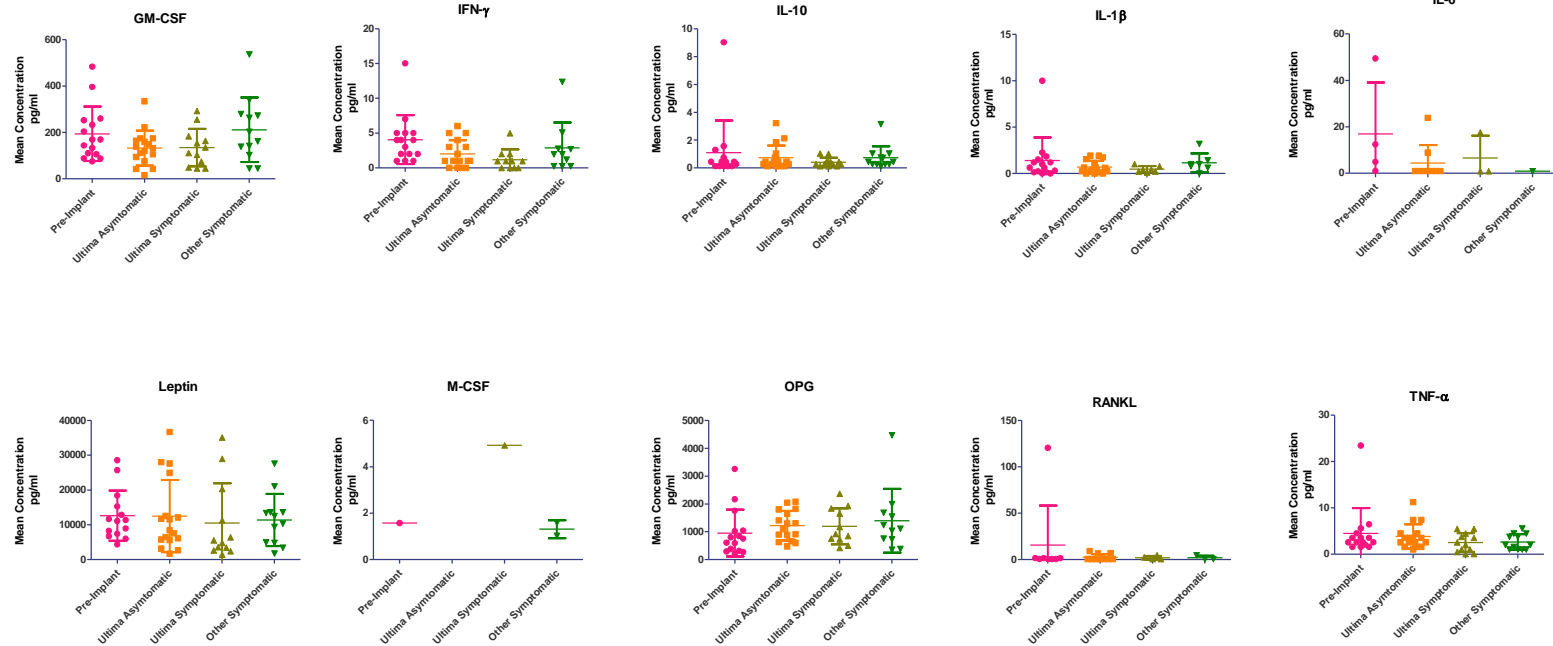


Figure 4-9: Serum cytokine levels

Ten different cytokine levels were measured in patient's serum, displayed as pg/ml. Data was stratified according to clinical groups and was analysed using one-way ANOVA. There were no statically significant differences between groups. (Pre-implant n=15, Ultima Asymptomatic n=17, Ultima Symptomatic n=12, Other =12).

SF

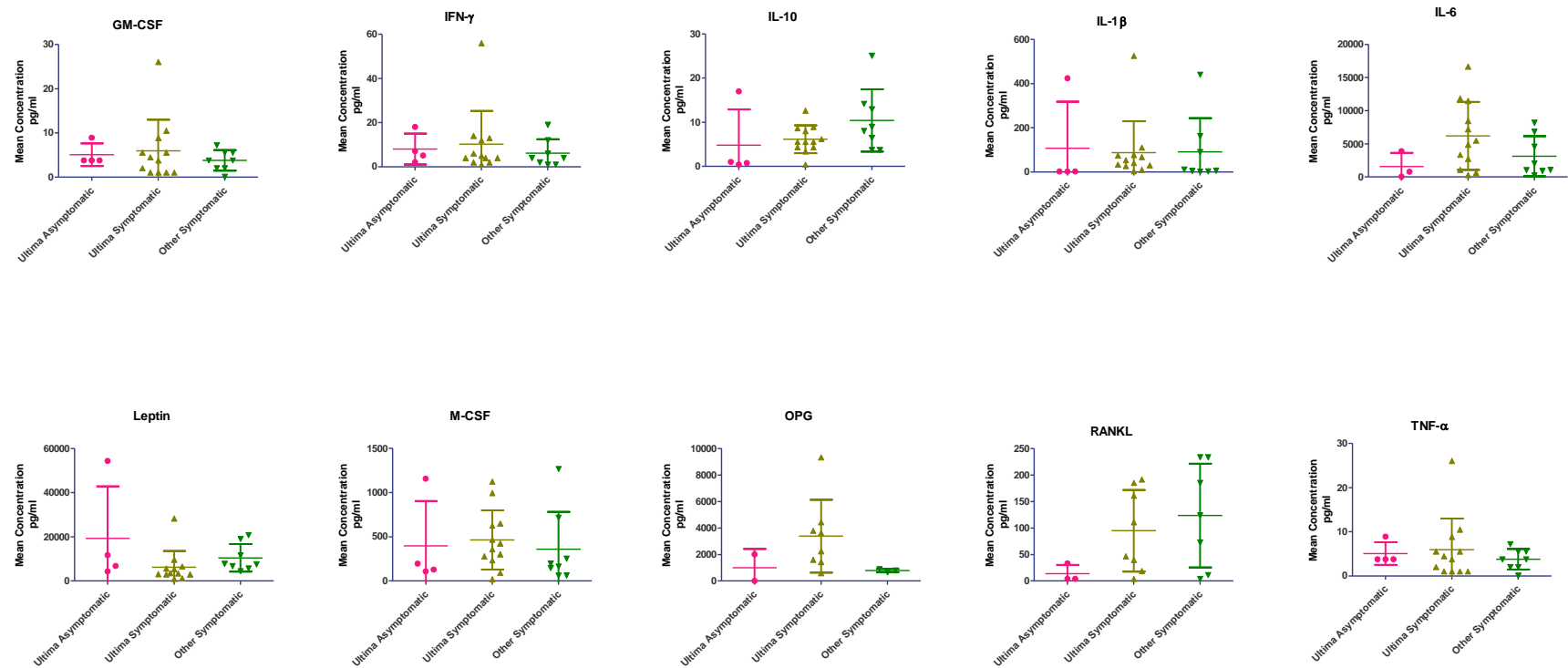


Figure 4-10: SF cytokine levels

Synovial fluid was collected intra-operatively and analysed for ten different cytokine levels, displayed as pg/ml. Data was stratified according to clinical groups and was analysed using one-way ANOVA. There were no statically significant differences between groups. (Pre-implant n=15, Ultima Asymptomatic n=17, Ultima Symptomatic n=12, Other Symptomatic n=12).

Table 4-5: Summated cytokine concentration in patient's serum and SF

Serum (pg/ml)	GM-CSF	IFN-γ	IL-10	IL-1β	IL-6	Leptin	M-CSF	OPG	RANKL	TNF-α
Minimum	30.94	0.1884	0.0313	0.2500	0.4290	1463	0.2500	2.000	0.3732	0.2500
25% Percentile	93.15	0.6538	0.2346	0.2500	0.4290	5046	0.2500	442.5	0.3732	1.380
Median	145.9	1.892	0.5348	0.5260	0.4290	9148	0.5604	656.2	0.3732	2.391
75% Percentile	221.4	3.936	0.8149	0.8210	8.715	15354	0.8707	1370	8.301	4.641
Maximum	524.8	15.33	8.957	9.190	56.43	37725	2.357	3973	118.1	25.53
Mean	171.3	2.744	0.8262	0.8423	9.022	12011	0.6763	955.8	7.145	3.580
Std. Deviation	110.7	2.947	1.299	1.298	15.86	9228	0.5224	759.3	22.43	3.823
Std. Error	14.80	0.4254	0.1737	0.1800	3.738	1244	0.08158	102.4	4.316	0.5203
Lower 95% CI of mean	141.6	1.888	0.4782	0.4808	1.135	9516	0.5114	750.5	-1.727	2.536
Upper 95% CI of mean	200.9	3.599	1.174	1.204	16.91	14506	0.8412	1161	16.02	4.623
SF (pg/ml)										
Minimum	104.2	1.043	0.6923	0.7012	8.000	993.4	21.58	394.5	2.000	0.3850
25% Percentile	166.8	2.702	3.850	3.134	860.1	3506	149.4	856.6	7.736	0.3850
Median	202.5	5.064	6.205	32.86	3647	6168	274.0	1619	63.77	2.306
75% Percentile	307.3	13.30	9.649	104.4	10429	11170	666.4	9318	154.7	6.866
Maximum	579.4	55.70	25.39	491.0	27125	73145	1345	12390	236.8	25.59
Mean	254.2	8.912	7.589	91.48	6203	10816	434.9	4251	81.41	4.150
Std. Deviation	126.2	11.32	5.885	144.0	7096	15010	393.6	4613	79.07	5.512
Std. Error	25.77	2.311	1.201	29.39	1448	3064	80.35	1191	19.18	1.125
Lower 95% CI of mean	200.9	4.131	5.104	30.69	3206	4478	268.7	1697	40.76	1.823
Upper 95% CI of mean	307.5	13.69	10.07	152.3	9199	17154	601.1	6806	122.1	6.478

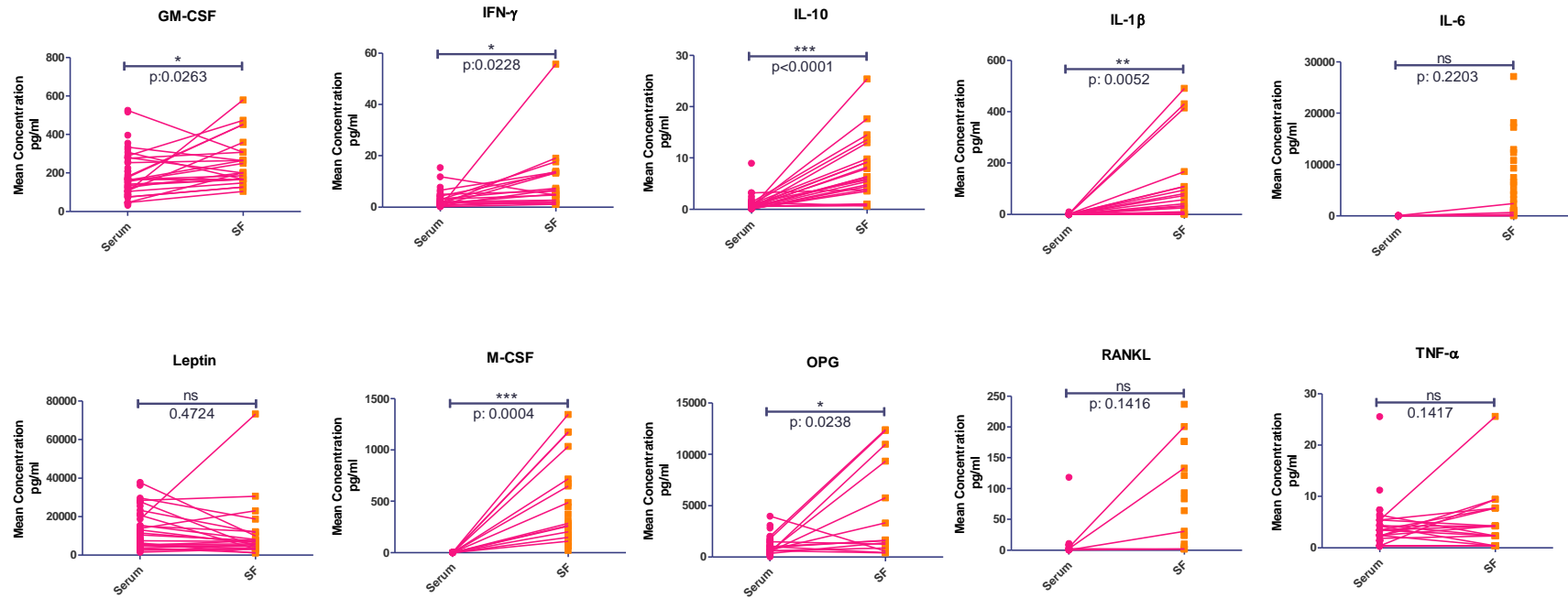


Figure 4-11: Comparison of cytokine levels in serum versus synovial fluid

Concentrations of respective analytes in serum (n = 56) and SF (n = 24) was compared. Each data point represents a patient. Matching samples were paired where possible. Serum concentration of cytokines levels were compared with SF concentrations using two tailed paired t-test.

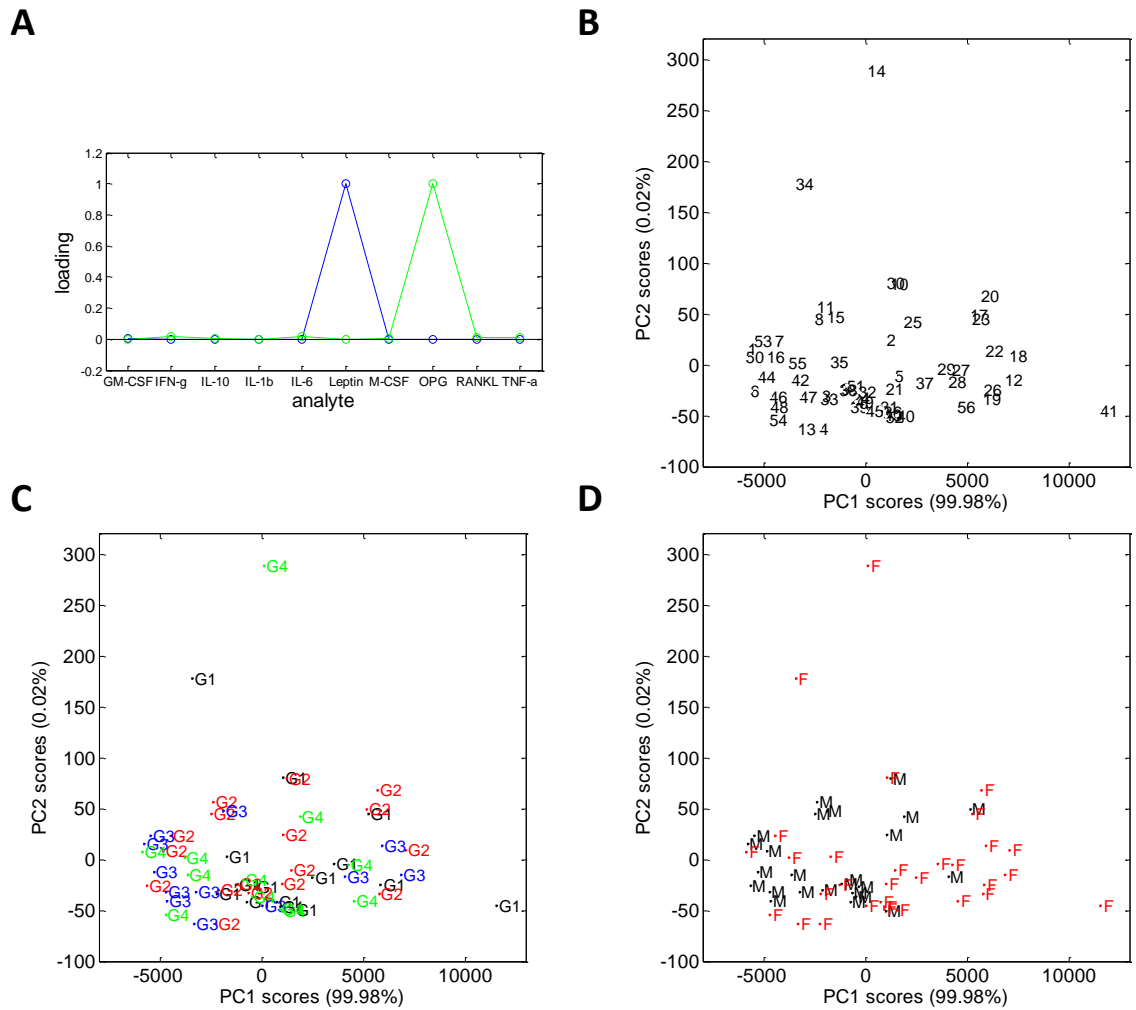


Figure 4-12: PCA analysis of cytokines in serum

G1: Pre-Implant, G2: Ultima Asymptomatic, G3: Ultima Symptomatic, G4: Other Symptomatic. F: Female, M: Male

Principal Components Analysis of serum mean MFI data (no scaling). **A:** Loadings for PC1 (blue) shown to be Leptin and PC2 (green) shown to be OPG **B:** showing individual patients demonstrated by their study number. **C:** Indicating patients stratified into their clinical groups **D:** Male versus female compared. Axes labels indicates percentage variance represented by each component.

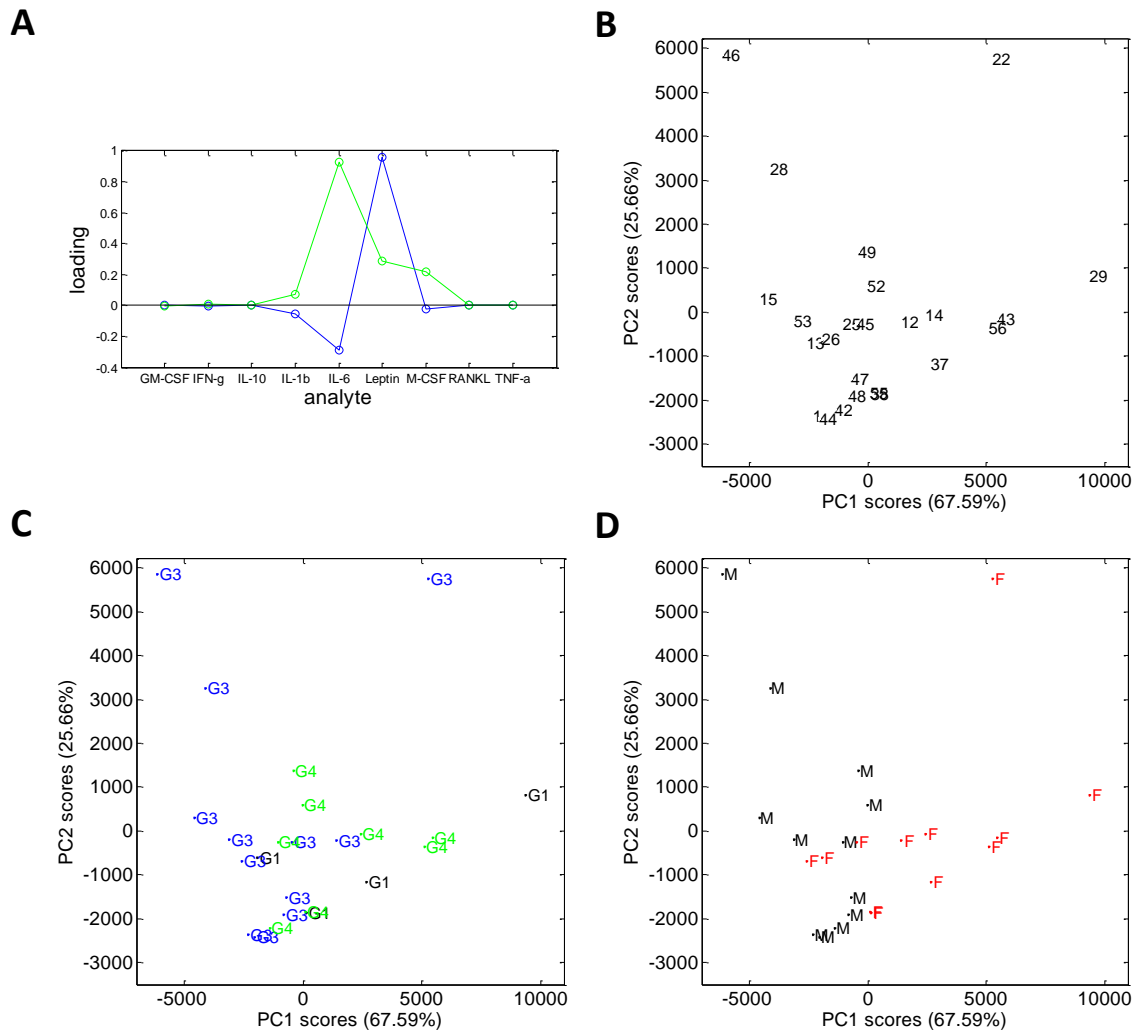
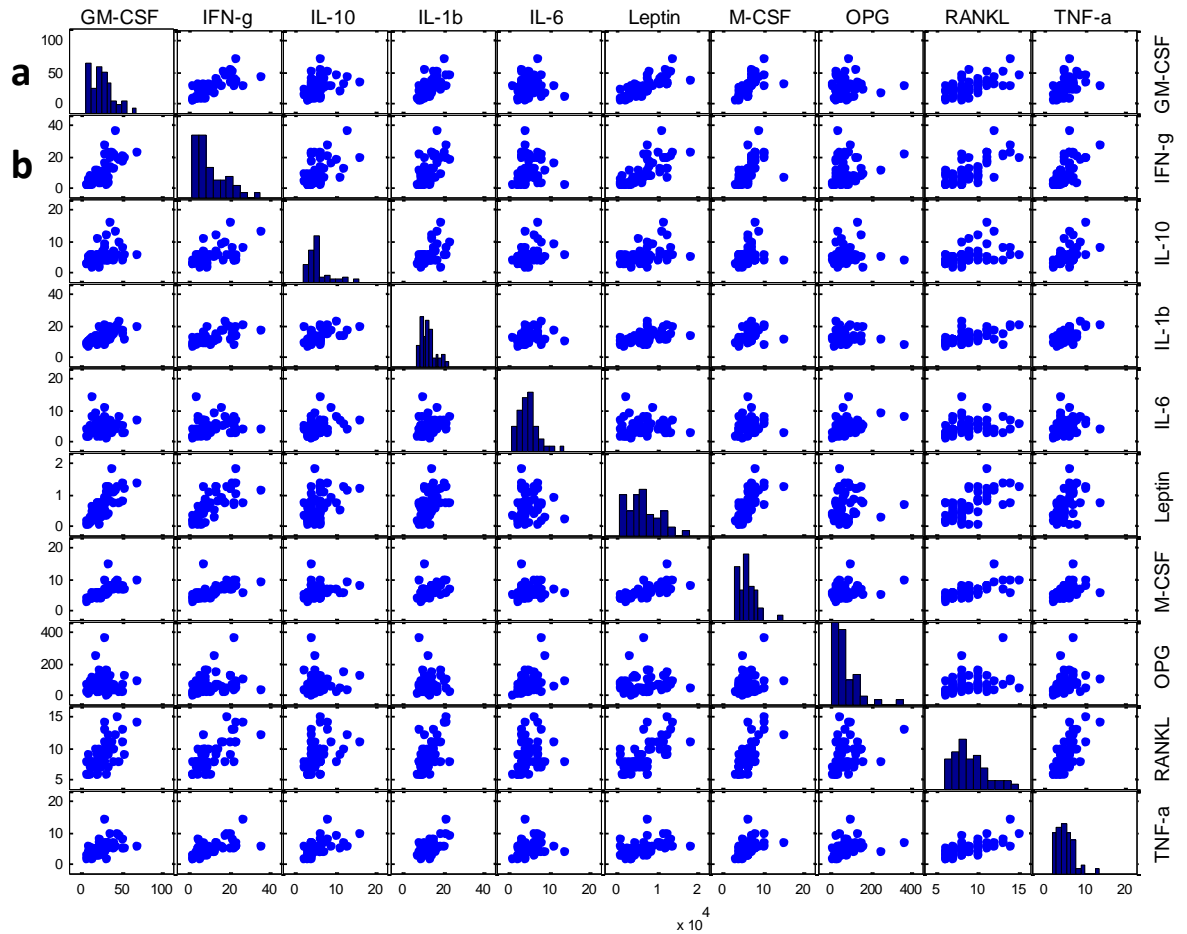


Figure 4-13: PCA analysis of cytokines in synovial fluid

Key: G1: Pre-Implant, G2: Ultima Asymptomatic, G3: Ultima Symptomatic, G4: Other Symptomatic. F: Female, M: Male

Principal Components Analysis of synovial fluid in operative patients; groups G1, G3 and G4. Mean MFI data (having removed OPG due to 7/24 missing values) (no scaling). **A:** Loadings for PC1 (blue) shown to be Leptin and PC2 (green) shown to be IL-6 **B:** showing individual patients demonstrated by their study number. **C:** Indicating patients stratified into their clinical groups **D:** Male versus female compared. Axes labels indicates percentage variance represented by each component.

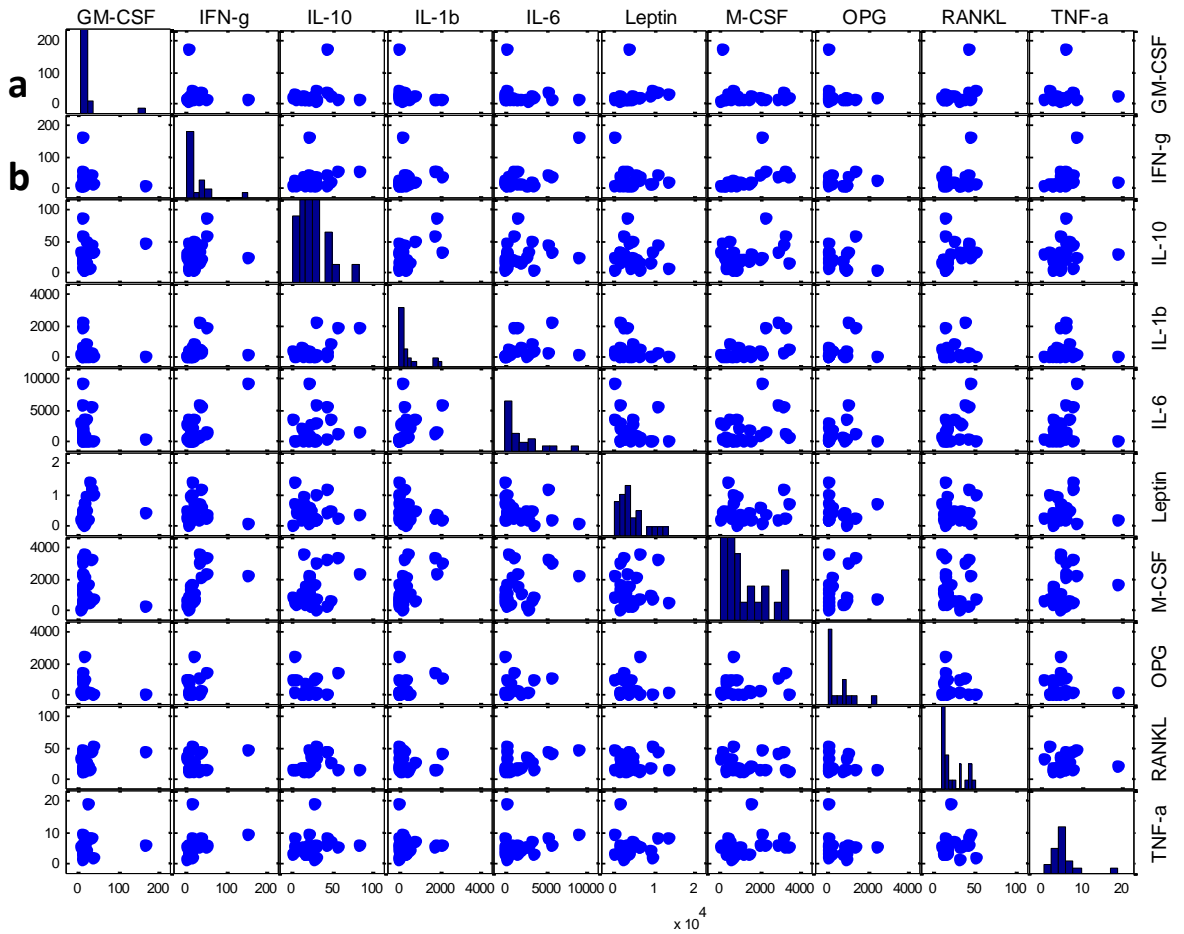


c

	GM-CSF	IFN-g	IL-10	IL-1b	IL-6	Leptin	M-CSF	OPG	RANKL	TNF-a
GM-CSF	1.000	0.730	0.376	0.651	0.102	0.778	0.690	0.053	0.656	0.489
IFN-g	0.730	1.000	0.498	0.600	0.136	0.717	0.600	0.206	0.704	0.609
IL-10	0.376	0.498	1.000	0.517	0.327	0.403	0.247	0.072	0.397	0.538
IL-1b	0.651	0.600	0.517	1.000	0.290	0.529	0.411	-0.024	0.582	0.668
IL-6	0.102	0.136	0.327	0.290	1.000	0.017	0.177	0.370	0.259	0.203
Leptin	0.778	0.717	0.403	0.529	0.017	1.000	0.712	0.078	0.656	0.486
M-CSF	0.690	0.600	0.247	0.411	0.177	0.712	1.000	0.232	0.707	0.464
OPG	0.053	0.206	0.072	-0.024	0.370	0.078	0.232	1.000	0.306	0.265
RANKL	0.656	0.704	0.397	0.582	0.259	0.656	0.707	0.306	1.000	0.696
TNF-a	0.489	0.609	0.538	0.668	0.203	0.486	0.464	0.265	0.696	1.000

Figure 4-14: Analysis of cytokine correlation coefficients in serum

a) Each histogram showing the distribution of one of the analytes (labelled respectively) X axis = unit of measurement (median fluorescence intensity), y axis = frequency. **b)** Scatter plots showing correlation matrix. The level of each cytokine (median fluorescence intensity) was compared to the other cytokine (9x9). **c)** Table displaying values for R. correlations that are higher than cut off value of 0.42 (determined by simulation test) were highlighted in blue, n = 55.



c

	GM-CSF	IFN-g	IL-10	IL-1b	IL-6	Leptin	M-CSF	OPG*	RANKL	TNF-a
GM-CSF	1.000	-0.161	0.198	-0.197	-0.169	0.181	-0.201	NaN	0.399	0.087
IFN-g	-0.161	1.000	0.227	0.276	0.689	-0.169	0.530	NaN	0.240	0.272
IL-10	0.198	0.227	1.000	0.608	0.149	-0.111	0.346	NaN	0.274	0.149
IL-1b	-0.197	0.276	0.608	1.000	0.295	-0.270	0.604	NaN	-0.059	0.003
IL-6	-0.169	0.689	0.149	0.295	1.000	-0.275	0.348	NaN	0.514	0.173
Leptin	0.181	-0.169	-0.111	-0.270	-0.275	1.000	-0.001	NaN	0.067	-0.022
M-CSF	-0.201	0.530	0.346	0.604	0.348	-0.001	1.000	NaN	-0.027	0.227
OPG*	NaN	NaN	NaN	NaN						
RANKL	0.399	0.240	0.274	-0.059	0.514	0.067	-0.027	NaN	1.000	0.062
TNF-a	0.087	0.272	0.149	0.003	0.173	-0.022	0.227	NaN	0.062	1.000

Figure 4-15: Analysis of cytokine correlation coefficients in synovial fluid

a) Each histogram showing the distribution of one of the analytes (labelled respectively) X axis = unit of measurement (median fluorescence intensity), y axis = frequency. **b)** Scatter plots showing correlation matrix. The level of each cytokine (median fluorescence intensity) was compared to the other cytokine (9x9). **c)** Table displaying values for R. there were no significant correlations that are higher than cut off value of 0.62 (determined by simulation test), n = 24.

Metal ion Levels

Serum metal ion levels were measured and the results revealed that both Co and Cr levels were elevated in patients with a MoM compared to the control Pre-implant group. Serum Co levels were significantly increased in both Ultima Asymptomatic ($p = 0.0007$) and Ultima Symptomatic group ($p = 0.002$) compared to pre-implant. Mean serum Co levels in the Other MoM group were also increased however it was not significant compared to the Pre-implant group (Fig 4-14 A). Showing Co levels were much higher in Ultima groups compared to other metal implant groups. Mean Co serum levels were $13.06 \mu\text{g/L}$ (range 3.66 to 47.42) for the Ultima asymptomatic group and $10.04 \mu\text{g/L}$ (range 1.49 to 29.05) for the Ultima symptomatic group. This indicates that both of the Ultima groups had serum levels higher than the diagnostic cut off ($7\mu\text{g/L}$).

Serum Cr levels also were raised in all three MoM implant groups compared to the Pre-implant group (Fig 4-14 B). The Ultima Asymptomatic and the Symptomatic groups had elevated Cr levels compared to the Pre-implant group ($p = 0.0015$ and $p = 0.0407$). However the mean serum levels were below the diagnostic cut off level of $7\mu\text{g/L}$.

Highest levels of both Co and Cr were found in the Ultima Asymptomatic group which had a well-functioning implant. This elevation was not due to the *in-situ* implant time as three groups had a similar average *in situ* period (G2: 130 ± 26 , G3: 139 ± 23 and G4: 123 ± 54 months). Mean cobalt levels were higher than chromium levels in the Ultima groups. Cobalt is the most abundant metal in the Ultima implant which may explain higher levels of Co compared with Cr.

The mean Co levels were much higher than clinical recommendation in Ultima groups, this was especially very significant in Ultima Asymptomatic group ($p = 0.0007$). This finding correlates with this group's cell counts demonstrated with immunophenotyping. This was

the only group had an aberrant immune cell values in peripheral blood. Increased Co levels may explain the altered immune cell composition in the Ultima Asymptomatic group.

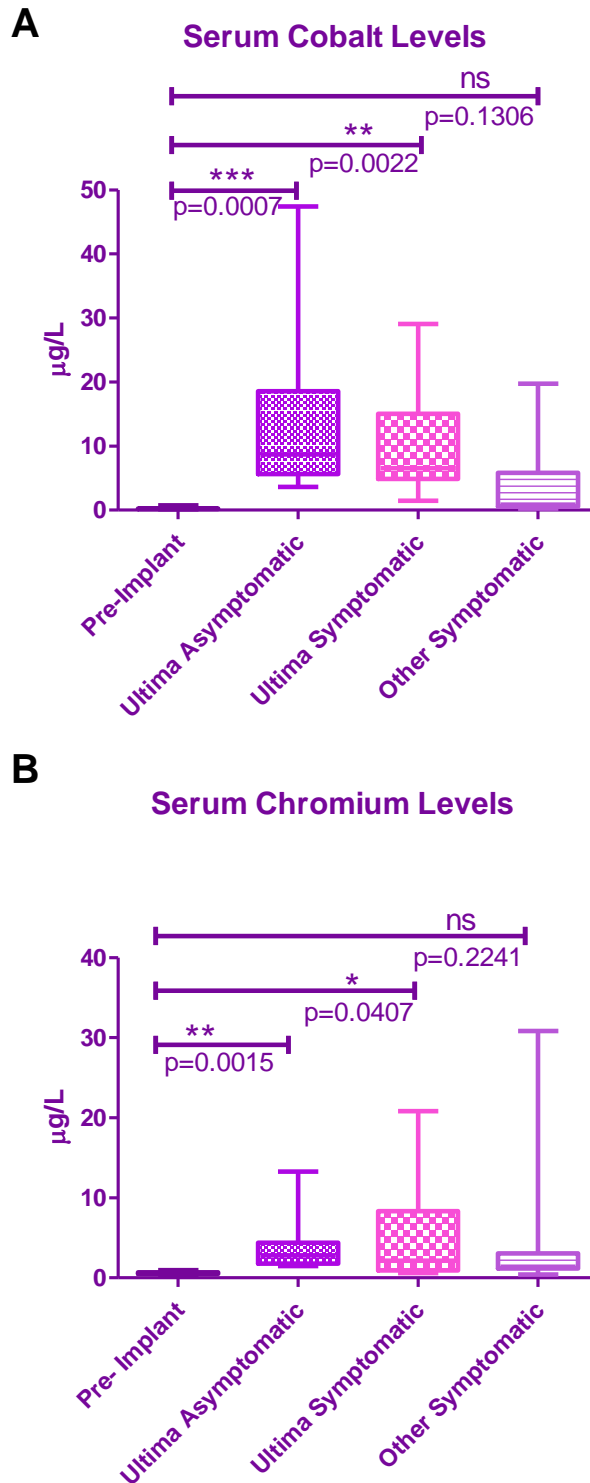


Figure 4-16: Serum cobalt and chromium levels

(A) Serum Cobalt and (B) Chromium Levels; Determined by ICP-MS. Levels expressed in $\mu\text{g/L}$ for Pre-Implant ($n = 11$), Ultima Asymptomatic ($n = 15$), Ultima Symptomatic ($n = 11$) and Other Symptomatic patients ($n = 9$). Metal ion levels were compared between groups using unpaired t test with Welch's correction and p values displayed on the graphs.

4.5 Discussion

MoM implant patients were investigated for their immune cell composition, serum and SF cytokine levels and serum metal ion concentrations.

Assessment of the quantitative and phenotypic modifications of peripheral blood leukocytes was conducted by flow cytometry. An extensive immunophenotyping was undertaken; investigating 18 different antigenic targets concurrently. Blood leukocyte levels were normal in all groups studied apart from the Ultima Asymptomatic group. In this group variation was evident in T lymphocytes with increased expression of HLADR and CD62L. Naïve T cells do not normally express HLADR antigen and increased abundance of it is an indication of immune stimulation hence CD3+HLADR+ phenotype identifies activated T lymphocytes. CD62L is a ligand for CD34, GlyCAM and MAdCAM-1 receptors in secondary lymph nodes and expression of this ligand is an indication of lymph node homing for T cells therefore T cell-mediated heighten immune surveillance was evident in this group. Whilst some groups showed CD8 lymphopaenia [168] others demonstrated the opposite; increased levels of CD8+HLADR+ lymphocytes in MoM patients [169, 170].

The MoM literature often demonstrates the relative cell numbers comparing one study group to another with single colour staining. However, in the current study the absolute cell numbers were determined with multiple markers ensuring lineage specificity. This is important to warrant integrity of the data and subsequent interpretation.

In the current study, there was also an increase of CD3+HLADR+ cells. This was due to the CD8 population in the Ultima Asymptomatic group but not in the failed groups.

Increased HLADR expression on CD8+ T cells attributed to enhanced telomerase activity and proliferation and are distinct from cytotoxic CD8+ T cells [171]. Elevation of

CD8+HLADR+ T cells were observed in stable Human Immunodeficiency virus-infected individuals [172] and proposed to be marker for a stable acquired immune deficiency syndrome in the presence of normal levels of CD4+ cells. This suggests a protective mechanism might have been maintained by this subset of T cells. The results of the current study is in agreement with literature where stable MoM patients demonstrated increased number of CD8+HLADR+ T cells in the presence of normal CD4+ counts.

Particulate debris generated by wear is the main initiator of the destructive process that leads to peri-prosthetic osteolysis [173]. The most important cells in this scenario are monocytes/macrophages which respond to particle challenge by phagocytosis. This mechanism should ensure decreased inflammation by containment of the wear particles. However monocytes are associated with tissue destruction in the literature [174].

Inflammation is a highly regulated process tightly linked to simultaneous stimulation of tissue protective and regenerative mechanisms to prevent collateral damage. Monocytes either could be inflammatory or homeostatic/regulatory. In the current study, finding an increased number of monocytes in the Asymptomatic group might be due to regulatory processes that are in place in this group.

Further, CD1c DCs were also increased in the same group. CD1c+ DCs are the most abundant subpopulation of DCs and have a specialised role in presentation of non-protein antigens. The presence of DCs in synovial fluid and synovial tissue is documented in arthritic conditions [175]. CD1c+ myeloid DCs have been shown to induce T cells in RA patients [176]. However, CD1c+ DCs also have shown to have an immunoregulatory function [177] [178]. The classical macrophages and myeloid dendritic cells are two major source of antigen presentation. APCs are needed for antigen-specific T cell activation which may explain increased number of APCs along with activated T cells in this group. Finding increased CD1c+ DCs, along with activated T cells and classical monocytes, might

be an indication of a regulatory mechanism that keeps metal sensitisation under control in the Asymptomatic Ultima group. The nature of this increase is not known in the current study hence specialised markers for regulatory cells were not investigated. However one would assume that the heightened immune status might be due to the immune surveillance or even a regulatory mechanism resulting in this group which has a well-functioning implant.

CD86 is a co-stimulatory molecule and binds to CD28 and CD152 (CTLA-4) on T cells. It is up regulated in activated monocytes and crucial for T cell activation. Investigation of CD86 up-regulation in all three monocyte subsets did not reveal any difference between the clinical groups. Altaf *et al* demonstrated increased CD86 expression on monocytes after challenge with Co/Cr particles *in vitro* [146] compared to non-challenged cells, demonstrating induction of antigen presentation upon metal challenge. This was not evident in the current study. Two investigation set up is quite different from each other. In the current study cell were not re-challenged *in vitro*, instead samples were analysed directly *ex-vivo* and only had been challenged *in vivo* by *in situ* implant.

A lymphocyte-mediated inflammatory reaction has been shown around the metal implants histologically [56], which demonstrated lymphocytic infiltration into implant site. In this study, the local cellular immune response was also investigated in synovial fluid. The cell composition was analysed using flow cytometry with panels above, utilising an enzymatic digestion prior (data not shown). It was not feasible to demonstrate reliable cell counts with this type of sample due to the nature of the SF matrix having complex proteins results in viscous material. It was concluded that SF was not a suitable sample type for a routine flow analysis. This difficulty was also reported by other groups [175] [179] however some groups have demonstrated the presence of T cells, macrophages and DCs in SF [176].

Soluble mediators such as cytokines, chemokines and growth factors are known to be involved in the pathophysiology of implant failure [150, 180]. Using a sensitive assay, investigation of ten different analytes has not shown a strong link between the known clinical groups examined and the array of cytokines measured in this study. However other sources of variability, not tested in the current study, might be present. Beekhuizen *et al* also investigated SF samples in OA patients for 47 different analytes. They looked at end-stage OA patients and found that IL-6, IP-10, MDC, PDGF, Leptin, IL-13, MIP-1b, CD40L and RANTES were higher, whereas eotaxin and G-CSF levels were lower in OA patients compared to healthy controls [181]. Comparing available data from Beekhuizen's study with the present study reveals that the Ultima cohort had higher levels of IL-10 and IL-1 β however lower levels of IFN- γ and Leptin. IL-10, IL-1 β and IFN- γ all were at very low levels in both studies questioning the reliability of these read outs. Wong *et al* reported that a screening study of healthy individuals also revealed the serum IL-1 β , IFN- γ were undetectable in the majority of samples [182]. All of these studies had too few numbers of subjects to come to definitive conclusions however this explorative approach might be a valuable reference for future experiments.

Serum cytokine levels might be transient in these patients therefore hard to monitor. Cytokines levels were almost always higher in SF compared to serum. SF might be a better sample type to study cytokine levels however this sample type is not easily obtainable. Investigation of serum and SF soluble mediators did not show strong evidence of inflammation in this cohort, which contradicts with the body of literature.

Having found significant differences in serum Co/Cr levels post-operatively has been described in MoM patients previously [183, 184] However, finding the higher levels of Co in the Asymptomatic metal implant group is striking. The mean serum Cr levels were also

highest in these patients, however they were mostly under the diagnostic cut off ($7 \mu\text{g/L}$) in this study. There is some dispute regarding acceptable levels of metal ions and their clinical significance [162] therefore these levels may need adjustment in future. On the other hand, the mean serum Co levels were above the clinical diagnosis cut off. The Ultima alloy consists predominantly of Co and this may be the main source of the problem. It has been shown that cobalt is more reactive than chromium in human macrophages. The cobalt exposure to peripheral immune cells results in inflammatory macrophage induction [185]. Hart *et al* investigated peri-prosthetic Ultima retrieval tissue using synchrotron-X-ray absorption spectroscopy (XAS). They found that cobalt was most abundant in the peri-prosthetic tissue of Ultima patients. They also compared the ratio of Co to Cr for each tissue and showed that Co is 10 times more abundant than Cr in the tissue surrounding Ultima hips [186].

The Ultima implant carrying patients are rare as this implant was discontinued in 2005 which limited the number of cases that were available for the study. The total number of subjects was 56, with the Ultima group consisting 29 patients. Even though the number of parameters studied were extensive, the number of subjects was limited which constrained the analysis. Therefore this pilot study in metal implant failure should inform of parameters studied and further work necessary to confirm these data.

5 CHAPTER 5 – *In vitro* assessment of metal particle impact on immune cells

5.1 Introduction

Aseptic loosening as a result of osteolysis is the most frequent cause of implant failure. The cell mechanisms involved in this phenomenon are of major research interest. Osteolysis in the MoM implant hip is described as active resorption of bone matrix at the location where bone meets the implant (peri-prosthetic osteolysis). Peri-prosthetic osteolysis leads to an imbalance in structural bone loading and chronic inflammation. In healthy individuals bone resorption by osteoclasts is followed by bone formation by osteoblasts and is a natural part of osteogenesis. However, in implant failure this cycle is disturbed; osteolysis overwhelms ossification process. In total hip replacement, osteolysis is thought to be the result of an immune response where immune cells attempt to clear implant wear particles. Clinically, osteolysis can be asymptomatic, however chronic exposure to wear particles results in continuous immune cell infiltration at the implant site. Subsequent inflammation can cause the symptoms seen in implant failure [187].

Osteoclasts are the main bone absorbing cells although macrophage-mediated bone resorption has been demonstrated [188]. Osteoclast activity is modulated by neighbouring stromal cell, osteoblasts and immune cells. In the absence of infection, macrophages have been shown to be activated by implant debris which leads to osteoclastogenic activity. Macrophages challenged by metal particles produce pro-inflammatory mediators that facilitate osteolysis [189]. IL-1 β , TNF- α and IL-6 secreted by macrophages and T cells enhance bone resorption by increasing the pool of osteoclastic progenitors and also by stimulating differentiation to mature osteoclasts [155, 190]. Therefore, secondary cell types, such as immune cells can contribute to bone remodelling by either direct contact or soluble factors i.e. cytokines and growth factors [191]. For example, M-CSF, GM-CSF

along with RANKL are necessary for osteoclast activation. On the other hand IFN- γ inhibits RANKL-induced osteoclastogenesis [192]. Leptin and IL-10 have been shown to inhibit osteoclastic activity by stimulating osteoblasts and blocking NF κ B pathway in osteoclasts, respectively [193].

How the metal wear debris incite an inflammatory response is not fully understood. However, host proteins are thought to be involved in metal particle recognition by immune cells. Serum protein coupling to alloy particles can be described as opsonisation which influences recognition and uptake of foreign material by phagocytotic cells. With respect to orthopaedic wear debris, opsonisation of alloy particles with serum has been shown to enhance phagocytic capacity and activation of macrophages [194]. The protein binding profile of Co-Cr-Mo alloy particles is different compared to elemental cobalt or chromium particles. It has been shown by micro-sequencing that Co-Cr-Mo alloy couples with two distinct serum proteins of 68 kDa albumin and 47 kDa alpha-1 antitripsin [195]. Also, serum coupling to metal alloys has been shown to increase lymphocyte reactivity [196]. Opsonisation therefore, might be important in the activation of lymphocytes contributing to implant failure. This was investigated in the current study where cells were cultured in the presence of autologous serum.

Interactions between metal particles and cells depend on the size, number of particles present, material composition, chemical state and interaction matrix [197-199]. It has been shown that nanoparticles smaller than 10 nm are internalised by the cells in an energy-independent manner using pre-existing pores in the membrane. Whereas the large particles with size distribution of 20-100 nm, are taken up through micropinocytosis and larger particles utilise macropinocytotic pathways [200]. Particles larger than 100 nm are not extravasated into blood vessels and remain trapped at the location of generation. They are

therefore expected to dominate the immune reaction at the site of generation. On the other hand smaller particles can accumulate in distant organs via blood circulation, or can be transported from organ to organ *in vivo*.

Doorn *et al* studied 13 Co-Cr-Mo revision patients. Enzymatic digestion of peri-prosthetic tissue revealed that most of the Co-Cr-Mo wear particles were smaller than 50 nm on average (range 6-834 nm) and round to oval in shape with irregular boundaries. This size range is considerably smaller than that reported for polyethylene particles [201]. It has been estimated that patients with MoM implants generate between 6.7×10^{12} and 2.5×10^{14} metal particles a year [64]. However, it not possible to measure precisely the particle load in tissues *in vivo*.

Aims and Hypothesis

In the current study, to better understand the immune cells response to metal alloy particles an *in vitro* cell culture model was set up. PBMCs were exposed to metal alloy particles and their response was then assessed. Dose dependent immune activation profile was investigated using metal particles that were characterised for shape, size and concentration. It was hypothesised that metal ions/particles induce reactivity in PBMCs which results in a pro-inflammatory response. The hypothesis was tested by studying proliferation profile of PBMCs and cytokine production capacity upon metal particle exposure.

5.2 Materials and Methods

5.2.1 *In vitro* metal nanoparticle generation

Several studies have described MoM wear particle characteristics and the resulting general consensus is that the average particle size generated *in vivo* is on a nanometer scale rather than micrometer range [34, 52]. Taking this into consideration, an *in vitro* system was used to generate nano-size metal alloy particles which would represent *in vivo* wear particles. A novel approach was undertaken where a metal hip implant was broken into nanoscale particles using a laser.

An Ultima[®] THR TPS implant, which has a Co-Cr-Mo alloy stem was laser ablated (Particular GmbH, Germany). Fig 5-1 shows a schematic description of the particle generation process. An Ultima implant was physically ablated in sterile water using a laser (TruMicro 5050, TRUMF USA), at a repetition rate of 200 Hz and a reduced pulse energy of 50 μ J (average power: 10 W) with the laser pulse duration of 10 picoseconds. This procedure uses no chemicals hence it produces ligand free samples for biological applications. The concentration of the alloy-colloid solution was determined to be 100 mg/L by atomic absorption spectrometry.

The procedure above produced an alloy colloid suspension. Properties of this colloid suspension were investigated for particle size and particle number using NanoSight system (NanoSight, Malvern). Furthermore, transmission electron microscopy (TEM) was used to determine shape characteristics of alloy particles.

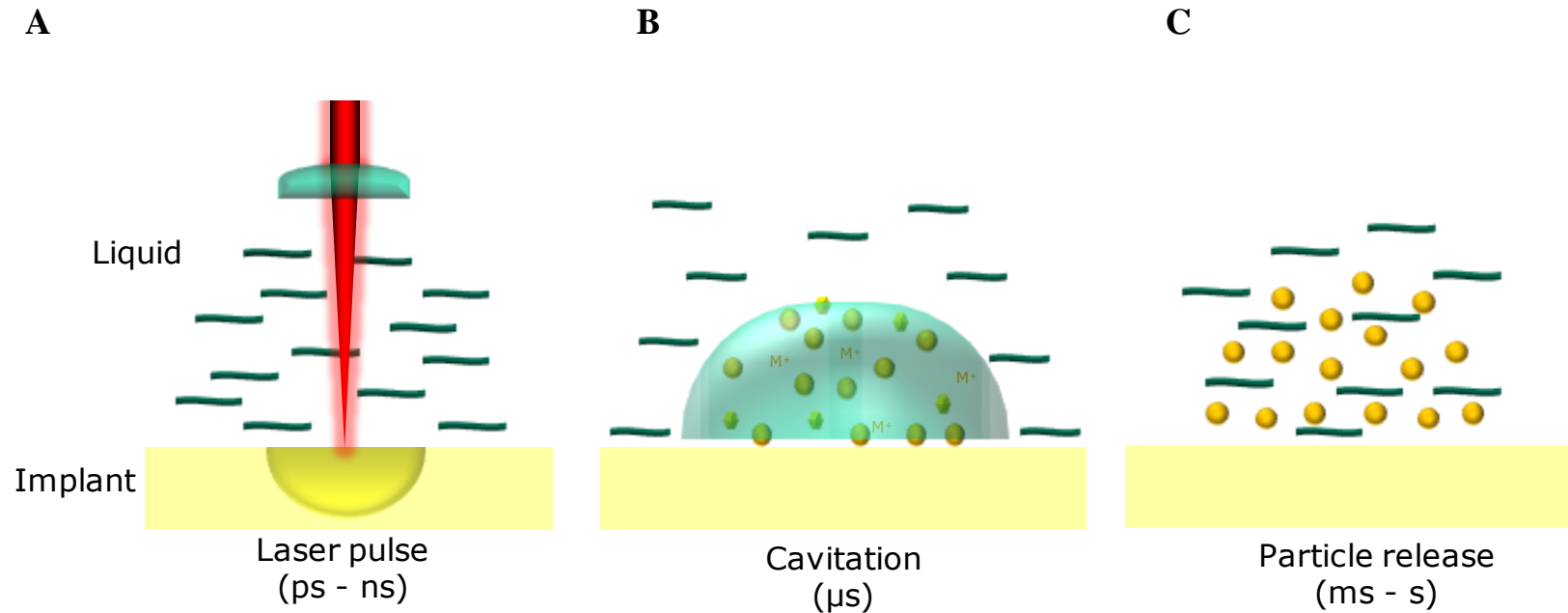


Figure 5-1: Colloid generation by laser ablation

An Ultima[®] TPS implant, a Co-Cr-Mo alloy MoM THR, was laser ablated to generate metal particles of a similar size to those seen *in vivo*. **A:** Laser irradiation: Laser (10 W) applied to material in water with 10 picosecond pulses. **B:** Particle nucleation: Cleaved nanoparticles stay in cavitation bubble for a microsecond (μ s). M^+ represents ionised metal particles. **C:** Particle release: Cavitation bubble bursts and releases nanoparticles within millisecond (ms) to second (s).

5.2.2 Characterisation of metal colloid size and particle number

Metal nanoparticle suspensions generated in water by laser ablation system were tested for particle size and number using NanoSight technology (Model: LM10 model, Malvern UK). Fig 5-2 depicts the instrument set up and its compartments schematically. When the laser hits the particles in the sample this produces a side scatter profile which is then measured using image capture (Fig 5-2 A). The instrument images individual particles using a microscope plus camera system. Nanoscale particles in liquid move with Brownian motion and smaller particles move faster than larger particles. The camera captures movement of each particle within a given time (Fig 5-2 B). Therefore the average distance of movement (particle diffusion coefficient, Dt) is recorded in the video. The rate of movement is influenced by the viscosity of the liquid that the sample is in, the temperature and size of the particle, and it is not related to particle density or refractive index. Because each particle is tracked individually this produces high resolution results for particle size determination. The particles' motion is recorded by the software for each frame and the particle size is then calculated using the Stokes-Einstein equation.

Equation 5-1: Stokes-Einstein formula

$$Dt \langle x,y \rangle^2 = \frac{K_B T t_s}{3 \pi \eta dh}$$

Dt : diffusion coefficient, mean square of displacement

T : temperature

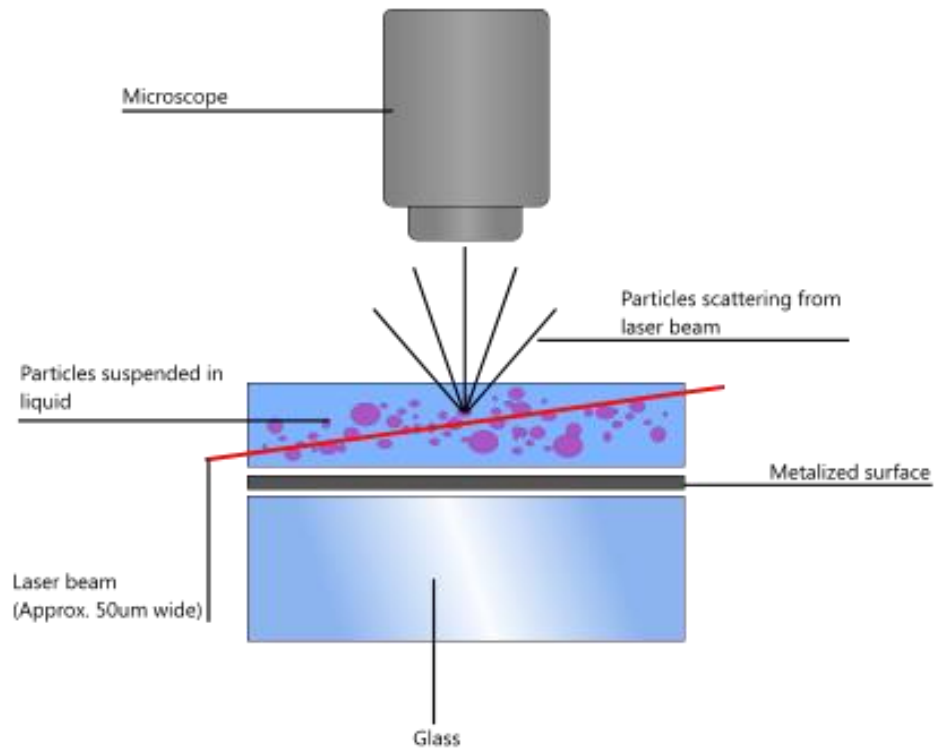
η : solvent viscosity

dh : hydrodynamic diameter

K_B : Boltzmann's constant = $1.3806488 \times 10^{-23}$

$\pi = 3.14159$

A



B

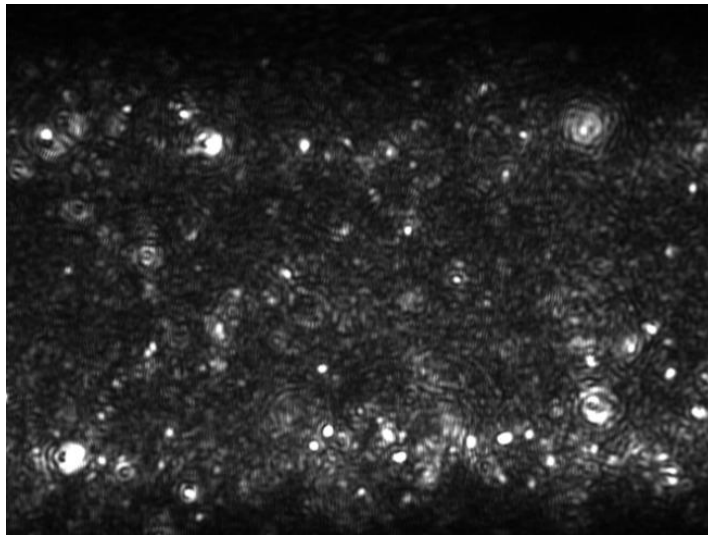


Figure 5-2: The NanoSight System

Size distribution of nanoparticles was determined using NanoSight

<http://www.nanosight.com/technology>. **A:** Instrument set up **B:** A representative read out of Co-Cr-Mo alloy particles

5.2.3 Characterisation of metal particle shape and cellular uptake

Transmission electron microscopy produces high resolution images and provides information of sub-cellular biological structures, morphology of organelles and their interactions with treatment compounds at the molecular level. Therefore this method was chosen as one of the methods to test the metal alloy's impact on immune cells.

Cell cultures

Primary cells were isolated as PBMCs from three healthy volunteers using Ficoll-Hypaque density gradient separation. The required amount of Na-Heparin whole blood was layered over Histopaque 1077 density (Sigma, Cat No: 10771) in an Acuspin tube (Sigma, Cat No: A2055-10EA) and centrifuged 15 mins at 800g at 21°C, followed by aspiration of opaque layer consisting of mononuclear cells. Cells were washed with isotonic Hanks' Balanced Salt solution (HBSS) twice at 300g for 5 mins and resuspended in Ex-ViVo 15 plus 10% autologous serum for down-stream processing. Cells were incubated with 100 µg/L metal nanoparticles for 2, 24 and 48 hours at 37°C in 95% O₂+ 5% CO₂. After the incubation period, the cells were transferred into 1.5 ml Eppendorfs and centrifuged at 300g for 2.5 minutes. The supernatant was then carefully removed and replaced with 1 ml of 2.5% glutaraldehyde in 0.1M PIPES buffer. Cells were resuspended in glutaraldehyde and fixed for 2 hours at 21°C.

Transmission Electron Microscope method

Cell suspensions were centrifuged and washed in 0.1M piperazine-N,N'-bis-2-ethanesulfonic acid (PIPES) buffer three times. After the final centrifugation, the cell pellets were mixed 1:1 with molten 2% low gelling temperature agarose (Type VII Sigma, Cat No: A-4018), which was solidified by chilling and then chopped into small pieces

(approximately 1mm³). Sample pieces were post-fixed in 1% aqueous osmium tetroxide for 2 hours then, after PIPES buffer washes, dehydrated through a series of ethanol solutions (10, 20, 30, 40, 50, 60, 70, 80, 90, 3x 100%). After the 3rd change of 100% ethanol: the ethanol was replaced with a 1:1 mix of 100% ethanol to LR White medium grade resin and put on a rotator for 1 hour 21°C. This was followed by a 1:2 and a 1:3 mix of 100% ethanol to LR White resin and finally 100% resin, with at least 1 hour between each change. The resin was changed twice with fresh 100% resin with periods of at least 8 hours between changes. The sample pieces were each transferred into BEEM[®] embedding capsules with fresh resin and polymerised overnight at 60°C. 90 nm thick sections were cut using an ultramicrotome (Ultracut E, Reichert-Jung) with a glass knife, collected on film/carbon coated copper grids, and stained sequentially with uranyl acetate and lead citrate. The sections were examined and imaged in a FEI Tecnai G2 20 Twin transmission electron microscope at 200kV.

Images were acquired by Kathryn Cross at the Norwich Research Park Bioimaging Centre.

5.2.4 Measurement of cell proliferation

Colorimetric assay tetrazolium salt reduction in mitochondria: 2,3-Bis(2-methoxy-4-nitro-5-sulphophenyl)-2H-tetrazolium-5-carboxanilide (XTT) assay or fluorescent labelling of cytoplasmic amine groups by Carboxyfluorescein succinimidyl ester (CFSE) were utilised for proliferation measurement.

Measurement of cell proliferation with XTT

Colorimetric assays that primarily use reduction of tetrazolium salts provide an estimate of cell proliferation indirectly by measuring mitochondrial activity in an entire cell population

[202]. The XTT assay is based on the principle that tetrazolium salts are reduced to formazan by mitochondrial dehydrogenases in viable cells.

Foetal Bovine Serum (FBS) is commonly used in immunological experiments and human lymphocytes may proliferate in response to xenogeneic proteins in FBS. For this reason using FBS was omitted, instead autologous serum samples were supplied to culture media of Ex-ViVo15 (Lonza, BE04-744Q without phenol red and gentamicin).

Phytohemagglutinin (PHA) mitogen was used as a positive control, which primarily stimulates T cell proliferation. PBMC proliferation was measured using XTT at 1 µg/ml plus 1% phenazine methosulfate (PMS), (Sigma-Aldrich, Cat no; TOX2). The solution of XTT prepared in media is yellowish in colour; viable cells reduce the XTT ring which causes colorimetric change into orange. The absorbance of the resulting orange solution is measured spectrophotometrically at 450 nm. An absorbance reading of 690 nm was also measured and subtracted from the 450 nm value as background correction.

The protocols published by Mull *et al* and Roehm *et al*, were followed [202, 203]. Briefly, PBMC were cultured in serum free X-ViVo 15 media plus heat inactivated (at 56°C for an hour) 10% autologous serum was added to each well. As a positive proliferation control lectin from *Phaseolus vulgaris* (PHA, Sigma-Aldrich Cat no: 61764-1MG) was used at 1 µg/ml final concentration.

PBMCs were seeded at 2×10^5 cells/well in triplicates and cultured with metal particles at concentrations of 10, 50 and 100 µg/L. They were then incubated at 37°C with 5% CO₂ in 96-well flat bottom tissue culture plates. XTT was reconstituted in media and pre-warmed at 56°C for an hour to dissolve, then vortexed briefly just before use. At the end of the incubation period the XTT was added at a volume equal to 20% of the total culture volume (i.e. 50 µl in 200 µl cells). This was followed by an incubation of 4 hours on a

gyratory rocker at 37°C with 95% O₂ plus 5% CO₂. All procedures were carried out aseptically. The absorbance was measured using a spectrophotometer (BioRad, Benchmark Plus microplate).

Measurement of lymphocyte expansion rate with PI+CFSE

CFSE (eBiosciences CatNo: 65-0850-84) staining was combined with propidium iodide (PI Sigma, P4170) to assess lymphocyte expansion rate and to discriminate live/dead cell populations.

CFSE crosses intact cell membranes readily where intracellular esterases cleave the acetate groups of CFSE to yield the carboxyfluorescein molecule which is fluorescent and measured by flow cytometry using 488 nm laser (λ_{ex} / λ_{em} : 494/521 nm). The succinimidyl ester group reacts with primary amines of the cell, this crosslinks the dye to intracellular proteins. By each cell division daughter cell contains half of the CFSE relative to mother cells and this is used as indication of proliferation. PI only stains dead cells through penetrating damaged cell walls. PI binds to nucleic acids in cells intercalating to DNA. Negative PI signal is indication of intact cell membrane therefore cell vitality (λ_{ex} / λ_{em} : 535/617 nm).

PBMCs were prepared as described above and incubated with CFSE at 1 μ M/final concentration. Cells were mixed by vortexing and incubated 10 mins at 21°C in the dark. CFSE labelling was stopped by adding 5 x volume of complete media chilled in 4°C. Cells were washed three times with complete media and cultured with metal alloys at concentrations of (20, 100 and 200 μ g/L) or staphylococcal enterotoxin B (SEB), (Sigma, S4881) at 5 μ g/mL final for 6 days. On day 6, PI was added to a final concentration of 10 μ g/mL. Cells were acquired on a flow cytometry instrument (Accuri C6, BD

Biosciences). Data was analysed using FlowJo version 7.6.4. (TreeStar Inc) proliferation curve fitting algorithm.

5.2.5 Assessment of cytokine production

Cells were cultured as described above using XTT protocol. After a 6 days of culture period 100 µl of culture supernatants were collected and frozen at 80°C until used. Levels of cytokine production by cells that exposed to metal particles were measured with a commercial kit Procarta 10-Plex Human (Cat No: EPX100-14040-801). Analysis of Leptin, GM-CSF, IFN- γ , IL-1 β , IL-10, IL-6, M-CSF, OPG, sRANKL and TNF- α were conducted according to manufacturer's instructions (detailed in Chapter 4). Assays were read in Luminex 200 system, methodology is also described in Chapter 4.

5.2.6 Statistics

The treatment groups were compared with one way ANOVA and Dunnett's Multiple Comparison Test was applied as post hoc analysis for collective comparison. The individual treatment group comparison was conducted by unpaired, two-tailed Student t test with 95% Confidence Interval using GraphPad Prism.

5.3 Results

In vitro generated Ultima alloy particles were measured for size and particle number as a colloid suspension. Fig 5-3 shows size distribution for the colloid suspension. It was observed that almost all particles were in nano-size scale with a mean of 256 (± 124) nm and mode 183 nm. Particle number in the suspension was also calculated and found to be 6.97×10^6 particles/ ml. This equates around 7×10^4 particles in 10 μg , 3.5×10^5 particles in 10 μg dose and 7×10^5 particles in 100 μg treatment concentrations. A representative result displayed in Fig 5-3 also details the instrument settings.

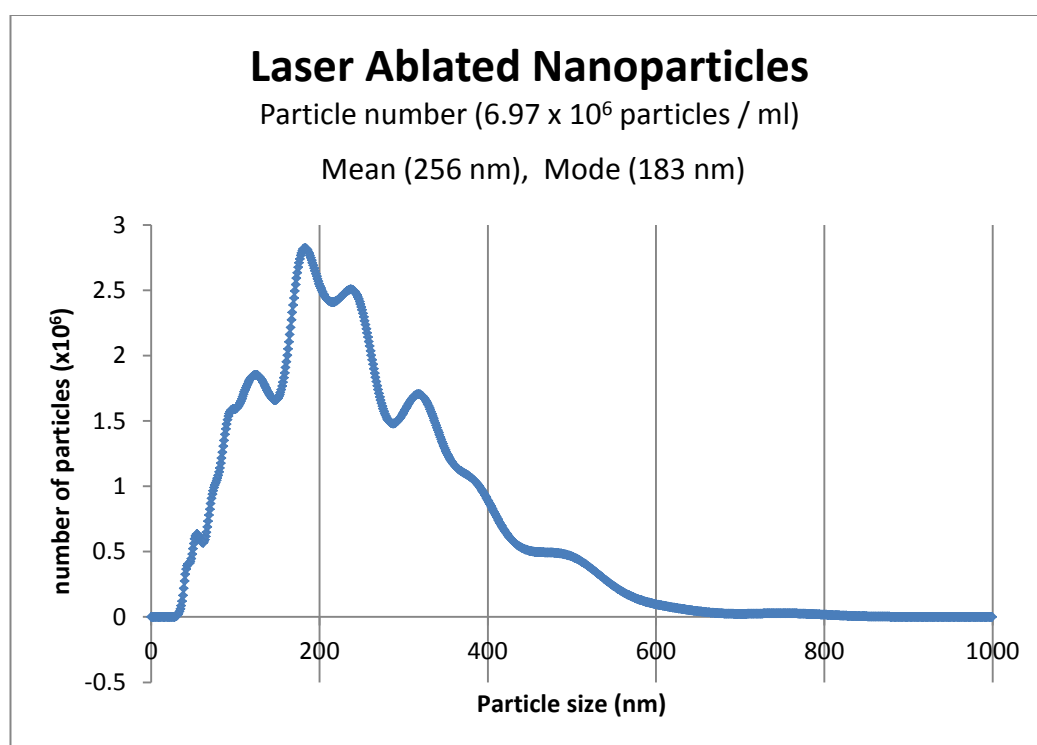


Figure 5-3: Co-Cr-Mo metal alloy particle size and number distribution

Characteristics of the metal colloid suspension were measured with NanoSight using the settings; camera shutter: 30 ms, camera gain: 560 V, Frame rate 30 fps, temperature 23.1 $^{\circ}\text{C}$, viscosity: 0.929 centipoise (cP). Particles size was calculated frame by frame and plotted against the number of particles of that size (measured between 10-1000 nm).

PBMCs were cultured with metal alloy suspension at 100 µg/L final concentration and incubated for 2, 24 or 48 hours. This concentration of metal particle treatment was chosen for two reasons; first at lower concentrations it was not possible to visualise metal particles in cells by TEM, so specificity of the affect was not clear. Second this concentration was found to be detrimental for lymphocyte activity where proliferation of the PBMCs was ceased therefore, metal particles at 100 µg/L concentration thought be appropriate to investigate.

Cells types were identified by morphology using TEM. Macrophages characterised by size and lobular nucleus taking up around 2/3 of cytoplasm (Fig 5-4 A). Lymphocytes are characterised by being smaller in size compared to macrophages, however they contain larger rounded nucleus which covers around 80% of the cytoplasm (Fig 5-4 B). Metal alloy particles were imaged by themselves and found to be mainly spherical in shape (Fig 5-4 C & D). Particles were between 50-200 nm in size, consistent with NanoSight readings (Fig 5-3).

Metal alloy particle affect on PBMCs were assessed by comparing with non-treated cells over same period of time. The time course experiment revealed that non-treated cells remained healthy with cell and nuclear membranes appearing intact with no cytoplasmic extraction evident (Fig 5-5 A, C & E). On the other hand metal-treated cells displayed vacuolisation of plasma by 2 hours (Fig 5-5 B). The integrity of the cells was compromised; evident by disintegrated cell and nuclear membranes at 24 hours (Fig 5-5 D). 48 hours of incubation resulted in the death of majority of the monocytes (Fig 5-5 F). These changes in cellular structure were confined to monocyte/macrophages mainly whereas lymphocytes were unaffected.

Metal alloy particles were engulfed as quickly as 2 hours by monocytic cells (Fig 5-6 A). Metal particles were mainly confined to vesicular pouches (Fig 5-6 B). Longer incubation time did not result in increased phagocytosis rate. However some cytolysis of monocyte/macrophages was observed at 48 hours (Fig 5-6 C). Also at this time point increased mitochondria size was noted which is the hallmark of necrosis.

Fig 5-7 shows a monocyte/macrophage labelled as “necrosis” in contact with a lymphocyte. Monocyte/macrophage is undergoing necrosis indicated by loss of plasma membrane and extracted cytoplasm with intact nucleus. Another monocyte is present labelled as “apoptosis” which shows typical signs of apoptosis recognised by condensed chromatin in the nucleus and shrunk cell size. This is probably displaying an early apoptotic stage since signs of late apoptotic cellular events were not present i.e breakdown of nuclear membrane and formation of apoptotic bodies. However surrounding lymphocytes appeared unaffected with both plasma and nuclear membrane intact and do not show any signs of necrosis or apoptosis. Some of the lymphocytes were very close to the monocyte/macrophage showing cell-to-cell contact after uptake of particles, suggesting potential antigen presentation in progress (Fig 5-7).

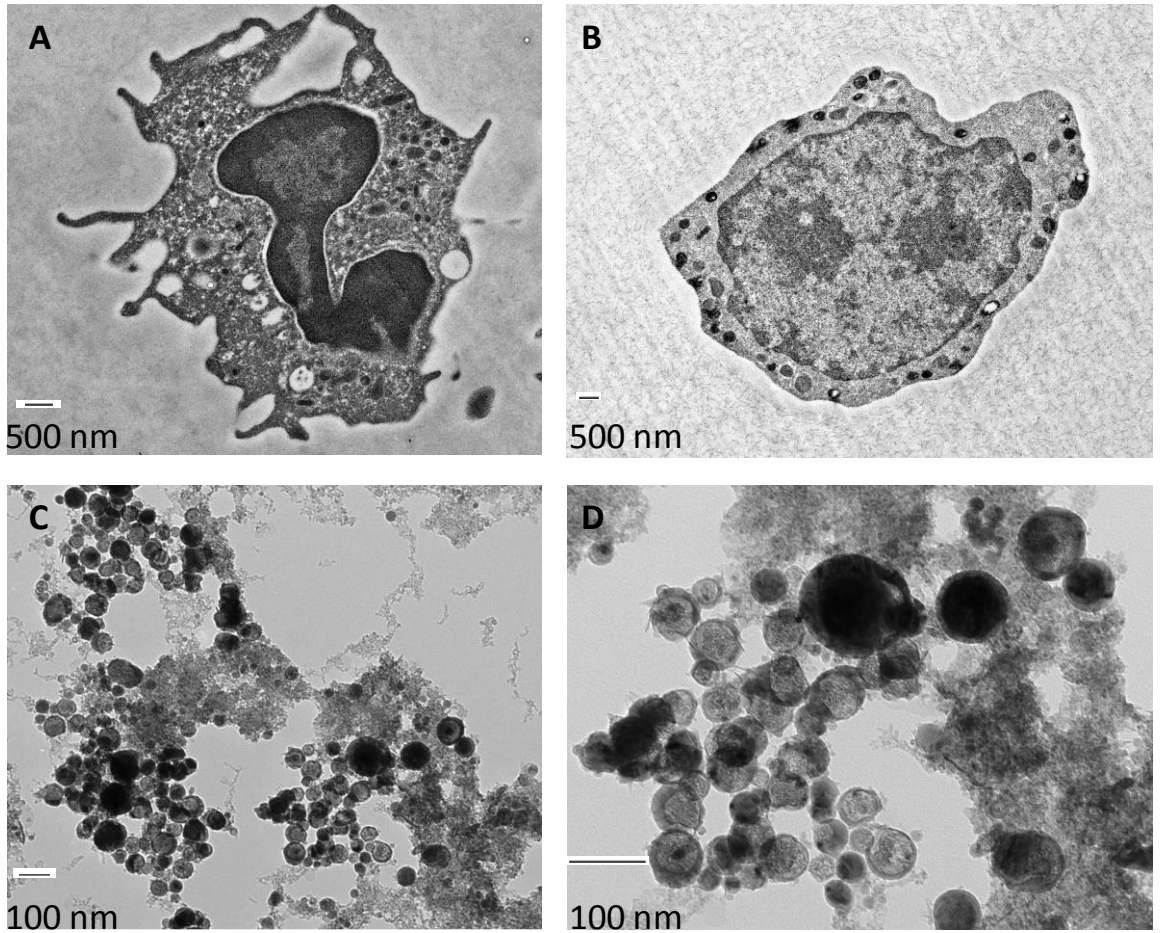
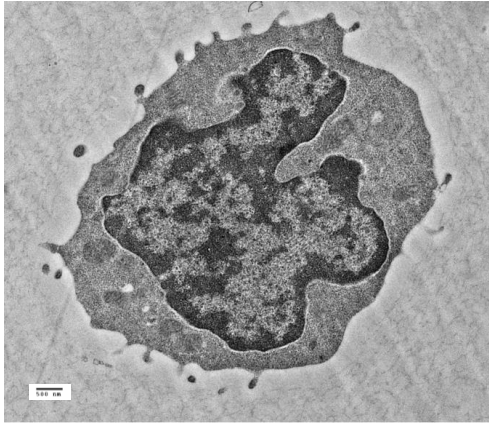


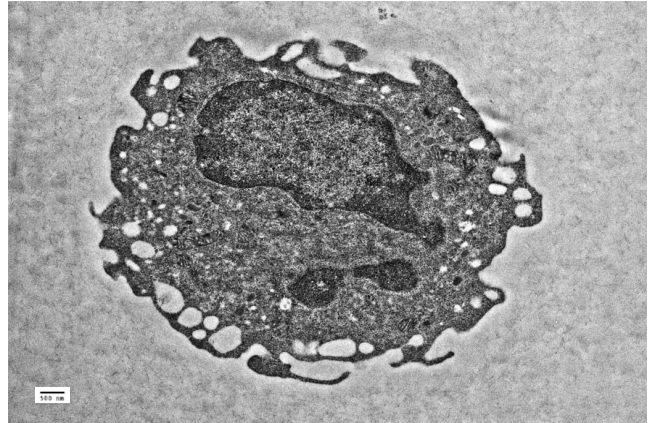
Figure 5-4: PBMC and metal alloy particle morphology

Representative TEM micrographs are displaying typical cell types within PBMCs and metal alloy particles alone **A:** A macrophage displaying characteristics of this cell type lobular nucleus and dendrites branched from cytoplasm which is typical for activated macrophages **B:** A lymphocyte characterised by cells size, smooth cell membrane and larger nucleus/cytoplasm ratio. **C:** Whole particles were placed on plastic coated grids and imaged unstained. Metal alloy particles by themselves. Varying in size, and shape (oval and spherical). **D:** Showing zoomed in version of metal alloy particles displaying electron dense spheres with varying strength of density.

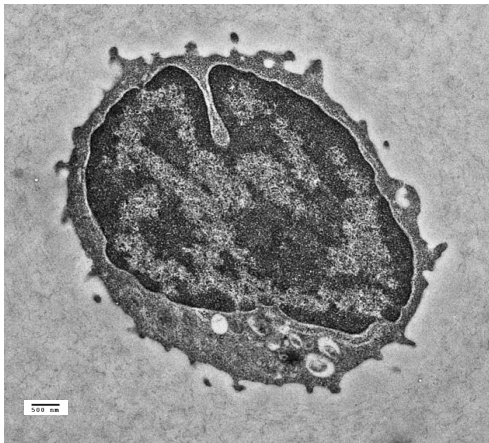
A: 2 hours PBMCs alone



B: 2 hours PBMCs + particles



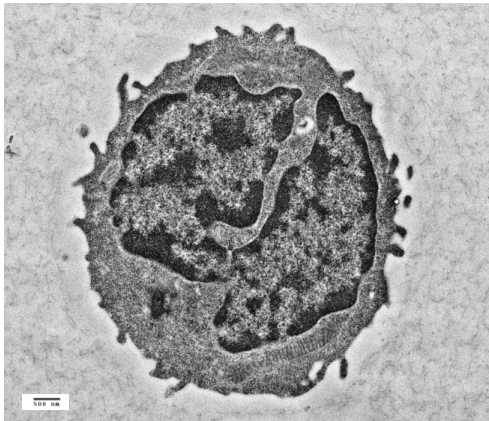
C: 24 hours PBMCs alone



D: 24 hours PBMCs + particles



E: 48 hours PBMCs alone



F: 48 hours PBMCs + particles

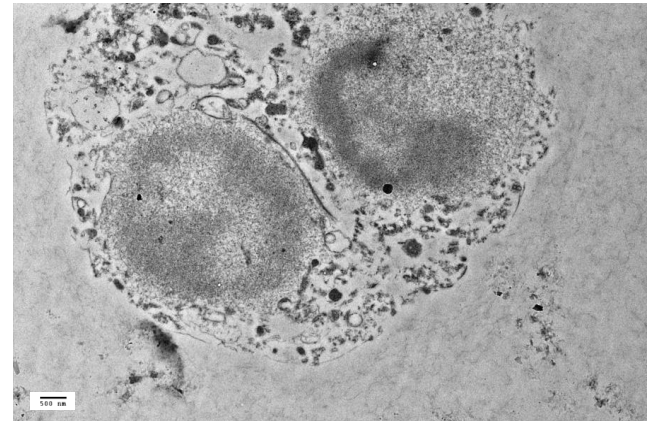


Figure 5-5: Time course treatment of PBMCs with metal alloy particles

PBMCs were cultured with and without metal particles to visualise metal particle effect on them by TEM. Monocytes/macrophages were photographed at 2, 24 and 48 hours. **A:** monocytes in culture for 2 hours. **B:** Monocytes plus metal particle culture. **C:** Monocytes in culture for 24 hours. **D:** monocytes plus metal particle culture. Cells are starting to show necrotic stage, evident with vacuolised cytoplasm. **E:** monocytes are shown after 48 hour of PBMCs cell culture alone. **F:** PBMCs cultured with metal particles; loss of cytoplasmic and nuclear membrane inflicted by metal particle exposure for 48 hours resulting in cell death.

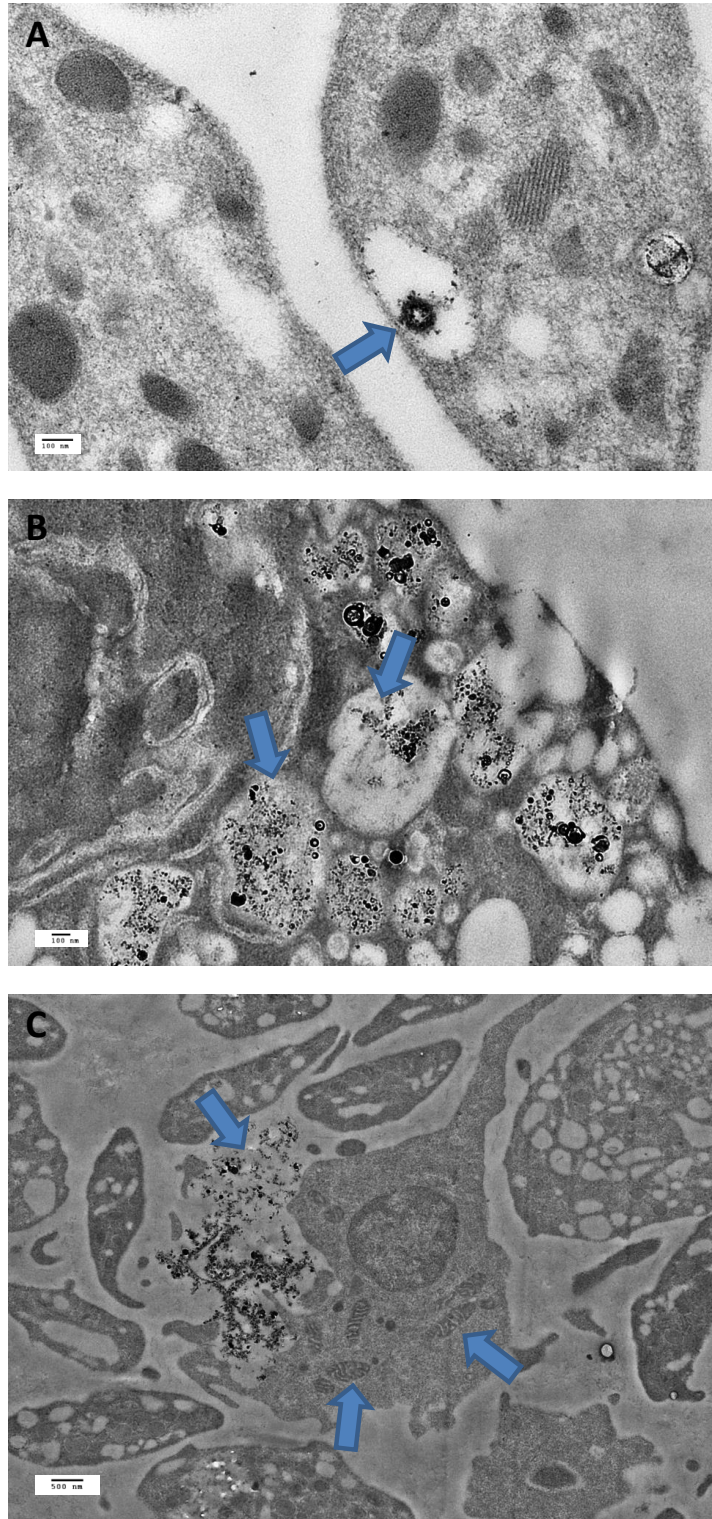


Figure 5-6: Metal particle phagocytosis and its impact on monocytes/macrophages

TEM images showing electron dense (visualised dark) metal particles and their cellular uptake by monocytes/macrophages. **A:** A macrophage showing recently endocytosed metal alloy particles (arrow) at 2 hours incubation time **B:** extensive engulfment of metal particles by monocytes, confined to vesicles indicated by arrows. **C:** A macrophage in the processes of containing metal particles; healthy looking cytoplasm and several active mitochondria are present (arrows). Neighbouring cells displaying high levels of cytoplasmic vacuolisation plus loss of nucleus and mitochondrial structures.

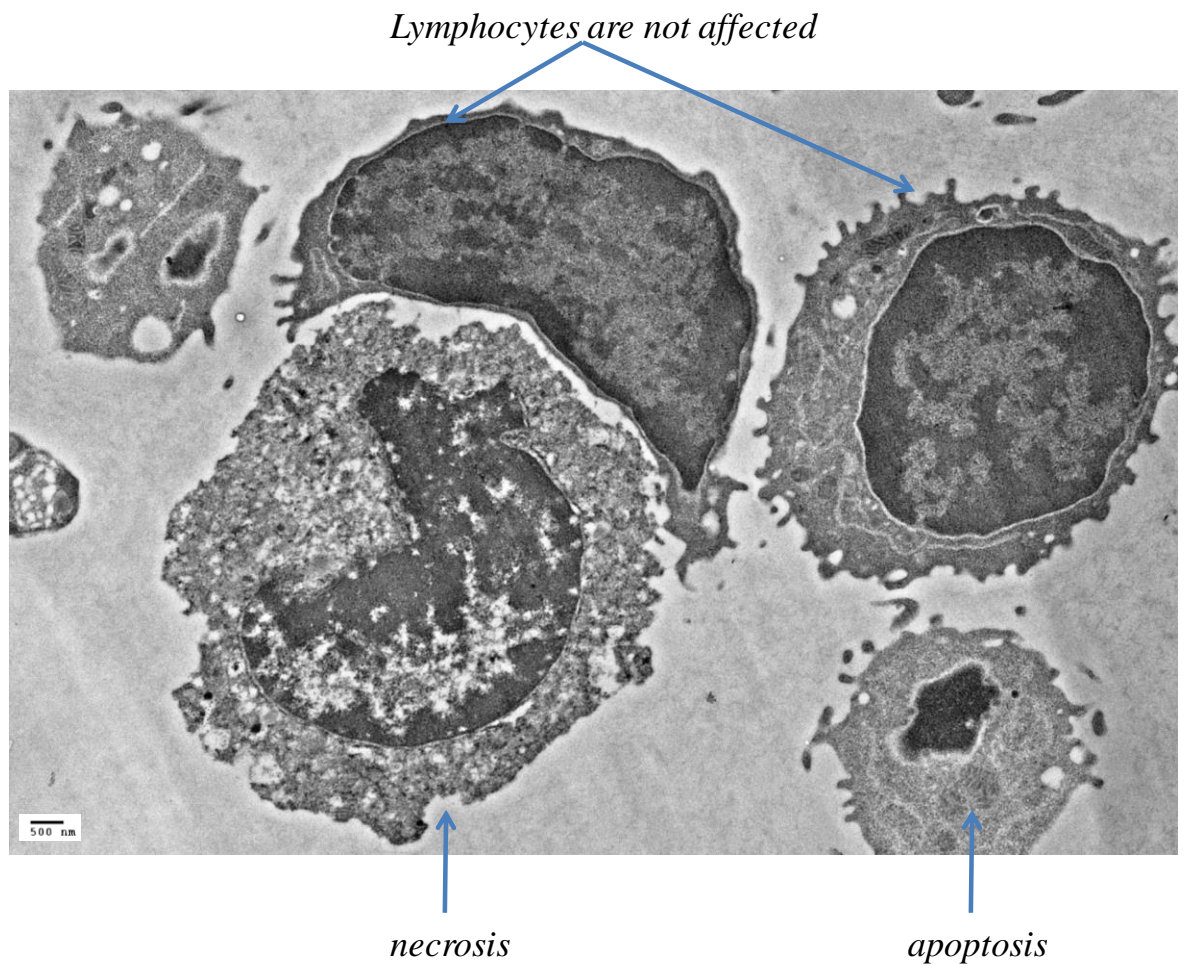


Figure 5-7: Cell toxicity, necrosis and apoptosis after metal particle exposure

Figure is showing a representative image of cells within PBMC population and their interactions after metal particle exposure, visualised by TEM. The micrograph is depicting metal particle impact on cells and interaction between lymphocytes and macrophages. A macrophage is undergoing necrosis (arrow) showing classical signs; enlarged cell size and collapse of the plasma membrane. The cell's integrity is compromised and is displaying highly vacuolated cytoplasm. Another macrophage is going through apoptosis (arrow) as characterised by dense chromatin and shrunken cell size. This cell is probably at an early stage of apoptosis since cellular fragmentation is not yet evident and no sign of apoptotic bodies. On the other hand lymphocytes appear to be morphologically unaffected by metal particles.

The metal alloy particles were studied for their potential stimulatory effects on PBMCs using physiological concentrations seen in metal implant patients (10, 50 and 100 µg/L). Particles were generated by a laser ablation technique at a concentration 100 mg/L measured by atomic absorption spectroscopy and diluted with media to achieve the treatment concentration used in this study. Assay optimisation was carried out with these concentrations plus negative (PBMC only) and positive (PHA) controls. Proliferation assays were used as a measurement of lymphocyte reactivity.

A time course experiment was carried out to assess the optimal response time for PBMC proliferation using XXT assay. Cell cultures were incubated for 1, 2, 3 and 6 days with increasing concentrations of metal particles (Fig 5-8). There technical repeats were conducted.

Low concentration metal particle treatment (10 µg/L) resulted in an increased proliferation response at day 2 compared to non-treated PBMCs ($p = 0.023$). This effect was even more prominent at day 3 ($p = 0.0072$) and reaching its peak at day 6 ($p = 0.0007$). On day 6 the stimulating effect of this concentration was even greater than positive PHA control ($p = 0.0044$).

Intermediate concentration metal particle treatment (50 µg/L) was also stimulatory to PBMCs up to day 3 ($p = 0.0003$) but this effect was slightly decreased by day 6 compared to negative control ($p = 0.0054$) (Fig 5-8).

High concentration metal particle treatment (100 µg/L) produced detrimental effects on PBMC proliferation (Fig 5-8). The number of viable cells with this treatment concentration was not statistically different from PBMCs only cells. However, it was considerably lower than all other treatment groups. This indicates there was no expansion of PBMCs at this concentration.

The results of optimisation experiments revealed that 6 day cultures were optimal in assessing metal particle impact on PBMCs. This time scale is also representative of the time lag associated with antigen specific responses *in vivo* and used as the standard culture time for measurement of lymphocyte proliferation in DTH responses. Because the donors are believed not to be pre-sensitized with these particles beforehand the results seen in this study is an indication of generic mechanism against metal ions/particles that has resulted in exorbitant proliferation response.

The assessment above was repeated using different donors to identify any host-related differences in response to metal particles. Again a similar pattern of response was noted in different donors (Fig 5-9 A). Low concentration metal particle treatment (10 µg/L) showed high stimulatory capacity compared to non-treated cells ($p = 0.0055$). The proliferation response was also higher with intermediate concentration metal particle treatment (50 µg/L) compared with non-treated cells ($p = 0.0211$). However, high concentration metal particle treatment (100 µg/L) showed no stimulatory effect on PBMCs as measured at day 6.

The Stimulation Index (SI) was calculated by dividing treatment response value by negative control value of non-treated cells. Mean SI values were found to be 3.181 for 10µg/L concentration, 2.079 for 50 µg/L concentration, 1.193 for 100 µg/L concentration and 3.342 for PHA. These results indicate that 10 µg/L concentration activated immune cells as well as PHA positive control (Fig 5-9 B).

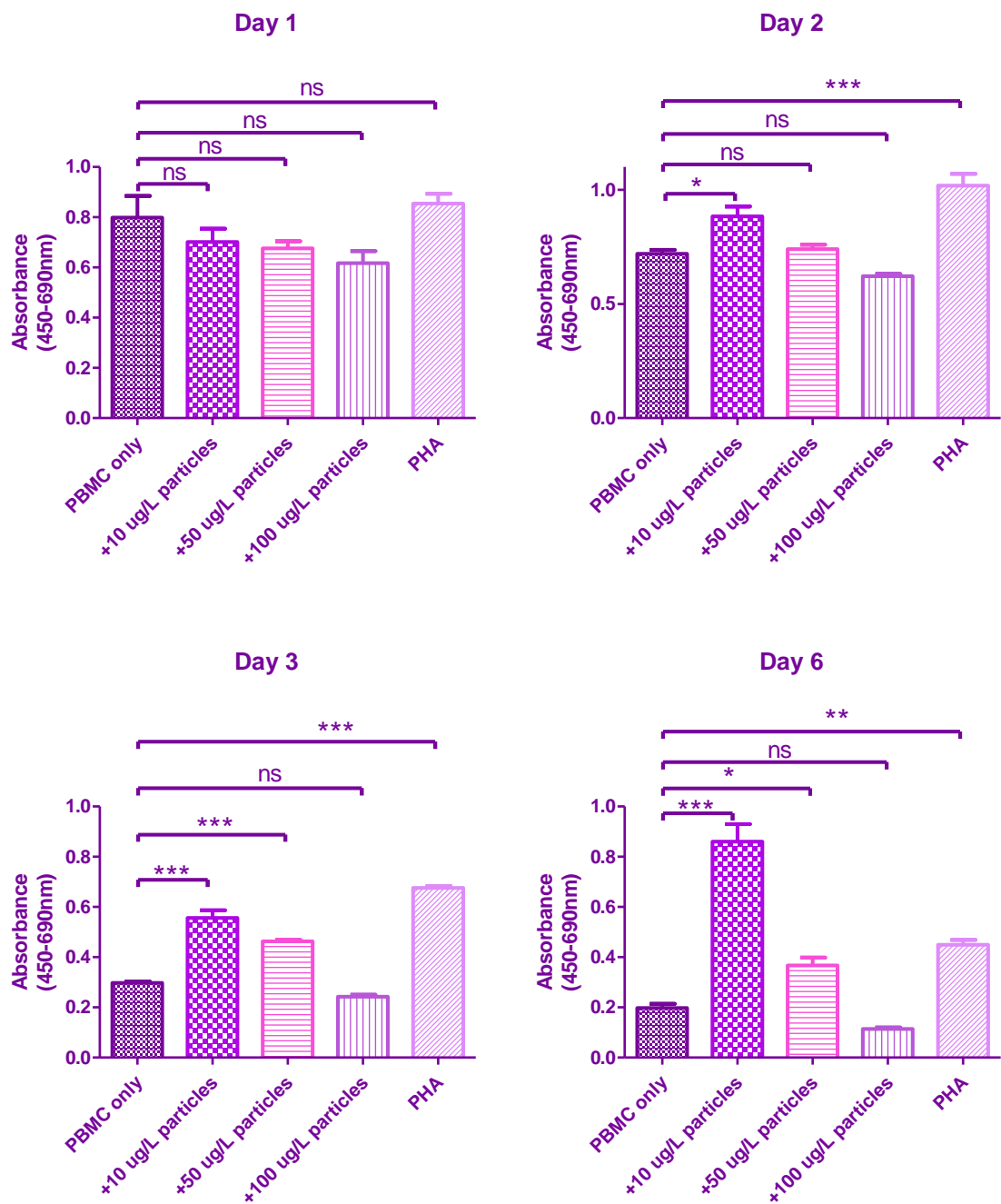


Figure 5-8: PBMC response to metal alloy particles

Cellular proliferation as determined by XTT was assessed at different time points (Day 1, 2, 3 and 6). Three different particle concentrations were used. Control cultures consist of PBMC only (negative control) and PBMC+PHA (positive control). Results showing a representative donor with 3 technical replicates.

ns ($p \geq 0.05$), * ($p \leq 0.05$), ** ($p \leq 0.01$), *** ($p \leq 0.001$), **** ($p \leq 0.0001$)

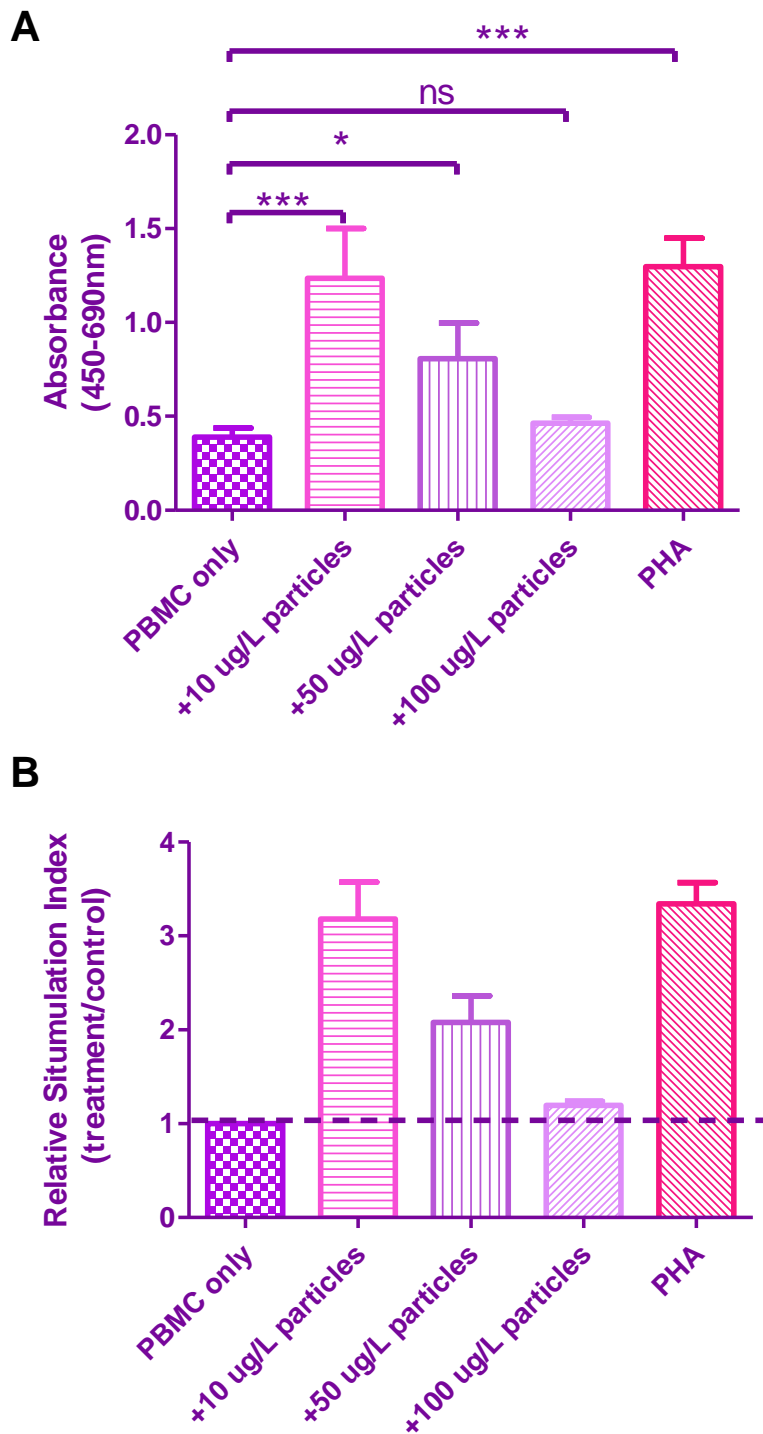


Figure 5-9: Stimulation Index after metal alloy particle induced proliferation

PBMCs were cultured with increasing concentration of metal alloy particles for 6 days and cell proliferation was measured by XTT. **A:** Proliferation response after treatment 10, 50 and 100 $\mu\text{g/L}$ metal alloy particles. **B:** Relative stimulation index determined by dividing treatment cell response by control PBMC only. $n = 3$ with three technical replicates.

ns ($p \geq 0.05$), * ($p \leq 0.05$), ** ($p \leq 0.01$), *** ($p \leq 0.001$), **** ($p \leq 0.0001$)

In order to measure cell viability and identify individual proliferation cycles after metal particle exposure a PI+CFSE assay was conducted. PBMCs were cultured with metal particles (20, 100 and 200 $\mu\text{g/L}$) or SEB (5 $\mu\text{g/mL}$) as positive control for 6 days. Fig 5-10 shows the gating strategy adopted for this acquisition. A consecutive gating was applied to flow data as follows;

- 1) Singlet cell population gated utilising FCS-Area versus FSC-Height (Fig 5-10 A)
- 2) Lymphocyte gate constructed with FSC-Area versus SSC-Area (Fig 5-10 B)
- 3) Negative PI staining to differentiate live from dead cells (Fig 5-10 C)
- 4) Live cells gated and analysed for proliferation index (Fig 5-10 D)

Live/dead staining with PI revealed that there were no significant differences in the frequency of dead cells between different treatment groups (Table 5-1). After 20 $\mu\text{g/L}$ concentration of metal particle treatment 95.2% of the cells were alive at day 6. This was very similar for 100 $\mu\text{g/L}$ treatment (94.5%) and 200 $\mu\text{g/L}$ treatment (93.7 %) concentrations within lymphocyte population.

The Proliferation Index (PI) was calculated within the “proliferating” gate (Fig 5-10 D) and results are depicted in Table 5-2. The 20 $\mu\text{g/L}$ treatment concentration produced a lymphocyte proliferation index rate at 2.070 which declined to 1.903 with 100 $\mu\text{g/L}$ concentration. The further decline was evident with 200 $\mu\text{g/L}$ concentration at 1.783 of proliferation index.

Fig 5-11 depicts results for the effect of different treatment concentration on PBMCs. The 20 $\mu\text{g/L}$ concentration resulted in 6 cycles of division (Fig 5-11 A) whereas this was reduced to 4 with 100 $\mu\text{g/L}$ concentration (Fig 5-11 B) and there were only 2 cycles of division with 200 $\mu\text{g/L}$ (Fig 5-11 C). Fig 5-11 D shows treatment with SEB, positive

control where 7 cycles of proliferation was seen. It was noted that there was a subpopulation of lymphocytes going through high proliferation rate at peak 4 (10^5 signal). This equates around 2 days of culture (lymphocyte dividing rate is around 12 hours). This is an indication of a subset of lymphocytes are reacting to the metal particles similar fashion to reacting to SEB hence same peak was also present with SEB treatment (Fig 5-11).

These results indicate that metal particles do not cause cell death within the lymphocyte population. This is also in agreement with TEM images in this study where lymphocytes were unaffected morphologically (Fig 5-7). The 20 $\mu\text{g/l}$ concentration of metal particle has a stimulatory effect on lymphocytes and this effect was reduced at concentrations of 100 $\mu\text{g/L}$ and higher. The lymphocytes are only proliferative cells within PBMC culture therefore proliferation that observed can be solely attributed to this population. This effect may be due to APC activation by metal particles and subsequent effect on lymphocytes induced by antigen presentation cells i.e monocytes. Alternatively, metal particle might have activated lymphocytes directly. To dissect these two different mechanisms further studies are required studding different cell subpopulations.

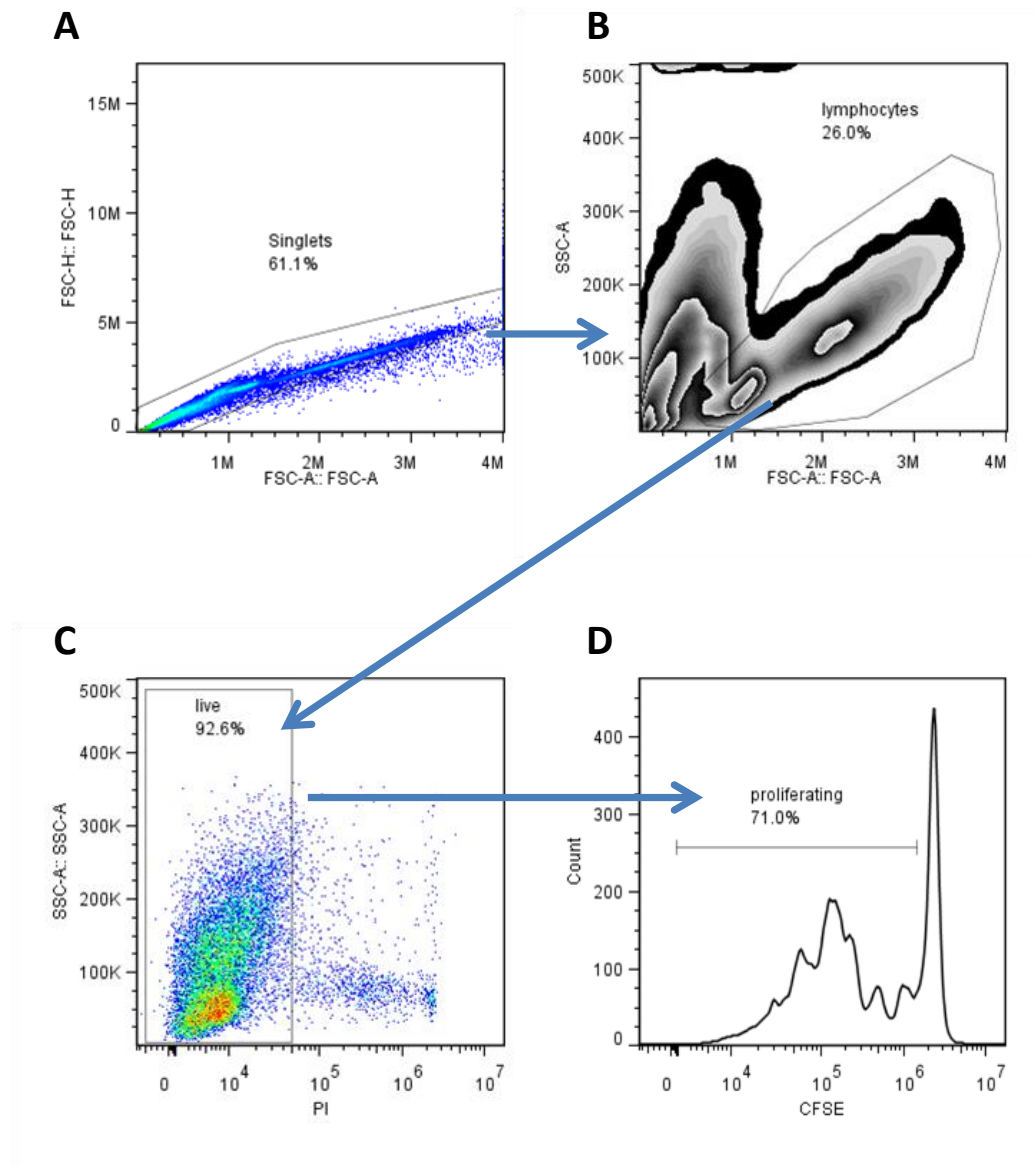
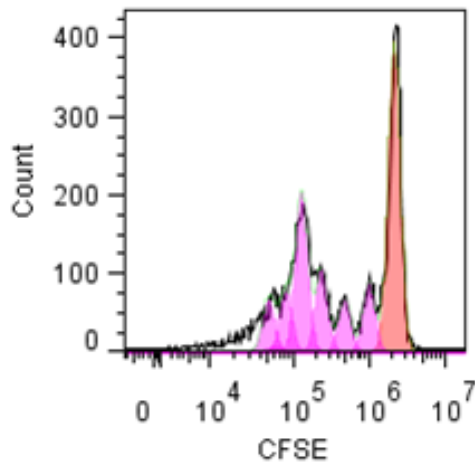


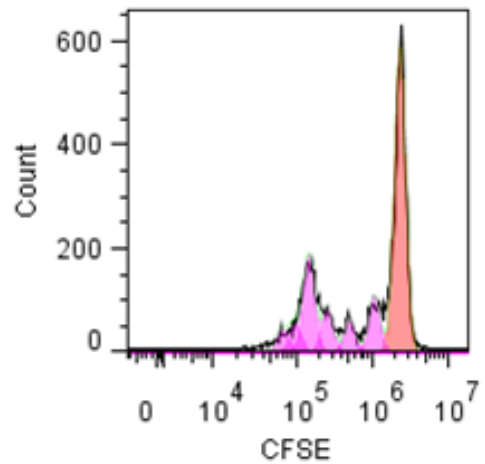
Figure 5-10: CFSE Gating Strategy

A: Cells were cultured for 6 days during which some aggregation can occur in cell population therefore it was necessary to exclude doublets and aggregates. Cells are spherical in shape such that their diameter is proportional to cross section area; plotting Height versus Area creates a correlation line for single cells. Deviations off this line occur when cells stick together and they appear as outliers from the line. “Singlets” gate was drawn around this line. **B:** lymphocytes identified by their SSC vs FCS characteristics. In a culture two separate lymphocyte populations were observed, small lymphocytes which are dormant and larger lymphocyte which are proliferating as indicated by larger FCS showing size expansion and larger SSC showing increased granularity during mitosis. Small and large lymphocytes were gated together as “lymphocytes”. **C:** PI stains dead cells; negative PI staining identifies live cells. Therefore PI negative cells were gated as “live”. **D:** CFSE signal in FL1 channel displaying proliferated/proliferating lymphocytes where the frequency of 7-8 generation of daughter cells was calculated.

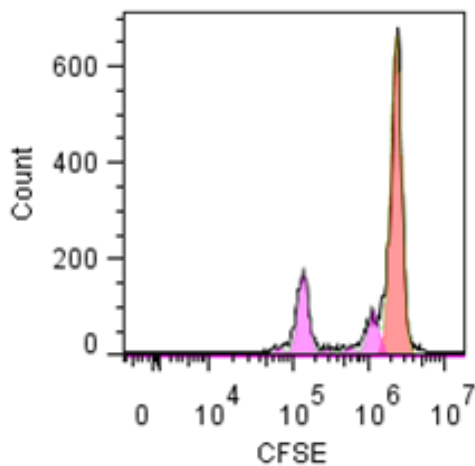
A: 20 $\mu\text{g/L}$



B: 100 $\mu\text{g/L}$



C: 200 $\mu\text{g/L}$



D: SEB

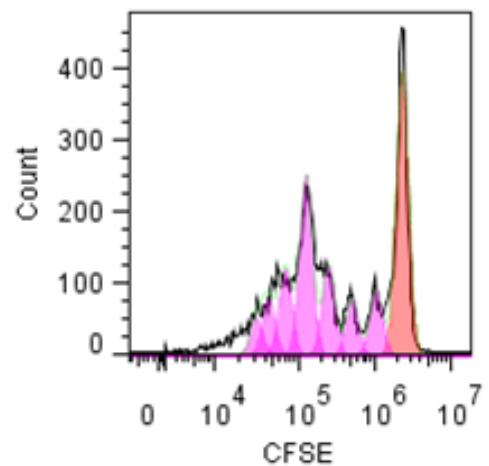


Figure 5-11: PBMC proliferation assessed by CFSE staining

PBMCs were treated with different concentrations of metal particles and incubated for 6 days. CFSE staining was conducted on day one and on day 6 cells were analysed for proliferation response. Data was fitted using the Watson (Pragmatic) model in FlowJo version 7.6.5. **A:** 20 $\mu\text{g/L}$ metal particles **B:** 100 $\mu\text{g/L}$ metal particles **C:** 200 $\mu\text{g/L}$ metal particles **D:** SEB at 5 $\mu\text{g/mL}$

Table 5-1: Live/Dead staining with PI

Frequency of cells	Treatment concentrations			
	20 µg/L	100 µg/L	200 µg/L	SEB (5µg/mL)
Live cells	95.2%	94.5%	93.7%	95.6%
Dead Cells	4.73%	5.37%	6.12%	4.27%

Table 5-2: Proliferation Index calculated after CFSE staining

	Treatment concentrations			
	20 µg/L	100 µg/L	200 µg/L	SEB (5µg/mL)
Mean Proliferation Index (±SD)	2.070 (±0.02646)	1.903 (±0.06110)	1.783 (±0.2139)	2.240 (±0.06928)
Mean Division Index (±SD)	0.3760 (±0.01609)	0.2773 (±0.02219)	0.1613 (±0.008386)	0.4697 (±0.01823)

In order to assess cytokine production by PBMCs after metal particle exposure (10 µg/L, 50 µg/ and 100 µg/L), culture supernatants were collected after 6 days and analysed by the Luminex system. Ten different cytokine levels were investigated; GM-CSF, IFN-γ, IL1-β, IL-10, M-CSF, OPG, sRANKL, TNF-α, IL-6 and Leptin. Leptin was undetectable in all samples hence this analyte was excluded from further analysis. IL-6 was high in all samples with all treatment concentrations. It was no possible to differentiate treatment effect on immune cells therefore this analyte was also excluded from further analysis. Leptin and IL-6 were concluded not to be confounding factors on PBMC functions upon particle exposure. Therefore the remaining eight analytes were analysed further.

Analysis was conducted using three different donors. Low concentration metal particle treatment (10 µg/L) did not show increased levels of cytokine production for the analytes GM-CSF, IFN-γ, IL1-β, IL-10, OPG and TNF-α compared to non-treated cells. However levels of M-CSF (233.8 ± 53.25 , $p = 0.0016$) and sRANKL (39.09 ± 11.15 , $p = 0.0037$) were increased with this treatment concentration (Fig 5-12, Table 5-3).

Intermediate concentration metal particle treatment (50 µg/L) produced an altered cytokine secretion profile of PBMCs where levels all seven cytokines were statistically significant compared to non-treated cells apart from IL-10 (Fig 5-12, Table 5-3).

High concentration metal particle treatment (100 µg/L) induced elevated levels of cytokine release from PBMCs for all eight analytes analysed (Fig 5-12, Table 5-3). IL-10 production was also increased at this treatment concentration to 60.91 ± 26.77 pg/ml from 7.984 ± 5.498 of low concentration of particle treatment ($p = 0.0285$).

Cytokine release assay showed a dose dependent response for all eight analytes analysed where increased metal particle concentrations resulted in increased cytokine production of PBMCs. This increase was statistically significant for M-CSF and sRANK-L at the 10 $\mu\text{g/L}$ concentration whereas increased treatment concentrations of 100 $\mu\text{g/L}$ resulted in statistically significant levels of cytokine production for all analytes. These results indicate that leukocytes are reactivated by metal alloy particles and the immune reactive concentration was determined to be 10 $\mu\text{g/L}$. This reaction might be mediated by M-CSF and RANKL in the first instance however increased treatment concentration resulted in a more heterogeneous response which involved several cytokines.

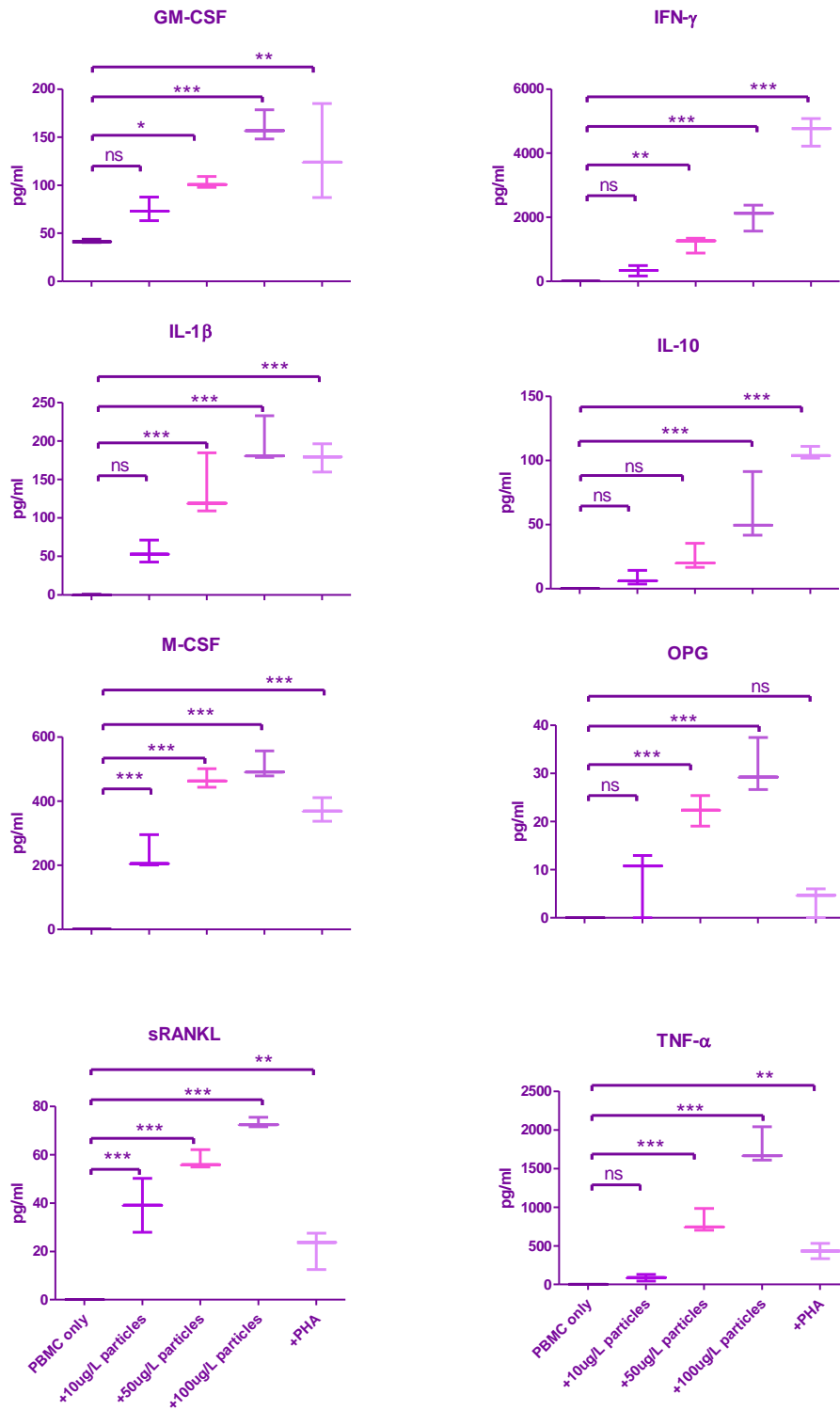


Figure 5-12: PBMC cytokine secretion after exposure to metal alloy particles

Culture supernatants were collected and assayed on the Luminex platform to determine PBMC cytokine production following metal alloy exposure. Production of cytokine is represented in pg/mL and values are shown by whisker plots displaying min to max with mean. n = 3 biological/ 2 technical replicates.

ns (p ≥ 0.05), * (p ≤ 0.05), ** (p ≤ 0.01), *** (p ≤ 0.001), **** (p ≤ 0.0001)

Table 5-3: Cytokine production of PBMCs cultured with metal particles

Cytokine levels in culture supernatants mean value pg/mL (\pm SD) n = 3 biological/ 2 technical replicates					
	PBMC only	+ 10 μg/L metal	+ 50 μg/L metal	+ 100 μg/L metal	+ PHA
GM-CSF	41.82 (1.784)	74.55 (12.31)	102.5 (5.812)	161.2 (15.51)	132.0 (49.44)
IFN-γ	0.2793 (0.1343)	330.5 (160.3)	1166 (247.6)	2024 (413.6)	4691 (435.8)
IL-1β	0.3042 (0.4296)	55.57 (14.37)	137.8 (40.94)	197.5 (30.70)	178.5 (18.45)
IL-10	ND	7.984 (5.498)	23.96 (9.948)	60.91 (26.77)	105.6 (4.795)
M-CSF	ND	233.8 (53.25)	469.1 (29.39)	509.0 (41.69)	372.3 (36.76)
OPG	ND	7.915 (6.939)	22.27 (3.170)	31.13 (5.639)	3.579 (3.170)
sRANKL	ND	39.09 (11.15)	57.68 (3.905)	73.21 (2.116)	21.27 (7.828)
TNF-α	ND	86.94 (44.62)	810.8 (151.4)	1773 (233.9)	433.4 (98.83)

ND: Not detectable

5.4 Discussion

This *in vitro* study showed that Ultima alloy particles were immunologically active and capable of inducing lymphocyte proliferation demonstrated by CFSE+PI assay. This was particularly evident with 10 µg/L treatment concentration whereas concentrations higher than 100 µg/L resulted in detrimental effects on lymphocyte proliferation. Increased lymphocyte expansion rate after stimulation is a hallmark of immune system activation. Cytokine production profile substantiated this finding where non-treated cells produce very little or no cytokines however metal particle-treated cells produced several cytokines in a concentration dependant manner.

High concentrations of metal particles (100 µg/L and 200 µg/L) did not adversely affect lymphocyte survival. However cells could not proliferate any longer, suggesting the functional mechanism was halted after metal exposure in these cells. Serum levels of metal ions are generally lower than that used to challenge PBMCs in the current study. However it was deemed that metal challenge concentrations used in this study are clinically significant because metal concentration of peri-prosthetic environment is highly elevated [65] and estimated to be an order of magnitude higher locally compared to serum levels.

At high concentrations particles might be toxic to monocytes/macrophages but not to lymphocytes. After exposure to 100 µg/L of metal particles, TEM images revealed that macrophages uptake particles readily resulting in necrosis of these cells. Necrosis is an inflammatory process and results in activation of other immune cells. This might be one of the mechanisms, another one could involve a more specific route of antigen presentation. If lymphocyte activation by metal particles requires antigen presentation by APCs; necrotic status of macrophages might be the reason why lymphocyte proliferation was limited at higher concentrations.

There were also some apoptotic cells observed. TEM provides the analysis of sectioned specimens and allows qualitative output. The number of cells that can be processed for imaging is very limited therefore quantitative data is not possible. However it appeared that apoptotic cells were less frequent than necrotic cells, whether this is representative of entire sample cannot be established. Regardless how cells die, maintenance of normal functions in the multi-cellular organism dictates that dying cells are cleared by phagocytes. Metal particle-induced necrosis/apoptosis of macrophages in large scale would result in inefficient clearance of cellular debris. Defective clearance may contribute to persistence of inflammation and subsequent pathologies.

Samples tested in these experiments were donated by healthy individuals with no metal implant *in situ* nor any known metal allergy. Therefore the expansion seen in lymphocytes is most likely due to *de novo* activation of these cells which suggests a primary activation rather than a memory response. Previous studies have shown that people with no implants or metal sensitivity do not display activation of immune cells after a metal challenge [204], whereas subjects with a history of metal sensitivity respond to metal challenge strongly via T and B cells [65] suggesting the immune activation involves adaptive arm of immune system. In the current study it is demonstrated that metal challenge also induces a lymphocyte-mediated immune response in donors without a history of metal sensitivity. However, it is not known whether activation of lymphocytes is caused directly by metal particles or indirectly by accessory cells due to metal particles effect on these cells. It has been shown in the current study that metal particles are phagocytised and processed by macrophages. Therefore, it could be postulated that metal particles alters antigen presentation and results in subsequent lymphocyte activation.

It was striking to note that low concentrations of metal particles induced stimulation comparable to mitogen driven responses. Metal particles may act as super-antigen hence

the response observed was much stronger than any potential antigen-specific response would be. The exact molecular mechanism of this activation was not investigated. However one could postulate a haptens effect after coupling to serum proteins might be possible. It has been demonstrated that metal ions couple with serum proteins such as albumin [205] [206]. Rachmawati *et al* showed that Cobalt activates dendritic cells through direct TLR-4 ligation whereas chromium mediated activation requires tissue-derived cofactors to induce clinical sensitization [207] . To be able to identify the exact mechanism of metal recognition the immunogenic epitopes need to be identified first. This was not possible within the scope of the current study. In the current study cells were cultured in autologous serum from donors to emulate the *in vivo* environment where the cells would be in a protein-rich milieu. The increased stimulation index after metal particle exposure suggests that serum protein coupling might be necessary for cellular uptake, however a serum-free system was not tested.

Monocyte/macrophage involvement in metal particle uptake has been demonstrated before [195, 198]. Cytokines IL-1 β , IL-6 and TNF- α were used as indicators of macrophage activation [197] in cell culture models in the absence of accessory cells. In the current study, PBMC cultures consisting of both monocytes/dendritic cells and lymphocytes were used in which lymphocyte and APC interactions can occur. Cytokine release assays showed concentration-dependent responses for all eight of the cytokines analysed where increased metal particle concentration resulted in increased cytokine production by PBMCs. At 10 $\mu\text{g/L}$ concentration only M-CSF and sRANKL had significantly increased levels compared to non-treated cells. T cells are known to produce these two cytokines and the presence of these stimulates myeloid lineage cells including monocytes and osteoclasts. M-CSF is necessary along with sRANKL for the complete differentiation of osteoclastic precursors into mature osteoclasts [208]. Osteoclasts are the main bone absorbing cells and

the most common indication of implant failure is peri-prosthetic osteolysis which is driven by osteoclasts. T cell activation by macrophages and subsequent M-CSF and sRANKL release might mediate osteoclast differentiation *in vivo*. Metal wear debris is believed to be continuously released from implants *in vivo* at low concentrations, however there are no reliable means of measuring the immune reactive dose of these particles *in vivo*. Normal serum levels of sRANKL range between 0.45-0.89 pg/ml [209] and in healthy individual M-CSF is present at 2.36 ± 0.18 ng/ml [210]. These levels were exceeded greatly in the current study identifying them as potential drivers of osteoclast activation and immune mediated osteolysis. This study determined the immune reactive dose to be 10 μ g/L *in vitro* and M-CSF and sRANKL might be the main drivers.

Intermediate concentration particle treatment (50 μ g/L) resulted in elevated levels of all pro-inflammatory cytokines apart from IL-10. IL-10 is an anti-inflammatory cytokine and its role in immune regulation is well established. Whereas increasing the treatment concentration to 100 μ g/L showed a statistically significant IL-10 response along with other cytokines. Both osteogenic (IFN- γ , IL-10, OPG) and osteoclastogenic (GM-CSF, M-CSF, IL-1 β , IL-6, RANKL, TNF- α) cytokine levels were raised indiscriminately in culture. This appears to be similar to the cytokine storm first described in Graft Versus host disease (GVHD) patients [211]. The current study was restricted to an *in vitro* system, the *in vivo* response might be different in metal implant failure. However, the production of IL-10 following the onset of a cytokine storm is a marker of a counter-inflammatory response that has been termed as immunoparalysis. This phenomenon is associated with down-regulation of monocyte activity. It indicates a cut-off point where the anti-inflammatory response starts to kick in at higher concentrations. A compensating mechanism is expected at higher concentrations as indicated in the current study.

Constrained proliferation capacity at higher concentrations might be due to increased IL-10 production where macrophages cannot process metal alloy particles any longer.

Catelas *et al* showed intracellular endocytosis of Cr²⁺ and Cr³⁺ ions in a macrophage cell line consisting of clusters of nanoforms. Further energy-dispersive X-ray spectroscopy (EDS) analysis revealed that nanoforms were chromium phosphate with an organic phase attached to it. Such nanoforms were not observed with Co²⁺ ions [71]. The current study also demonstrates wear particle endocytosis (Fig 5-6 A and B) at a concentration of 100 µg/L using primary immune cells. TEM images revealed that metal alloy particle uptake mainly involved monocytes, whereas lymphocytes seemed unaffected. Monocytes are phagocytic cells and comprise the first line of immune response, therefore one can expect to see monocyte driven phagocytosis.

Colognate *et al* reported that Co nanoparticles were internalised by PBMC at higher rates compared to Co²⁺ ions and that this was time dependent. They have observed an 80 fold increase at 24 hours and 140 fold increase at 48 hours determined by tracking radio-labelled Co molecules [212]. The data from the current study failed to demonstrate any time-dependent increase of metal particle uptake. However, the two testing systems are very different. The cellular uptake quantification by TEM is not possible hence the number of samples imaged is extremely limited. The lack of concentration dependent observations in TEM images might be also due to increased necrosis and apoptosis over a period of time because only the intact macrophages were imaged.

Transition metals such as Ni, Co, Cr, Palladium have been found to be potent clinical sensitisers [207]. These compounds are usually tested in elemental state or their salt forms. However, the current study used the original alloy to reproduce a more realistic scenario. Using similar sizes and shapes of metal alloy particles as seen *in vivo*, generates a more

appropriate experimental set up. The use of exogenous FCS serum was avoided to prevent xenogenic activation. Instead heat-inactivated autologous serum was used to determine the intrinsic stimulation capacity of metal alloys. Whether serum proteins are the carrier molecules for metal ions or not, the immune cells are in serum proteins naturally *in vivo*. In the current study this was assumed to be a pre-requisite and an alternative system was not tested.

To summarise, this study demonstrates that Co-Cr-Mo alloys induce a proliferative and cytokine response in PBMCs and provides evidence of immune activation. At first instance a high throughput whole population approach was utilised and followed by single cell assay of proliferation to answer initial questions. Phenotypic characterisation of PBMC subsets was not undertaken which could identify responding cell subsets. Further studies should focus on identifying affected cell subsets and their functions in metal implant failure.

6 CHAPTER 6: General Conclusions

This study investigated immunological factors in both innate and adaptive immunity that may play a role in metal hip implant failure. Orthopaedics patients were recruited and stratified into four clinical sub-groups;

- Pre-implant group as control where OA patients going through their first hip arthroplasty and never been exposed to a hip implant before.
All other three groups had a metal hip implant at the point of sample collection.
- Ultima asymptomatic group; where implant is well tolerated.
- Ultima symptomatic group; showing signs of implant failure hence going through a revision surgery
- Other symptomatic group; patients having another type of metal implant and going through a revision surgery due to implant failure.

The majority of hip implants perform well while a sub-group of THR patients experienced implant failure. This phenomenon is even more pronounced with MoM implants. Some of the patients avoided developing peri-prosthetic osteolysis whereas others did not. To investigate a potential genetic disposition for metal implant failure, HLA tissue typing was conducted in the Norfolk cohort.

Possessing certain set of HLA alleles can lead to risk of increased susceptibility to some conditions as discussed in Chapter 3. HLA molecules can present disease triggering peptides that result in disease disposition. This could be due to alterations in self-peptides or MHC molecules itself induced by metal ions. Alternatively, metal ions could influence regulatory mechanisms where presentation of self-peptides results in a disturbed homeostatic mechanism due to altered MHC presentation to regulatory cells. In the

absence of appropriate regulatory mechanisms the host would develop aberrant immune response to hip implants. On the other hand some HLA alleles might be protective against activation of immune response after hip arthroplasty where having certain haplotype helps immune response to control hypersensitivity more tightly. Missing these protective alleles within the gene pool may contribute to disturbance in regulatory functions therefore results in increased susceptibility to implant failure. Therefore HLA molecules can have a direct role in the fate of disease development.

It should also be noted that disease associated HLA molecules may not have a direct role in disease development but it might simply be a result of extensive LD at MHC loci where other linked genes to given haplotype are the cause of the disease but not HLA itself. SNPs at the location of TNF- α , IL1RA, IL-6 and MMP-1 genes were implicated to be associated with implant failure previously [213] , however there is no study reporting HLA association with osteolysis.

Strong genetic association does not necessarily mean causation. Therefore several criteria should be considered before making an assumption; such as strength of the association, biological plausibility and consistency of the results. To be able to differentiate these two phenomenon (association versus causation), functional assays need to be conducted where the role of the molecule can be tested. The first step in this direction is to identify disease associated/related determinants. To attempt to do so, 25 different MHC class II loci were typed in the current study and two alleles were found to be strongly associated with protecting from implant failure (HLA-DQA1*01:02 and HLA-DQB1*06). Heterodimers of DQA1*01:02/DQB1*06:02 confer dominant protection against type 1 diabetes (T1D) and strong susceptibility to narcolepsy [214]. The potential role of this haplotype in metal implant failure is reported for the first time through this study. The statistical testing for

these alleles withstood multiple testing correction which gives confidence in the potential biological role of these genes. Allele HLDR-DQA1*05 was found to be associated with implant failure development in the current study. However after multiple testing corrections the statistical significance was lost. This allele can be checked again with a second study in other population with a similar condition, repeated frequency results would ensure testing specificity. Multiple correction avoids type I error of getting false-positive results but it also increases the chance of getting type II errors where a genuine finding may be ruled out. Therefore a second study with *a priori* hypothesis offers the best explanation for marginal results. The degree of agreement and reproducibility of the current results needs to be confirmed with another population of people experiencing MoM hip implant failure.

The number of subjects that were studied was limited because the implant of interest was discontinued around 10 years ago. HLA molecules are encoded by many genes and there are several variations of each gene. Also high LD is present at HLA regions requiring large number of subjects to be tested. The minimum number of subjects required depends on the frequency of that allele and whether it is rare/common in both the study and control populations. Study power was calculated retro-respectively and concluded that the current study was underpowered. As it is demonstrated in the results section by the worst and the best case scenario analysis; the current study needed to recruit between twice and ten times more patients for HLA analysis depending on which alleles studied.

It was hypothesised in this study that antigen presenting cells were altered phenotypically and functionally in the failed implant patients. To test this research question an extensive immunophenotyping was conducted. The results of this work showed that immunophenotypic alterations were only present in the Ultima Asymptomatic group where there was increased numbers of activated T cells, classical monocytes and myeloid

dendritic cells. Altered numbers of immune cells have been shown in many inflammatory conditions [176, 215]. Such increase could be related to three main reasons;

- 1) Increase in differentiation from bone marrow
- 2) Expanded half-life in the periphery due to chronic stimulation
- 3) Reduced recruitment to secondary tissues.

The blood transit time of some cells might be short lived hence single point readings must not be over interpreted. However, only the Ultima Asymptomatic group showed signs of immune-activation and the results were consistent between different cell types. This outcome might be an indication of immune stimulation being protective against implant failure. On the other hand, the number of cells and expression of activation markers were within normal range for the other three groups. This might be due to the fact that in the failed groups, there is no more systemic inflammation and cells were now polarised and moved to the local site of implant. However, local inflammatory responses are expected to be reflected in the periphery to some extent, hence the scientific justification for blood phenotyping in tissue-associated inflammatory conditions and tumour biology.

The immunophenotyping approach undertaken in this study was novel as 18 different parameters were investigated simultaneously. Flow cytometry is a powerful technique which allows concurrent detection of several cell types and functional markers in large numbers. This assessment is the first of its kind in metal implant failure which uses a detailed and robust system for immune cell monitoring. Non-manipulated *ex vivo* blood samples were assayed on the same day with a perspective that it would reflect *in vivo* immune state. Immunophenotyping is a sensitive but not specific measurement therefore it

cannot pin point the causative reason for metal implant failure, however, blood dyscrasia is considered to be an indication of immune dysfunction.

Antigen presenting cells were scrutinised to an extent which has not been reported in metal implant failure previously. This investigation was supported with an assessment of soluble mediators in blood and SF with an extensive panel of osteogenic and osteoclastogenic cytokines/growth factors. Surprisingly, there was no indication of systemic inflammation in the failed implant groups substantiated by immune cells analysis and cytokine measurements. Local inflammation was measured in SF samples. There was higher levels of tested cytokines in SF compared to serum samples of matched individuals however this analysis did not substantiated any indication differences between clinical groups. This might be due to sample size being too small hence it was not possible to obtain this sample type for every patient.

Unfortunately, sampling time in these patients reflects late stages of the implant failure process where patients have been experiencing failure-related symptoms for many months or even years. This period reflects a long lag-period from the time of initial surgery when local homeostasis was first disturbed. It is likely that after major surgery of hip replacement, surgical trauma causes an inflammatory response in the peri-prosthetic tissue causing necrosis and ischaemia. In many patients, the inflammatory responses are averted and bone and soft tissue architecture is restored. However in the presence of excess implant wear, homeostasis can be disturbed and peri-prosthetic osteolysis may develop leading to aseptic loosening. The time-scale of these events is not known therefore a prospective study of well-functioning implants, monitoring immune response periodically from pre-implant to post-implant stages could provide valuable information in future studies. One of the limitations of the current study was that patients were sampled at only one time point. Pre- and post-ablution studies monitoring regulatory mechanism such as

M2 macrophages, Tregs and IL-10, TGF- β mediated pathways could provide more insight to metal implant failure.

The serum cobalt and chromium levels were also high in the Ultima Asymptomatic group which correlated with increased cells counts. The results were externally validated by comparing absolute cell readings with established normal cell counts of healthy individuals. Therefore this approach not only allows comparisons between clinical groups, but also permits comparisons against normal ranges of immune cells. Increased metal ion levels might be directly associated with increased cell counts in a well-functioning group as a result of a compensation/ regulatory mechanism.

For the reasons mentioned above this study did not look at peri-prosthetic tissue samples hence this type of sample is often only available after metal implant failure where there is almost always extensive tissue damage, hence it might be too late. An aim of the study was to develop a practical assay to monitor immune response without resulting in invasive methodology.

Following the results of immune monitoring it was noted that alterations in circulating immune cell numbers or activity are likely to be too subtle to determine *ex vivo* therefore the analysis may require an amplification which is only possible *in vitro*. For these reasons an *in vitro* testing system was set up to measure immune response to metal particles with an opinion to assess immediate effects of these particles on primary human immune cells which is something that is not possible *in vivo*. *In vitro* testing revealed that these particles were immune-reactive at low concentrations as demonstrated by T cell proliferation. The particles that were tested were generated from the Ultima implant in a form of nano-scale beads representing the original composition of Co-Cr-Mo alloys. To our knowledge this was the first attempt to use such material in assessment of these chemical's bio-inertness. It

was interesting to see that 10 µg/L concentration of metal alloy particles resulted in an immune stimulation as strong as positive mitogen controls. At these concentration levels of M-CSF and RANKL were significantly increased, both are known to be osteoclastogenic factors. The immune reactive concentration of metal alloys is determined to be 10 µg/L perhaps modulated by these two cytokines.

It has been shown with TEM images with the current study that macrophages phagocytose metal alloy particles resulting in necrosis of macrophages, however lymphocytes were unaffected morphologically. This data correlates with proliferation results where lymphocytes were proliferated after treatment with metal particles in mix cultures i.e. monocytes present. Monocytes could be involved with two different ways; initially in the attempt to clear wear debris results in necrotic bodies, cytokines, DAMPs which activates lymphocytes directly. Follow with macrophages involvement in APC-mediated lymphocyte activation. Either way macrophages deemed to be involved in the process and the results of this study provides evidence for macrophage-initiated immune activation. Increased metal particle concentrations resulted in cell proliferation arrest although lymphocytes were still viable suggesting metal ion particles are not affecting lymphocyte survival although they affect their cellular function. This aspect could be investigated in future studies by looking at cell cycle analysis and dissect which phase of mitosis might be affected. Investigation of molecular pathways involved in relevant cell cycle arrest might help to elucidate this phenomenon further.

Peri-prosthetic osteolysis resulting in implant failure considered to have multi-factorial aetiology involving genetic predisposition plus immunological dysregulation, however the exact mechanisms that is involved needs further elucidation. Therefore a broad and comprehensive investigational approach was undertaken in the current study. This study

demonstrates that immune system alterations were present in successful THR group and these mechanisms might be due to protective and homeostatic regulations. More selective and targeted approaches should follow for future studies taking into consideration of finding of the current study.

7 References

1. Zhang, Y. and J.M. Jordan, *Epidemiology of osteoarthritis*. Clin Geriatr Med, 2010. **26**(3): p. 355-69.
2. Birell, F. *Osteoarthritis: pathogenesis and prospects for treatment*. 2011; Available from: <http://www.arthritisresearchuk.org/health-professionals-and-students/reports/topical-reviews/topical-reviews-autumn-2011.aspx>.
3. UK, A.R. *Data and statistics on osteoarthritis*. 2013 2014.09.03
]; Available from: <http://www.arthritisresearchuk.org/arthritis-information/data-and-statistics/osteoarthritis.aspx>.
4. UK, A.R. *Data on osteoarthritis of the hip*. 2013 2014.09.03]; Available from: <http://www.arthritisresearchuk.org/arthritis-information/data-and-statistics/osteoarthritis/data-on-hip-oa.aspx>.
5. Pearle, A.D., R.F. Warren, and S.A. Rodeo, *Basic science of articular cartilage and osteoarthritis*. Clin Sports Med, 2005. **24**(1): p. 1-12.
6. Amin, A.R., M. Attur, and S.B. Abramson, *Nitric oxide synthase and cyclooxygenases: distribution, regulation, and intervention in arthritis*. Curr Opin Rheumatol, 1999. **11**(3): p. 202-9.
7. Wang, M., et al., *MMP13 is a critical target gene during the progression of osteoarthritis*. Arthritis Res Ther, 2013. **15**(1): p. R5.
8. Song, R.H., et al., *Aggrecan degradation in human articular cartilage explants is mediated by both ADAMTS-4 and ADAMTS-5*. Arthritis Rheum, 2007. **56**(2): p. 575-85.
9. Lark, M.W., et al., *Aggrecan degradation in human cartilage. Evidence for both matrix metalloproteinase and aggrecanase activity in normal, osteoarthritic, and rheumatoid joints*. The Journal of Clinical Investigation, 1997. **100**(1): p. 93-106.
10. Martel-Pelletier, J., *Pathophysiology of osteoarthritis*. Osteoarthritis Cartilage, 2004. **12 Suppl A**: p. S31-3.
11. Kapoor, M., et al., *Role of proinflammatory cytokines in the pathophysiology of osteoarthritis*. Nat Rev Rheumatol, 2011. **7**(1): p. 33-42.
12. Kafienah, W., et al., *Inhibition of cartilage degradation: a combined tissue engineering and gene therapy approach*. Arthritis Rheum, 2003. **48**(3): p. 709-18.
13. Dieppe, P.A. and L.S. Lohmander, *Pathogenesis and management of pain in osteoarthritis*. Lancet, 2005. **365**(9463): p. 965-73.
14. Hannan, M.T., D.T. Felson, and T. Pincus, *Analysis of the discordance between radiographic changes and knee pain in osteoarthritis of the knee*. J Rheumatol, 2000. **27**(6): p. 1513-7.
15. Altman, R., et al., *The American College of Rheumatology criteria for the classification and reporting of osteoarthritis of the hip*. Arthritis Rheum, 1991. **34**(5): p. 505-14.
16. NICE, G. *Osteoarthritis: Care and management in adults*. 2014 November 2014]; Available from: <http://www.nice.org.uk/guidance/cg177>.
17. Qvist, P., et al., *The disease modifying osteoarthritis drug (DMOAD): Is it in the horizon?* Pharmacol Res, 2008. **58**(1): p. 1-7.
18. NJR. *National Joint Registry for England, Wales and Northern Ireland- 10th Annual Report*. 2013 [cited 2014 12 March]; Available from:

- [http://www.njrcentre.org.uk/njrcentre/Portals/0/Documents/England/Reports/10th annual report/NJR%2010th%20Annual%20Report%202013%20B.pdf](http://www.njrcentre.org.uk/njrcentre/Portals/0/Documents/England/Reports/10th%20annual%20report/NJR%2010th%20Annual%20Report%202013%20B.pdf).
19. NJR. *National Joint Registry of England, Wales and Northern Ireland, Annual Report 2011*. 2011; Available from: [http://www.njrcentre.org.uk/njrcentre/Portals/0/Documents/England/Reports/Public %20&%20Patient%20Guide%20to%20the%20NJR%20Annual%20Report%202011.pdf](http://www.njrcentre.org.uk/njrcentre/Portals/0/Documents/England/Reports/Public%20&%20Patient%20Guide%20to%20the%20NJR%20Annual%20Report%202011.pdf).
 20. NICE. *Total hip replacement and resurfacing arthroplasty for end-stage arthritis of the hip (review of technology appraisal guidance 2 and 44)*. 2014; Available from: <http://www.nice.org.uk/guidance/ta304/>.
 21. Boardman, D.R., F.R. Middleton, and T.G. Kavanagh, *A benign psoas mass following metal-on-metal resurfacing of the hip*. *Journal of Bone and Joint Surgery-British Volume*, 2006. **88B**(3): p. 402-404.
 22. Hart, A.J., et al., *The painful metal-on-metal hip resurfacing*. *Journal of Bone and Joint Surgery-British Volume*, 2009. **91B**(6): p. 738-744.
 23. Langton, D.J., et al., *Blood metal ion concentrations after hip resurfacing arthroplasty A COMPARATIVE STUDY OF ARTICULAR SURFACE REPLACEMENT AND BIRMINGHAM HIP RESURFACING ARTHROPLASTIES*. *Journal of Bone and Joint Surgery-British Volume*, 2009. **91B**(10): p. 1287-1295.
 24. Langton, D.J., et al., *Early failure of metal-on-metal bearings in hip resurfacing and large-diameter total hip replacement A CONSEQUENCE OF EXCESS WEAR*. *Journal of Bone and Joint Surgery-British Volume*, 2010. **92B**(1): p. 38-46.
 25. Bozic, K.J., et al., *Risk of complication and revision total hip arthroplasty among Medicare patients with different bearing surfaces*. *Clin Orthop Relat Res*, 2010. **468**(9): p. 2357-62.
 26. MHRA. *Medicines and Healthcare products Regulatory Agency 2010 05/01/2011*]; Available from: <http://www.mhra.gov.uk/>.
 27. MHRA. 2012; Available from: <http://www.mhra.gov.uk/home/groups/dts-bs/documents/medicaldevicealert/con155767.pdf>.
 28. Toms, A.P., et al., *MRI of early symptomatic metal-on-metal total hip arthroplasty: a retrospective review of radiological findings in 20 hips*. *Clin Radiol*, 2008. **63**(1): p. 49-58.
 29. Donell, S.T., et al., *Early failure of the Ultima metal-on-metal total hip replacement in the presence of normal plain radiographs*. *J Bone Joint Surg Br*, 2010. **92**(11): p. 1501-8.
 30. Hart, A.J., et al., *Cup inclination angle of greater than 50 degrees increases whole blood concentrations of cobalt and chromium ions after metal-on-metal hip resurfacing*. *Hip Int*, 2008. **18**(3): p. 212-9.
 31. Hart, A.J., et al., *Insufficient acetabular version increases blood metal ion levels after metal-on-metal hip resurfacing*. *Clin Orthop Relat Res*, 2011. **469**(9): p. 2590-7.
 32. Knahr, K., *Tribology in Total Hip Arthroplasty*. 2011.
 33. Hallam, P., F. Haddad, and J. Cobb, *Pain in the well-fixed, aseptic titanium hip replacement. The role of corrosion*. *J Bone Joint Surg Br*, 2004. **86**(1): p. 27-30.
 34. Catelas, I. and M.A. Wimmer, *New insights into wear and biological effects of metal-on-metal bearings*. *J Bone Joint Surg Am*, 2011. **93 Suppl 2**: p. 76-83.
 35. Wimmer, M.A., et al., *The acting wear mechanisms on metal-on-metal hip joint bearings: in vitro results*. *Wear*, 2001. **250**(1-12): p. 129-139.

36. Wimmer, M.A., et al., *Tribochemical reaction on metal-on-metal hip joint bearings: A comparison between in-vitro and in-vivo results*. *Wear*, 2003. **255**(7–12): p. 1007-1014.
37. Hesketh, J., et al., *Biotribocorrosion of metal-on-metal hip replacements: How surface degradation can influence metal ion formation*. *Tribology International*, 2013. **65**(0): p. 128-137.
38. Bryant, M., et al., *Characterisation of the surface topography, tomography and chemistry of fretting corrosion product found on retrieved polished femoral stems*. *J Mech Behav Biomed Mater*, 2014. **32**: p. 321-34.
39. Bryant, M., et al., *Failure analysis of cemented metal-on-metal total hip replacements from a single centre cohort*. *Wear*, 2013. **301**(1–2): p. 226-233.
40. Bryant, M., et al., *Crevice corrosion of biomedical alloys: a novel method of assessing the effects of bone cement and its chemistry*. *J Biomed Mater Res B Appl Biomater*, 2013. **101**(5): p. 792-803.
41. Bryant, M., et al., *Fretting corrosion of fully cemented polished collarless tapered stems: The influence of PMMA bone cement*. *Wear*, 2013. **301**(1–2): p. 290-299.
42. Meyer, H., et al., *Corrosion at the cone/taper interface leads to failure of large-diameter metal-on-metal total hip arthroplasties*. *Clin Orthop Relat Res*, 2012. **470**(11): p. 3101-8.
43. Stangl, G.I., D.A. Roth-Maier, and M. Kirchgessner, *Vitamin B-12 deficiency and hyperhomocysteinemia are partly ameliorated by cobalt and nickel supplementation in pigs*. *J Nutr*, 2000. **130**(12): p. 3038-44.
44. Heldt, D., et al., *Aerobic synthesis of vitamin B12: ring contraction and cobalt chelation*. *Biochem Soc Trans*, 2005. **33**(Pt 4): p. 815-9.
45. Centers for Disease Control and Prevention, C. *Workplace Safety & Health Topic : Cobalt*. 2013 2014.06.24]; Available from: <http://www.cdc.gov/niosh/topics/cobalt/>.
46. NIH, M.P. *Cobalt poisoning*. 2014 2014.06.24]; Available from: <http://www.nlm.nih.gov/medlineplus/ency/article/002495.htm>
47. Langton, D.J., et al., *The clinical implications of elevated blood metal ion concentrations in asymptomatic patients with MoM hip resurfacings: a cohort study*. *BMJ Open*, 2013. **3**(3).
48. NIH, M.P. *Chromium*
Dietary Supplement Fact Sheet 2013 2014.09.05]; Available from: <http://ods.od.nih.gov/factsheets/Chromium-HealthProfessional/>.
49. Shrivastava, R., et al., *Effects of chromium on the immune system*. *FEMS Immunol Med Microbiol*, 2002. **34**(1): p. 1-7.
50. IPCS. *Concise International Chemical Assessment: Inorganic Chromium (VI) Compounds*. 2013 21/07/2014]; Available from: http://www.who.int/ipcs/publications/cicad/cicad_78.pdf.
51. Registry, A.f.T.S.a.D. *Chromium Toxicity*. 2013 21/07/2014]; Available from: <http://www.atsdr.cdc.gov/csem/csem.asp?csem=10&po=0>.
52. Goode, A.E., et al., *Chemical speciation of nanoparticles surrounding metal-on-metal hips*. *Chem Commun (Camb)*, 2012. **48**(67): p. 8335-7.
53. Hart, A., et al., *Synchrotron Xray Spectroscopy Reveals Chemical Form of in-Human Metal-on-Metal Hip Wear Debris: Ultima and Current Generation Hips*. *J Bone Joint Surg Am*, 2012. **94**(B): p. 89.
54. WHO. 2014 2014.09.09

]; Available from:

http://www.who.int/water_sanitation_health/publications/2011/9789241548151_ch12.pdf?ua=1.

55. Reid, S.D., *Homeostasis and Toxicology of Essential Metals*. 2012.
56. Davies, A.P., et al., *An unusual lymphocytic perivascular infiltration in tissues around contemporary metal-on-metal joint replacements*. J Bone Joint Surg Am, 2005. **87**(1): p. 18-27.
57. Natsu, S., et al., *Adverse reactions to metal debris: histopathological features of periprosthetic soft tissue reactions seen in association with failed metal on metal hip arthroplasties*. J Clin Pathol, 2012. **65**(5): p. 409-18.
58. Willert, H.G., et al., *Metal-on-metal bearings and hypersensitivity in patients with artificial hip joints. A clinical and histomorphological study*. J Bone Joint Surg Am, 2005. **87**(1): p. 28-36.
59. Witzleb, W.C., et al., *Neo-capsule tissue reactions in metal-on-metal hip arthroplasty*. Acta Orthop, 2007. **78**(2): p. 211-20.
60. Hart, A.J., et al., *Pseudotumors in association with well-functioning metal-on-metal hip prostheses: a case-control study using three-dimensional computed tomography and magnetic resonance imaging*. J Bone Joint Surg Am, 2012. **94**(4): p. 317-25.
61. Hart, A.J., et al., *Understanding why metal-on-metal hip arthroplasties fail: a comparison between patients with well-functioning and revised birmingham hip resurfacing arthroplasties. AAOS exhibit selection*. J Bone Joint Surg Am, 2012. **94**(4): p. e22.
62. Goodman, S.B., *Wear particles, periprosthetic osteolysis and the immune system*. Biomaterials, 2007. **28**(34): p. 5044-8.
63. Gawkrödger, D.J., *Metal sensitivities and orthopaedic implants revisited: the potential for metal allergy with the new metal-on-metal joint prostheses*. British Journal of Dermatology, 2003. **148**(6): p. 1089-1093.
64. Mabilieu, G., et al., *Metal-on-metal hip resurfacing arthroplasty: a review of periprosthetic biological reactions*. Acta Orthop, 2008. **79**(6): p. 734-47.
65. Hallab, N.J., et al., *In vitro reactivity to implant metals demonstrates a person-dependent association with both T-cell and B-cell activation*. J Biomed Mater Res A, 2010. **92**(2): p. 667-82.
66. Liu, F., et al., *Inhibition of titanium particle-induced osteoclastogenesis through inactivation of NFATc1 by VIVIT peptide*. Biomaterials, 2009. **30**(9): p. 1756-62.
67. Tyson-Capper, A.J., et al., *Metal-on-metal hips: cobalt can induce an endotoxin-like response*. Ann Rheum Dis, 2013. **72**(3): p. 460-1.
68. Schmidt, M., et al., *Crucial role for human Toll-like receptor 4 in the development of contact allergy to nickel*. Nat Immunol, 2010. **11**(9): p. 814-9.
69. Paulus, A.C., et al., *Polyethylene wear particles induce TLR 2 upregulation in the synovial layer of mice*. J Mater Sci Mater Med, 2014. **25**(2): p. 507-13.
70. Catelas, I., et al., *TNF-alpha secretion and macrophage mortality induced by cobalt and chromium ions in vitro-qualitative analysis of apoptosis*. Biomaterials, 2003. **24**(3): p. 383-91.
71. Catelas, I., et al., *Quantitative analysis of macrophage apoptosis vs. necrosis induced by cobalt and chromium ions in vitro*. Biomaterials, 2005. **26**(15): p. 2441-53.
72. Jakobsen, S.S., et al., *Cobalt-chromium-molybdenum alloy causes metal accumulation and metallothionein up-regulation in rat liver and kidney*. Basic & Clinical Pharmacology & Toxicology, 2007. **101**(6): p. 441-446.

73. Xia, Z.D., et al., *Characterization of metal-wear nanoparticles in pseudotumor following metal-on-metal hip resurfacing*. *Nanomedicine-Nanotechnology Biology and Medicine*, 2011. **7**(6): p. 674-681.
74. Rae, T., *THE MACROPHAGE RESPONSE TO IMPLANT MATERIALS - WITH SPECIAL REFERENCE TO THOSE USED IN ORTHOPEDICS*. *Crc Critical Reviews in Biocompatibility*, 1986. **2**(2): p. 97-126.
75. Kong, Y.Y., et al., *Activated T cells regulate bone loss and joint destruction in adjuvant arthritis through osteoprotegerin ligand*. *Nature*, 1999. **402**(6759): p. 304-309.
76. Liu, F., et al., *Inhibition of titanium particle-induced osteoclastogenesis through inactivation of NFATc1 by VIVIT peptide*. *Biomaterials*, 2009. **30**(9): p. 1756-1762.
77. Sabokbar, A., O. Kudo, and N.A. Athanasou, *Two distinct cellular mechanisms of osteoclast formation and bone resorption in periprosthetic osteolysis*. *J Orthop Res*, 2003. **21**(1): p. 73-80.
78. Sabokbar, A., et al., *Arthroplasty membrane-derived fibroblasts directly induce osteoclast formation and osteolysis in aseptic loosening*. *J Orthop Res*, 2005. **23**(3): p. 511-9.
79. Fritz, E.A., et al., *Chemokine IL-8 induction by particulate wear debris in osteoblasts is mediated by NF-kappaB*. *J Orthop Res*, 2005. **23**(6): p. 1249-57.
80. Yin, L., et al., *T-cell receptor (TCR) interaction with peptides that mimic nickel offers insight into nickel contact allergy*. *Proceedings of the National Academy of Sciences of the United States of America*, 2012. **109**(45): p. 18517-18522.
81. Falta, M.T., et al., *Identification of beryllium-dependent peptides recognized by CD4+ T cells in chronic beryllium disease*. *The Journal of Experimental Medicine*, 2013. **210**(7): p. 1403-1418.
82. Clayton, G.M., et al., *Structural Basis of Chronic Beryllium Disease: Linking Allergic Hypersensitivity and Autoimmunity*. *Cell*, 2014. **158**(1): p. 132-142.
83. Thierse, H.J., et al., *T cell receptor (TCR) interaction with haptens: metal ions as non-classical haptens*. *Toxicology*, 2005. **209**(2): p. 101-7.
84. Gamerdinger, K., et al., *A new type of metal recognition by human T cells: contact residues for peptide-independent bridging of T cell receptor and major histocompatibility complex by nickel*. *J Exp Med*, 2003. **197**(10): p. 1345-53.
85. Moroni, A., et al., *Does Ion Release Differ Between Hip Resurfacing and Metal-on-metal THA?* *Clinical Orthopaedics and Related Research*, 2008. **466**(3): p. 700-707.
86. Kraus, V.B., et al., *Application of biomarkers in the development of drugs intended for the treatment of osteoarthritis*. *Osteoarthritis Cartilage*, 2011. **19**(5): p. 515-42.
87. Thorsby, E., *A short history of HLA*. *Tissue Antigens*, 2009. **74**(2): p. 101-116.
88. Dausset, J., *Iso-lueco-anticorps*. *Acta Haematologica*, 1958. **20**: p. 156-166.
89. Van Rood, J.J., J.G. Eernisse, and A. Van Leeuwen, *Leucocyte Antibodies in Sera from Pregnant Women*. *Nature*, 1958. **181**(4625): p. 1735-1736.
90. Payne, R. and M.R. Rolfs, *Fetomaternal Leukocyte Incompatibility*¹². *The Journal of Clinical Investigation*, 1958. **37**(12): p. 1756-1763.
91. Graw, R.G., Jr., et al., *Complication of bone-marrow transplantation. Graft-versus-host disease resulting from chronic-myelogenous-leukaemia leucocyte transfusions*. *Lancet*, 1970. **2**(7668): p. 338-41.
92. Vredevoe, D.L., et al., *HISTOCOMPATIBILITY TYPING OF KIDNEY HOMOGRAFT PATIENTS*. *Federation Proceedings*, 1965. **24**(2P1): p. 181-&.
93. Mozes, E., et al., *NATURE OF ANTIGENIC DETERMINANT IN A GENETIC CONTROL OF ANTIBODY RESPONSE*. *Journal of Experimental Medicine*, 1969. **130**(3): p. 493-&.

94. Kindred, B. and D.C. Shreffler, *H-2 Dependence of Co-Operation Between T and B Cells in Vivo*. The Journal of Immunology, 1972. **109**(5): p. 940-943.
95. Rosenthal, A.S. and E.M. Shevach, *Function of macrophages in antigen recognition by guinea pig T lymphocytes. I. Requirement for histocompatible macrophages and lymphocytes*. J Exp Med, 1973. **138**(5): p. 1194-212.
96. Doherty, P.C. and R.M. Zinkernagel, *BIOLOGICAL ROLE FOR MAJOR HISTOCOMPATIBILITY ANTIGENS*. Lancet, 1975. **1**(7922): p. 1406-1409.
97. Zinkernagel, R.M. and P.C. Doherty, *Restriction of in vitro T cell-mediated cytotoxicity in lymphocytic choriomeningitis within a syngeneic or semiallogeneic system*. Nature, 1974. **248**(5450): p. 701-2.
98. Frei, R., et al., *MHC class II molecules enhance Toll-like receptor mediated innate immune responses*. PLoS One, 2010. **5**(1): p. e8808.
99. Liu, X., et al., *Intracellular MHC class II molecules promote TLR-triggered innate immune responses by maintaining activation of the kinase Btk*. Nat Immunol, 2011. **12**(5): p. 416-24.
100. Mak, T.W., M.E. Saunders, and B.D. Jett, *Primer to The Immune Response*. 2013: Elsevier Science.
101. Murphy, K.P., et al., *Janeway's Immunobiology*. 2008: Garland Science.
102. Robinson, J., et al., *The IMGT/HLA database*. Nucleic Acids Research, 2011. **39**: p. D1171-D1176.
103. Marsh, S.G.E., et al., *Nomenclature for factors of the HLA system, 2010*. Tissue Antigens, 2010. **75**(4): p. 291-455.
104. JC, A., *Study of the leucocyte phenotypes in Hodgkin's disease*. Histocompatibility Testing 1967, 1967: p. 79-81.
105. van Lummel, M., et al., *Type 1 diabetes-associated HLA-DQ8 transdimer accommodates a unique peptide repertoire*. J Biol Chem, 2012. **287**(12): p. 9514-24.
106. Freeston, J., et al., *Ankylosing spondylitis, HLA-B27 positivity and the need for biologic therapies*. Joint Bone Spine, 2007. **74**(2): p. 140-3.
107. Jones, E.Y., et al., *MHC class II proteins and disease: a structural perspective*. Nat Rev Immunol, 2006. **6**(4): p. 271-82.
108. Bowes, J. and A. Barton, *Recent advances in the genetics of RA susceptibility*. Rheumatology (Oxford), 2008. **47**(4): p. 399-402.
109. Wordsworth, B.P., et al., *HLA-DR4 subtype frequencies in rheumatoid arthritis indicate that DRB1 is the major susceptibility locus within the HLA class II region*. Proc Natl Acad Sci U S A, 1989. **86**(24): p. 10049-53.
110. Andersson, E.C., et al., *Definition of MHC and T cell receptor contacts in the HLA-DR4restricted immunodominant epitope in type II collagen and characterization of collagen-induced arthritis in HLA-DR4 and human CD4 transgenic mice*. Proc Natl Acad Sci U S A, 1998. **95**(13): p. 7574-9.
111. Rosloniec, E.F., et al., *An HLA-DR1 transgene confers susceptibility to collagen-induced arthritis elicited with human type II collagen*. J Exp Med, 1997. **185**(6): p. 1113-22.
112. Riyazi, N., et al., *HLA class II is associated with distal interphalangeal osteoarthritis*. Annals of the Rheumatic Diseases, 2003. **62**(3): p. 227-230.
113. Merlotti, D., et al., *HLA antigens and primary osteoarthritis of the hand*. Journal of Rheumatology, 2003. **30**(6): p. 1298-1304.
114. Rovetta, G., et al., *HLA-DRB1 alleles and osteoarthritis in a group of patients living in Liguria-Italy*. Minerva medica, 2006. **97**(3): p. 271-5.

115. Moos, V., et al., *Association of HLA-DRB1*02 with osteoarthritis in a cohort of 106 patients*. Rheumatology, 2002. **41**(6): p. 666-669.
116. Wang, Y. and S. Dai, *Structural basis of metal hypersensitivity*. Immunol Res, 2013. **55**(1-3): p. 83-90.
117. Fischer, T., et al., *HLA -A, -B, -C and -DR antigens in individuals with sensitivity to cobalt*. Acta Derm Venereol, 1984. **64**(2): p. 121-4.
118. Thomson, W., et al., *Juvenile idiopathic arthritis classified by the ILAR criteria: HLA associations in UK patients*. Rheumatology, 2002. **41**(10): p. 1183-1189.
119. Szumilas, M., *Explaining odds ratios*. J Can Acad Child Adolesc Psychiatry, 2010. **19**(3): p. 227-9.
120. Benjamini, Y. and Y. Hochberg, *CONTROLLING THE FALSE DISCOVERY RATE - A PRACTICAL AND POWERFUL APPROACH TO MULTIPLE TESTING*. Journal of the Royal Statistical Society Series B-Methodological, 1995. **57**(1): p. 289-300.
121. Howell, W.M., *HLA and disease: guilt by association*. Int J Immunogenet, 2014. **41**(1): p. 1-12.
122. Sollid, L.M. and B.A. Lie, *Celiac disease genetics: current concepts and practical applications*. Clin Gastroenterol Hepatol, 2005. **3**(9): p. 843-51.
123. Han, F., et al., *HLA-DQ association and allele competition in Chinese narcolepsy*. Tissue Antigens, 2012. **80**(4): p. 328-35.
124. Glaxo Group Limited, U. 2014.06.26]; Available from: <http://www.google.com/patents/WO2011147763A1?cl=en>.
125. Price, P., et al., *Can MHC class II genes mediate resistance to type 1 diabetes?* Immunol Cell Biol, 2001. **79**(6): p. 602-6.
126. Patsopoulos, N.A., et al., *Fine-mapping the genetic association of the major histocompatibility complex in multiple sclerosis: HLA and non-HLA effects*. PLoS Genet, 2013. **9**(11): p. e1003926.
127. Nakajima, M., et al., *New Sequence Variants in HLA Class II/III Region Associated with Susceptibility to Knee Osteoarthritis Identified by Genome-Wide Association Study*. Plos One, 2010. **5**(3).
128. Shi, D., et al., *Association of single-nucleotide polymorphisms in HLA class II/III region with knee osteoarthritis*. Osteoarthritis and Cartilage, 2010. **18**(11): p. 1454-1457.
129. Valdes, A.M., et al., *Large Scale Replication Study of the Association between HLA Class II/BTNL2 Variants and Osteoarthritis of the Knee in European-Descent Populations*. Plos One, 2011. **6**(8).
130. Keller, M.R., et al., *Epitope analysis of the collagen type V-specific T cell response in lung transplantation reveals an HLA-DRB1*15 bias in both recipient and donor*. PLoS One, 2013. **8**(11): p. e79601.
131. Jankowska-Gan, E., S. Hegde, and W.J. Burlingham, *Trans-vivo delayed type hypersensitivity assay for antigen specific regulation*. J Vis Exp, 2013(75): p. e4454.
132. Freed, B.M., R.P. Schuyler, and M.T. Aubrey, *Association of the HLA-DRB1 epitope LA(67, 74) with rheumatoid arthritis and citrullinated vimentin binding*. Arthritis Rheum, 2011. **63**(12): p. 3733-9.
133. Dang, M., et al., *Human type 1 diabetes is associated with T cell autoimmunity to zinc transporter 8*. J Immunol, 2011. **186**(10): p. 6056-63.
134. Hetherington, S., et al., *Genetic variations in HLA-B region and hypersensitivity reactions to abacavir*. Lancet, 2002. **359**(9312): p. 1121-2.

135. Amstutz, U., et al., *Recommendations for HLA-B*15:02 and HLA-A*31:01 genetic testing to reduce the risk of carbamazepine-induced hypersensitivity reactions.* *Epilepsia*, 2014. **55**(4): p. 496-506.
136. Goncalo, M., et al., *HLA-B*58:01 is a risk factor for allopurinol-induced DRESS and Stevens-Johnson syndrome/toxic epidermal necrolysis in a Portuguese population.* *Br J Dermatol*, 2013. **169**(3): p. 660-5.
137. Campbell, P., et al., *Histological features of pseudotumor-like tissues from metal-on-metal hips.* *Clin Orthop Relat Res*, 2010. **468**(9): p. 2321-7.
138. Hengel, R.L., et al., *Cutting edge: L-selectin (CD62L) expression distinguishes small resting memory CD4+ T cells that preferentially respond to recall antigen.* *J Immunol*, 2003. **170**(1): p. 28-32.
139. Zhao, D.S., et al., *Ectopic expression of macrophage scavenger receptor MARCO in synovial membrane-like interface tissue in aseptic loosening of total hip replacement implants.* *J Biomed Mater Res A*, 2010. **92**(2): p. 641-9.
140. Takagi, M., et al., *Toll-like receptors in the interface membrane around loosening total hip replacement implants.* *J Biomed Mater Res A*, 2007. **81**(4): p. 1017-26.
141. Tamaki, Y., et al., *Increased expression of toll-like receptors in aseptic loose periprosthetic tissues and septic synovial membranes around total hip implants.* *J Rheumatol*, 2009. **36**(3): p. 598-608.
142. Kwon, Y.M., et al., *Dose-dependent cytotoxicity of clinically relevant cobalt nanoparticles and ions on macrophages in vitro.* *Biomed Mater*, 2009. **4**(2): p. 025018.
143. Ziegler-Heitbrock, L. and T.P. Hofer, *Toward a refined definition of monocyte subsets.* *Front Immunol*, 2013. **4**: p. 23.
144. Ziegler-Heitbrock, L., *The CD14+ CD16+ blood monocytes: their role in infection and inflammation.* *J Leukoc Biol*, 2007. **81**(3): p. 584-92.
145. Ziegler-Heitbrock, L., et al., *Nomenclature of monocytes and dendritic cells in blood.* *Blood*, 2010. **116**(16): p. e74-80.
146. Altaf, H. and P.A. Revell, *Evidence for active antigen presentation by monocyte/macrophages in response to stimulation with particles: the expression of NFkappaB transcription factors and costimulatory molecules.* *Inflammopharmacology*, 2013. **21**(4): p. 279-90.
147. Gerlini, G., et al., *Induction of CD83+CD14+ nondendritic antigen-presenting cells by exposure of monocytes to IFN-alpha.* *J Immunol*, 2008. **181**(5): p. 2999-3008.
148. Cobelli, N., et al., *Mediators of the inflammatory response to joint replacement devices.* *Nat Rev Rheumatol*, 2011. **7**(10): p. 600-608.
149. Maitra, R., et al., *Immunogenicity of modified alkane polymers is mediated through TLR1/2 activation.* *PLoS One*, 2008. **3**(6): p. e2438.
150. Goodman, S.B., et al., *Cellular profile and cytokine production at prosthetic interfaces. Study of tissues retrieved from revised hip and knee replacements.* *J Bone Joint Surg Br*, 1998. **80**(3): p. 531-9.
151. Lee, M.S., et al., *GM-CSF regulates fusion of mononuclear osteoclasts into bone-resorbing osteoclasts by activating the Ras/ERK pathway.* *J Immunol*, 2009. **183**(5): p. 3390-9.
152. Takayanagi, H., et al., *T-cell-mediated regulation of osteoclastogenesis by signalling cross-talk between RANKL and IFN-gamma.* *Nature*, 2000. **408**(6812): p. 600-5.

153. Attur, M.G., et al., *Autocrine production of IL-1 beta by human osteoarthritis-affected cartilage and differential regulation of endogenous nitric oxide, IL-6, prostaglandin E2, and IL-8*. Proc Assoc Am Physicians, 1998. **110**(1): p. 65-72.
154. Bresnihan, B., et al., *Treatment of rheumatoid arthritis with recombinant human interleukin-1 receptor antagonist*. Arthritis Rheum, 1998. **41**(12): p. 2196-204.
155. Kwan Tat, S., et al., *IL-6, RANKL, TNF-alpha/IL-1: interrelations in bone resorption pathophysiology*. Cytokine Growth Factor Rev, 2004. **15**(1): p. 49-60.
156. Mutabaruka, M.-S., et al., *Local leptin production in osteoarthritis subchondral osteoblasts may be responsible for their abnormal phenotypic expression*. Arthritis Research & Therapy, 2010. **12**(1).
157. Turner, R.T., et al., *Peripheral Leptin Regulates Bone Formation*. Journal of Bone and Mineral Research, 2013. **28**(1): p. 22-34.
158. Simonet, W.S., et al., *Osteoprotegerin: A novel secreted protein involved in the regulation of bone density*. Cell, 1997. **89**(2): p. 309-319.
159. Boyce, B.F., et al., *TNF alpha and pathologic bone resorption*. Keio Journal of Medicine, 2005. **54**(3): p. 127-131.
160. Keegan, G.M., I.D. Learmonth, and C.P. Case, *Orthopaedic metals and their potential toxicity in the arthroplasty patient: A review of current knowledge and future strategies*. J Bone Joint Surg Br, 2007. **89**(5): p. 567-73.
161. Gill, H.S., et al., *Molecular and immune toxicity of CoCr nanoparticles in MoM hip arthroplasty*. Trends Mol Med, 2012. **18**(3): p. 145-55.
162. Hart, A.J., et al., *Sensitivity and specificity of blood cobalt and chromium metal ions for predicting failure of metal-on-metal hip replacement*. J Bone Joint Surg Br, 2011. **93**(10): p. 1308-13.
163. de Smet, K., et al., *Metal Ion Measurement as a Diagnostic Tool to Identify Problems with Metal-on-Metal Hip Resurfacing*. Journal of Bone and Joint Surgery-American Volume, 2008. **90A**: p. 202-208.
164. Fung, E., et al., *Multiplexed immunophenotyping of human antigen-presenting cells in whole blood by polychromatic flow cytometry*. Nature Protocols, 2010. **5**(2): p. 357-370.
165. BD, B. *BD Trucount Tubes*. 07-02-2013]; Available from: <http://www.bdbiosciences.com/ptProduct.jsp?prodId=227679&catyId=782112&page=product>.
166. Nimmerjahn, F. and J.V. Ravetch, *Fc gamma receptors as regulators of immune responses*. Nat Rev Immunol, 2008. **8**(1): p. 34-47.
167. Haller Hasskamp, J., J.L. Zapas, and E.G. Elias, *Dendritic cell counts in the peripheral blood of healthy adults*. Am J Hematol, 2005. **78**(4): p. 314-5.
168. Hart, A.J., et al., *The association between metal ions from hip resurfacing and reduced T-cell counts*. Journal of Bone and Joint Surgery-British Volume, 2006. **88B**(4): p. 449-454.
169. Hailer, N.P., et al., *Elevation of circulating HLA DR++ CD8(++) T-cells and correlation with chromium and cobalt concentrations 6 years after metal-on-metal hip arthroplasty*. Acta Orthopaedica, 2011. **82**(1): p. 6-12.
170. Hart, A.J., et al., *Circulating levels of cobalt and chromium from metal-on-metal hip replacement are associated with CD8+ T-cell lymphopenia*. J Bone Joint Surg Br, 2009. **91**(6): p. 835-42.
171. Speiser, D.E., et al., *Human CD8(+) T cells expressing HLA-DR and CD28 show telomerase activity and are distinct from cytolytic effector T cells*. Eur J Immunol, 2001. **31**(2): p. 459-66.

172. Hua, S., et al., *Potential role for HIV-specific CD38-/HLA-DR+ CD8+ T cells in viral suppression and cytotoxicity in HIV controllers*. PLoS One, 2014. **9**(7): p. e101920.
173. Gallo, J., et al., *Particle disease: biologic mechanisms of periprosthetic osteolysis in total hip arthroplasty*. Innate Immun, 2013. **19**(2): p. 213-24.
174. SCHMALZRIED, T.P., et al., *The Role of Access of Joint Fluid to Bone in Periarticular Osteolysis: A Report of Four Cases**. Vol. 79. 1997. 447-52.
175. Takakubo, Y., et al., *Distribution of myeloid dendritic cells and plasmacytoid dendritic cells in the synovial tissues of rheumatoid arthritis*. J Rheumatol, 2008. **35**(10): p. 1919-31.
176. Moret, F.M., et al., *Intra-articular CD1c-expressing myeloid dendritic cells from rheumatoid arthritis patients express a unique set of T cell-attracting chemokines and spontaneously induce Th1, Th17 and Th2 cell activity*. Arthritis Res Ther, 2013. **15**(5): p. R155.
177. Kassianos, A.J., et al., *Human CD1c (BDCA-1)+ myeloid dendritic cells secrete IL-10 and display an immuno-regulatory phenotype and function in response to Escherichia coli*. European Journal of Immunology, 2012. **42**(6): p. 1512-1522.
178. Sato, T., et al., *Human CD1c(+) myeloid dendritic cells acquire a high level of retinoic acid-producing capacity in response to vitamin D(3)*. J Immunol, 2013. **191**(6): p. 3152-60.
179. Van Landuyt, K.B., et al., *Flow cytometric characterization of freshly isolated and culture expanded human synovial cell populations in patients with chronic arthritis*. Arthritis Res Ther, 2010. **12**(1): p. R15.
180. Podzimek, S., et al., *Influence of metals on cytokines production in connection with successful implantation therapy in dentistry*. Neuro Endocrinol Lett, 2010. **31**(5): p. 657-62.
181. Beekhuizen, M., et al., *An explorative study comparing levels of soluble mediators in control and osteoarthritic synovial fluid*. Osteoarthritis Cartilage, 2013. **21**(7): p. 918-22.
182. Wong, H.L., et al., *Reproducibility and correlations of multiplex cytokine levels in asymptomatic persons*. Cancer Epidemiol Biomarkers Prev, 2008. **17**(12): p. 3450-6.
183. Vendittoli, P.A., et al., *Metal Ion release with large-diameter metal-on-metal hip arthroplasty*. J Arthroplasty, 2011. **26**(2): p. 282-8.
184. Garbuz, D.S., et al., *The John Charnley Award: Metal-on-metal hip resurfacing versus large-diameter head metal-on-metal total hip arthroplasty: a randomized clinical trial*. Clin Orthop Relat Res, 2010. **468**(2): p. 318-25.
185. Caicedo, M.S., et al., *Soluble and Particulate Co-Cr-Mo Alloy Implant Metals Activate the Inflammasome Danger Signaling Pathway in Human Macrophages: A Novel Mechanism for Implant Debris Reactivity*. Journal of Orthopaedic Research, 2009. **27**(7): p. 847-854.
186. Hart, A.J., et al., *Cobalt from metal-on-metal hip replacements may be the clinically relevant active agent responsible for periprosthetic tissue reactions*. Acta Biomaterialia, 2012. **8**(10): p. 3865-3873.
187. Agarwal, S., *Osteolysis—basic science, incidence and diagnosis*. Current Orthopaedics, 2004. **18**(3): p. 220-231.
188. Athanasou, N.A., J. Quinn, and C.J. Bulstrode, *Resorption of bone by inflammatory cells derived from the joint capsule of hip arthroplasties*. J Bone Joint Surg Br, 1992. **74**(1): p. 57-62.

189. Rao, A.J., et al., *Revision joint replacement, wear particles, and macrophage polarization*. Acta Biomater, 2012. **8**(7): p. 2815-23.
190. Ishimi, Y., et al., *IL-6 is produced by osteoblasts and induces bone resorption*. J Immunol, 1990. **145**(10): p. 3297-303.
191. Teitelbaum, S.L., M.M. Tondravi, and F.P. Ross, *Osteoclasts, macrophages, and the molecular mechanisms of bone resorption*. J Leukoc Biol, 1997. **61**(4): p. 381-8.
192. Ji, J.D., et al., *Inhibition of RANK expression and osteoclastogenesis by TLRs and IFN-gamma in human osteoclast precursors*. J Immunol, 2009. **183**(11): p. 7223-33.
193. Gordeladze, J.O., et al., *Leptin stimulates human osteoblastic cell proliferation, de novo collagen synthesis, and mineralization: Impact on differentiation markers, apoptosis, and osteoclastic signaling*. J Cell Biochem, 2002. **85**(4): p. 825-36.
194. Maloney, W.J., et al., *Effects of serum protein opsonization on cytokine release by titanium-alloy particles*. J Biomed Mater Res, 1998. **41**(3): p. 371-6.
195. Sun, D.H., et al., *Human serum opsonization of orthopedic biomaterial particles: protein-binding and monocyte/macrophage activation in vitro*. J Biomed Mater Res A, 2003. **65**(2): p. 290-8.
196. Hallab, N.J., et al., *Differential lymphocyte reactivity to serum-derived metal-protein complexes produced from cobalt-based and titanium-based implant alloy degradation*. J Biomed Mater Res, 2001. **56**(3): p. 427-36.
197. Reddy, A., et al., *Implant debris particle size affects serum protein adsorption which may contribute to particle size-based bioreactivity differences*. J Long Term Eff Med Implants, 2014. **24**(1): p. 77-88.
198. Gonzalez, O., R.L. Smith, and S.B. Goodman, *Effect of size, concentration, surface area, and volume of polymethylmethacrylate particles on human macrophages in vitro*. J Biomed Mater Res, 1996. **30**(4): p. 463-73.
199. Albanese, A., P.S. Tang, and W.C. Chan, *The effect of nanoparticle size, shape, and surface chemistry on biological systems*. Annu Rev Biomed Eng, 2012. **14**: p. 1-16.
200. Lund, T., et al., *The influence of ligand organization on the rate of uptake of gold nanoparticles by colorectal cancer cells*. Biomaterials, 2011. **32**(36): p. 9776-84.
201. Doorn, P.F., et al., *Metal wear particle characterization from metal on metal total hip replacements: transmission electron microscopy study of periprosthetic tissues and isolated particles*. J Biomed Mater Res, 1998. **42**(1): p. 103-11.
202. Muul, L.M., et al., *Measurement of proliferative responses of cultured lymphocytes*. Current protocols in immunology / edited by John E. Coligan ... [et al.], 2011. **Chapter 7**: p. Unit7.10-Unit7.10.
203. Roehm, N.W., et al., *AN IMPROVED COLORIMETRIC ASSAY FOR CELL-PROLIFERATION AND VIABILITY UTILIZING THE TETRAZOLIUM SALT XTT*. Journal of Immunological Methods, 1991. **142**(2): p. 257-265.
204. Hallab, N.J., et al., *Lymphocyte responses in patients with total hip arthroplasty*. J Orthop Res, 2005. **23**(2): p. 384-91.
205. Zhang, Y. and D.E. Wilcox, *Thermodynamic and spectroscopic study of Cu(II) and Ni(II) binding to bovine serum albumin*. J Biol Inorg Chem, 2002. **7**(3): p. 327-37.
206. Bar-Or, D., et al., *Characterization of the Co(2+) and Ni(2+) binding amino-acid residues of the N-terminus of human albumin. An insight into the mechanism of a new assay for myocardial ischemia*. Eur J Biochem, 2001. **268**(1): p. 42-7.

207. Rachmawati, D., et al., *Transition metal sensing by Toll-like receptor-4: next to nickel, cobalt and palladium are potent human dendritic cell stimulators*. *Contact Dermatitis*, 2013. **68**(6): p. 331-8.
208. Arai, F., et al., *Commitment and differentiation of osteoclast precursor cells by the sequential expression of c-Fms and receptor activator of nuclear factor kappaB (RANK) receptors*. *J Exp Med*, 1999. **190**(12): p. 1741-54.
209. Jung, K., et al., *Osteoprotegerin and receptor activator of nuclear factor-kappaB ligand (RANKL) in the serum of healthy adults*. *Int J Biol Markers*, 2002. **17**(3): p. 177-81.
210. Shadle, P.J., et al., *Detection of endogenous macrophage colony-stimulating factor (M-CSF) in human blood*. *Exp Hematol*, 1989. **17**(2): p. 154-9.
211. Ferrara, J.L., S. Abhyankar, and D.G. Gilliland, *Cytokine storm of graft-versus-host disease: a critical effector role for interleukin-1*. *Transplant Proc*, 1993. **25**(1 Pt 2): p. 1216-7.
212. Colognato, R., et al., *Comparative genotoxicity of cobalt nanoparticles and ions on human peripheral leukocytes in vitro*. *Mutagenesis*, 2008. **23**(5): p. 377-382.
213. Del Buono, A., V. Denaro, and N. Maffulli, *Genetic susceptibility to aseptic loosening following total hip arthroplasty: a systematic review*. *Br Med Bull*, 2012. **101**: p. 39-55.
214. Nextprot. *HLA-DQA1 » HLA class II histocompatibility antigen, DQ alpha 1 chain* November 2014]; Available from: http://www.nextprot.org/db/entry/NX_P01909/medical.
215. Rimbart, M., et al., *Decreased numbers of blood dendritic cells and defective function of regulatory T cells in antineutrophil cytoplasmic antibody-associated vasculitis*. *PLoS One*, 2011. **6**(4): p. e18734.

8 Appendices

Appendix 1: Patient invitation letters and consent forms

Norfolk and Norwich University Hospital 
NHS Trust

Institute of Orthopaedics

Norfolk & Norwich University Hospital
Colney Lane
Norwich
NR4 7UY

Date :

direct dial: 01603 286706
direct fax: 01603 287498

Letter of Invitation: Out-Patients Clinic

Immune system involvement in prosthetic hip implants

Dear ,

I am writing to invite you to take part in a study into how wear debris from hip replacements is handled by the body. This study is being conducted by Ms Pinar Court as part of a PhD research project under my supervision.

Specialist cells from the blood move into tissues that can contain foreign material. These cells cause other cells from the blood and local tissue to remove this foreign material. We plan to investigate these cells and how they interact with tissues around hip implants.

This study is being run as a joint project between Norfolk and Norwich University Hospital, the Institute of Food Research, Norwich and the manufacturers of one particular hip replacement joint. The aim of the study is to increase our understanding of the immunological response to wear debris in patients with hip replacements.

If you agree to take part in this study, when you attend the out-patients clinic at Norfolk and Norwich University Hospital, we would like to take 50 ml (around a quarter of a cup) of blood from you. The blood sample would be a donation to the Norfolk and Norwich Human Tissue Bank from which we would be able to use for our study.

If you like to take part in this research, please read, complete and return the Patient Information Sheet and the Consent Form to us. If you have any further questions about the study please contact me by e-mail: simon.donell@nnuh.nhs.uk.

Thank you for considering this request.
Yours sincerely,



Professor Simon Donell, BSc FRCS(Orth) MD
Consultant Orthopaedic Surgeon
Honorary Professor, University of East Anglia

Institute of Orthopaedics

Norfolk & Norwich University Hospital
Colney Lane
Norwich
NR4 7UY

Date :

direct dial: 01603 286706
direct fax: 01603 287498

Letter of Invitation: Operative Patients

Immune system involvement in prosthetic hip implants

Dear ,

I am writing to invite you to take part in a study into how wear debris from hip replacements is handled by the body. This study is being conducted by Ms Pinar Court as part of a PhD research project under my supervision.

Specialist cells from the blood move into tissues that can contain foreign material. These cells cause other cells from the blood and local tissue to remove this foreign material. We plan to investigate these cells and how they interact with tissues around hip implants.

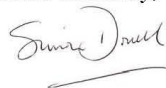
This study is being run as a joint project between Norfolk and Norwich University Hospital, the Institute of Food Research, Norwich and the manufacturers of one particular hip replacement joint. The aim of the study is to increase our understanding of the immunological response to wear debris in patients with hip replacements.

If you agree to take part in this study, we will study the discarded tissue taken by the surgeon during your operation which is no longer needed by you. In addition, an extra 50ml (around a quarter of a cup) of blood will also be removed. This will all be while you are anaesthetised. The tissue and blood samples would be a donation to the Norfolk and Norwich Human Tissue Bank from which we would be able to use for our study.

If you like to take part in this research, please read, complete and return the Patient Information Sheet and the Consent Form to us.

If you have any further questions about the study please contact me by e-mail: simon.donell@nnuh.nhs.uk. Thank you for considering this request.

Yours sincerely,



Professor Simon Donell, BSc FRCS(Orth) MD
Consultant Orthopaedic Surgeon
Honorary Professor, University of East Anglia

Institute of Orthopaedics
Norfolk & Norwich University Hospital
Colney Lane
Norwich
NR4 7UY

direct dial: 01603 286706
direct fax: 01603 287498

Participant Information Sheet: Out-Patients

Immune system involvement in prosthetic hip implants

You are being invited to take part in a research study.

Before deciding on whether you wish to take part in the study, we would like to inform you about the research being done and what we will be asking from you in the study. Please take your time and read the following information carefully. The research staff will go through the form with you. If you wish to have more information or if any details are unclear then please feel free to ask the research team. Further information can also be obtained through the chief investigator whose contact details are given at the end of this form.

What is the purpose of this study?

The purpose of the study is to investigate how the body handles metal ions that can be shed by an implant. In particular we are interested in which cells are involved both around the implant, and circulating in the blood.

Why have I been chosen?

You have been chosen because you have a metal-on-metal hip replacement and are undergoing follow-up.

Do I have to take part?

No. You are free to volunteer to take part in the study if you wish and at a later point if you decide you don't wish to continue with the study, you are free to withdraw without explanation. Also donating one type of sample does not commit you to donating any other samples types.

What will happen to me if I take part?

When you come for your routine follow-up appointment we will ask you, in addition to your blood metal ion level test, to donate an extra 50 ml (about a quarter of a cup) for this study.

What would I have to do?

After you have agreed to take part in the study and signed the consent form, the clinic nurse, a member of the clinical team, or a member of the research team, will take the blood sample during your appointment. You will be seated comfortably and the crook of your elbow will be sterilised with a swab. A tourniquet will be applied to your upper arm and tightened. Blood will be taken from a vein in your arm.

How long will it take?

Blood donation takes around 10 minutes.

What are the possible benefits of taking part?

It is not anticipated that there will be any direct benefits to you by taking part. We hope that we shall be able to understand the problem of metal reactions in the body to help other patients in the future. Some of this research could lead to the development of new products and processes, which may be developed commercially for the improvement of patients' care, in which case there would be no financial benefit to you.

What are the possible risks of taking apart?

The risk of blood donation is that of bruising to the patient's arm where the needle is inserted, this is considered to be minimal. The procedure will be undertaken by trained personnel in a clinical environment.

Will my details kept confidential?

Yes. We will keep some facts about you such as age and gender however we will not disclose any personal information such as name or address to anyone outside of your clinical care team. Medically qualified doctors and other suitably qualified staff may need to review your case notes as part of this research. It may be important to see how you progress and to see how your condition relates to what we learn in the research project.

What will happen to the results of the research study?

The primary research is for a PhD thesis. In addition the results will be published in international scientific journals and presented at scientific conferences.

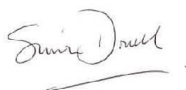
Who is organising and funding the research?

The study is being run as a Norwich Research Park joint project between Norfolk and Norwich University Hospital, the Institute of Food Research, Norwich and the University of East Anglia.

DePuy International is funding laboratory materials used in this research. It is a commercial company that produces hip replacements, including those that form part of this study.

If you would like to make a donation (gift) of tissue and/or blood for medical research please sign the form attached. We will respect your decision and it will not affect in any way the treatment you receive.

Yours sincerely,



Professor Simon Donell, BSc FRCS (Orth) MD
Chief Investigator - Consultant Orthopaedic Surgeon
Honorary Professor, University of East Anglia

Direct dial: 01603 286706
simon.donell@nnuh.nhs.uk

Institute of Orthopaedics
Norfolk & Norwich University Hospital
Colney Lane
Norwich
NR4 7UY

direct dial: 01603 286706
direct fax: 01603 287498

Participant Information Sheet: Operative Patients

Immune system involvement in prosthetic hip implants

You are being invited to take part in a research study.

Before deciding on whether you wish to take part in the study, we would like to inform you about the research being done and what we will be asking from you in the study. Please take your time and read the following information carefully. The research staff will go through the form with you. If you wish to have more information or if any details are unclear then please feel free to ask the research team. Further information can also be obtained through the chief investigator whose contact details are given at the end of this form.

What is the purpose of this study?

The purpose of the study is to investigate how the body handles metal ions that can be shed by an implant. In particular we are interested in which cells are involved both around the implant, and circulating in the blood.

Why have I been chosen?

You have been chosen because you are about to undergo an operation on your hip; either to revise an old one, or as a first procedure.

Do I have to take part?

No. You are free to volunteer to take part in the study if you wish and at a later point if you decide you don't wish to continue with the study, you are free to withdraw without explanation. Also donating one type of sample does not commit you to donating any other samples types.

What will happen to me if I take part?

As a part of your operation, tissue and other samples are routinely removed and sent to the pathology laboratory for examination. This is a standard part of treatment. In addition these specimens will be stored in the tissue bank and then used as part of this study. In addition to this we would also like to take an extra blood sample, 50 ml (about a quarter of a cup).

What would I have to do?

After you have agreed to take part in the study and signed the consent form, you do not have to do anything specific. Collection of the tissue is a part of your routine care. For the blood donation, this will be collected in the anaesthetic room just prior to your operation, when you are asleep.

How long will it take?

Tissue collection is part of the operation which takes between 1 to 3 hours depending on its complexity. Blood donation takes around 10 minutes.

What are the possible benefits of taking part?

It is not anticipated that there will be any direct benefits to you by taking part. We hope that we shall be able to understand the problem of metal reactions in the body to help other patients in the future. Some of this research could lead to the development of new products and processes, which may be developed commercially for the improvement of patients' care, in which case there would be no financial benefit to you.

What are the possible risks of taking apart?

The risk of blood donation is that of bruising to the patient's arm where the needle is inserted, this is considered to be minimal. The procedure will be undertaken by trained personnel in a clinical environment. The rest of the samples are taken during your operation and are necessary for patient care.

Will my details kept confidential?

Yes. We will keep some facts about you such as age and gender however we will not disclose any personal information such as name or address to anyone outside of your clinical care team. Medically qualified doctors and other suitably qualified staff may need to review your case notes as part of this research. It may be important to see how you progress and to see how your condition relates to what we learn in the research project.

What will happen to the results of the research study?

The primary research is for a PhD thesis. In addition the results will be published in international scientific journals and presented at scientific conferences.

Who is organising and funding the research?

The study is being run as a Norwich Research Park joint project between Norfolk and Norwich University Hospital, the Institute of Food Research, Norwich and the University of East Anglia.

DePuy International is funding laboratory materials used in this research. It is a commercial company that produces hip replacements, including those that form part of this study.

If you would like to make a donation (gift) of tissue and/or blood for medical research please sign the form attached. We will respect your decision and it will not affect in any way the treatment you receive.

Yours sincerely,



Professor Simon Donell, BSc FRCS (Orth) MD
Chief Investigator - Consultant Orthopaedic Surgeon
Honorary Professor, University of East Anglia

Direct dial: 01603 286706
simon.donell@nnuh.nhs.uk

Centre Number: Institute of Orthopaedics
 Study Number: Norfolk & Norwich University Hospital
 Trial Identification Number: Colney Lane Norwich NR4 7UY
 direct dial: 01603 286706
 direct fax: 01603 287498

CONSENT FORM

Title: Immune system involvement in prosthetic hip implants: Out-patients

Name of Researcher: Professor Simon Donell Please initial
as appropriate

- 1. I confirm that I have read and understand the information sheet dated December 2011, Version 03 for the above study. I have had the opportunity to consider the information, ask questions and have had these answered satisfactorily.
- 2. I understand that my participation is voluntary and that I am free to withdraw at any time without giving any reason, without my medical care or legal rights being affected.
- 3. I understand that relevant sections of my medical notes and data collected during the study may be looked at by individuals from the Institute of Food Research, from regulatory authorities or from the NNUH NHS Trust, where it is relevant to my taking part in this research. I give permission for these individuals to have access to my records.
- 4. I agree to my GP being informed of my participation in the study.
- 5. I agree to take part in the above study.

 Name of Patient Date Signature

 Name of Person Date Signature
 taking consent

Centre Number:
 Study Number:
 Trial Identification Number:

Institute of Orthopaedics
 Norfolk & Norwich University Hospital
 Colney Lane Norwich NR4 7UY
 direct dial: 01603 286706
 direct fax: 01603 287498

CONSENT FORM

Title: Immune system involvement in prosthetic hip implants: Operative patients

Name of Researcher: Professor Simon Donell

Please initial
 as appropriate

- 1) I confirm that I have read and understand the information sheet dated December 2011, Version 03 for the above study. I have had the opportunity to consider the information, ask questions and have had these answered satisfactorily.
- 2) I understand that my participation is voluntary and that I am free to withdraw at any time without giving any reason, without my medical care or legal rights being affected.
- 3) I understand that relevant sections of my medical notes and data collected during the study may be looked at by individuals from the Institute of Food Research, from regulatory authorities or from the NNUH NHS Trust, where it is relevant to my taking part in this research. I give permission for these individuals to have access to my records.
- 4) I agree to my GP being informed of my participation in the study.
- 5) I agree to take part in the above study.

 Name of Patient Date Signature

 Name of Person Date Signature
 taking consent

When completed: 1 for participants; 1 for researcher site file; 1(original) to be kept in medical notes.

Appendix 2: Raw data of HLA Typing

Study No	Group	HLA-DRB1	HLA-DRB1	HLA-DQB1	HLA-DQB1	HLA-DQA1	HLA-DQA1
001	G3	*03:01/50/68N	*13:01/105/109/112/117/121	*02:01:01	*06:03P	*01:03:01G	*05:01P
002	G2	*01:01P	*01:01P	*05:01/07/11/12	*05:01/07/11/12	*01:01:01G	*01:01:01G
003	G2	*01:01P	*03:01/50/68N	*02:01:01	*05:01/12	*01:01:01G	*05:01P
004	G2	*01:01P	*03:01/50/68N	*02:01:01	*05:01/12	*01:01:01G	*05:01P
005	G2	*07:01P	*11:01/97/100/117	*03:01/27-29/35	*03:03/31/33/34/39	*02:01	*05:01:01G
006	G2	*03:01/50/68N	*08:01P	*02:01:01	*04:02P	*04:01:01G	*05:01:01G
007	G2	*01:01P	*01:01P	*05:01/12	*05:01/12	*01:01:01G	*01:01:01G
008	G2	*13:01/105/109/112/117	*15:01P	*06:02P	*06:03P	*01:02:01G	*01:03:01G
009	G2	*01:01P	*15:01P	*05:01/12	*06:02P	*01:01:01G	*01:02:01G
010	G2	*03:01/50/68N	*11:04P	*02:01:01	*03:01/27-29/35	*05:01P	*05:01P
011	G2	*03:01/50/68N	*08:01P	*02:01:01	*04:02P	*04:01:01G	*05:01:01G
012	G3	*03:01/50/68N	*04:04/23	*02:01P	*03:02/37	*03:01:01	*05:01P
013	G3	*01:01P	*07:01P	*03:03/31/33/34/39	*05:01/12	*01:01:01G	*02:01
014	G4	*01:01P	*14:01/54/113/114	*05:01/07/11/12	*05:03/06/08-10/13	*01:01:01G	*01:01:01G
015	G3	*04:01P	*07:01P	*02:02	*03:01/27-29/35	*02:01	*03:01:01G
016	G2	*07:01P	*13:01/105/112/117	*02:02	*06:03P	*01:03:01G	*02:01
017	G2	*11:01/97/100/117	*15:01P	*03:01/27-29/35	*06:02P	*01:02:01G	*05:01:01G
018	G2	*03:01/50/68N	*15:01P	*06:02P	*06:02P	*01:02:01G	*01:02:01G
019	G2	*04:01P	*04:02P	*03:02/37	*03:02/37	*03:01:01G	*03:01:01G
020	G2	*01:01P	*04:01P	*03:01/27-29/35	*05:01/12	*01:01:01G	*03:01:01G
021	G2	*03:01/50/68N	*07:01P	*02:01P	*02:02	*02:01	*05:01P
022	G3	*03:01/50/68N	*03:01/50/68N	*02:01P	*02:01P	*05:01P	*05:01P
023	G1	*01:01/20	*04:04/05/08/23	*04:02P	*05:01/12	*01:01:01G	*03:01:01G
024	G2	*15:01P	*15:01P	*06:02P	*06:02P	*01:02:01G	*01:02:01G
025	G4	*08:01/39	*11:01/97/100/117	*03:01/27-29/35	*04:02P	*04:01:01G	*05:01:01G
026	G1	*01:03	*11:01/97/100/117	*03:01/27-29/35	*05:01/12	*01:01:01G	*05:01:01G
027	G4	*03:01/50/68N	*04:01P	*02:01P	*03:02/37	*03:01:01	*05:01P
028	G3	*08:04P	*13:03/115	*03:01/24/27-29/35/36	*03:01/24/27-29/35/36	*05:01:01G	*05:01:01G
029	G1	*04:04/23	*15:02P	*03:02/37	*06:01/43	*01:03:01G	*03:01:01G
030	G1	*03:01/50/68N	*15:01P	*02:01:01	*06:02P	*01:02:01G	*05:01P
031	G1	*01:01P	*07:01P	*02:02	*05:01/12	*01:01:01G	*02:01
032	G1	*01:01P	*04:01P	*03:02P	*05:01/12	*01:01:01G	*03:01:01G
033	G1	*04:01P	*12:01P	*03:01/27-29/35	*03:02/37	*03:01:01	*05:01:01G
034	G1	*07:01P	*07:01P	*02:02	*03:03/31/33/34/39	*02:01	*02:01
035	G1	*11:04P	*12:01P	*03:01/24/27-29/35/36	*03:01/24/27-29/35/36	*05:01:01G	*05:01:01G
036	G1	*01:01P	*15:01P	*05:01/12	*06:02P	*01:01:01G	*01:02:01G
037	G1	*01:01P	*04:03/52/97	*03:05P	*05:01/12	*01:01:01G	*03:01:01G
038	G1	*04:04/23	*11:04P	*03:01/27-29/35	*03:02/37	*03:01:01	*05:01:01G
039	G1	*07:01P	*15:01P	*03:03/30/31/33/34/39	*06:02/11/26N/47	*01:02:01G	*02:01
040	G1	*01:02P	*07:01P	*02:02	*05:01/12	*01:01:01G	*02:01
041	G1	*03:01/50/68N	*15:01P	*02:01:01	*06:02P	*01:02:01G	*05:01P
042	G4	*04:04/23	*11:01/97/100/117	*03:01/27-29/35	*03:02/37	*03:01:01	*05:01:01G
043	G4	*07:01P	*07:01P	*02:02	*03:03/31/33/34/39	*02:01	*02:01
044	G3	*01:03	*03:01/50/68N	*02:01:01	*05:01/12	*01:01:01G	*05:01P
045	G3	*01:01/17	*04:05/07/08/92	*03:01/27-29/35	*05:01/12	*01:01:01G	*03:01:01G
046	G3	*01:01/50/52N/53	*11:01/97/100/117/133/134/140/141	*03:01/27-29/35/42/47	*05:01/12/18	*01:01:01G	*05:01:01G
047	G3	*07:01P	*11:01/97/100/117/133/134/140/141	*02:02	*03:01/27-29/35/42/47	*02:01	*05:01:01G
048	G3	*07:01P	*15:01/74/75/79/85/86/90/91	*03:03/31/33/34/39	*06:02P	*01:02:01G	*02:01
049	G4	*03:01/50/68N/83	*04:01/11/112/119N/127/135	*02:01P	*03:01/27-29/35/42/47	*03:01:01G	*05:01P
050	G4	*03:01/50/68N/83	*07:01P	*02:01P	*02:02	*02:01	*05:01P
051	G4	*01:02/43/46	*04:04/23/108/118/120N/121/149	*03:02P	*05:01/12/18	*01:01:01G	*03:01:01G
052	G4	*04:01/11/112/119N/123/127/135/151	*11:01/97/100/117/133/134/140/141	*03:01/24/27-29/35/36/42/44/46/47	*03:01/24/27-29/35/36/42/44/46/47	*03:01:01G	*05:01:01G
053	G3	*07:01P	*07:01P	*02:02	*02:02	*02:01	*02:01
054	G4	*07:01P	*13:01/105/112/117/148/153	*03:03/31/33/34/39	*06:03P	*01:03/10	*02:01
055	G4	*03:01/50/68N/82-84/86/89	*03:01/50/68N/82-84/86/89	*02:01P	*02:01P	*05:01P	*05:01P
056	G4	*01:01/47/50/52N/53	*07:01P	*02:02	*05:01/12/18	*01:01:01G	*02:01

Appendix 3: List of Antibodies

<u>Target Ag</u>	<u>Flouorochrome</u>	<u>Clone</u>	<u>Isotype</u>	<u>Supplier</u>	<u>Cat No</u>	<u>Lot No</u>
CD3	FITC	UCHT1	m IgG1	BD	555916	28361
CD4	PE	RPA-T4	m IgG1	BD	555347	29420
CD16	AF 700	3G8	IgG1	Invitrogen	MHCD1629	999788C
CD62L	APC/Cy7	DREG-56	m IgG1	BioLgend	304814	B142100
CD303	APC	AC144	m IgG1	Miltenyi	130-090-905	5140117032
CD19	PacBlue	SJ25-C1	m IgG1	Invitrogen	MHCD1928	1022267A
CD83	APC	HB15e	m IgG1	BD	551073	2579
CD45	PerCP-Cy5.5	2D1	m IgG1	BD	332784	2172572
CD14	V500	M5E2	m IgG2a	BD	561391	2244666
CD1c	PE	AD5-8E7	m IgG2a	Miltenyi	120-000-889	5110928140
CX3CR1	FITC	2A9-1	rat IgG2b	MBL	D070-4	42
CD123	EF450	6H6	m IgG1	eBioscience	48-1239-42	E10099-1633
HLADR	PE-Cy7	G46-6	m IgG2a	BD	560651	2129616
CD8	PacOrg	3B5	m IgG2a	Invitrogen	MHCD0830	749011F
CD86	PE	2331 (FUN-1)	IgG1	BD	555658	7395
CD11b	AF700	VIM12	IgG1	Invitrogen	CD11B20	0200F
CD11c	APC	S-HCL-3	IgG2b	BD	333144	2153613
Lin cocktail	FITC	MφP9		BD	340546	2235900
		3G8				
		NCAM16.2				
		SJ25C1				
		SK7				
		L27				
<u>Isotype controls</u>						
	PE-Cy7	27-35	IgG2b	BD	560542	00368
	APC-Cy7	MOPC-21	IgG1	BD	557873	01018
	FITC	X39	IgG2a	BD	349051	09962
	APC	MOPC-21	IgG1	BD	555751	09379
	FITC	MOPC-21	IgG1	BD	555909	85506
	FITC	27-35	IgG2b	BD	556655	17322
	PE	MOPC-21	IgG1	BD	555749	04255
	APC	27-35	IgG2b	BD	555745	05608
	FITC	IR863	ratIgG2b	Life Tech	R2b01	0600E
	Alex700	not specified	IgG1	Life Tech	MG129	830859A
	PacBlue	not specified	IgG1	Life Tech	MG128	730189C
	PacOrg	not specified	IgG2a	Life Tech	MG2a30	428820E
	PerCP	X39	IgG2a	BD	349054	15788